1-1-2013

The Effect of Thymidylate Synthase Inhibitors On Bone Marrow Derived Cells In the Intestinal Tumor Microenvironment

Grishma Acharya
University of South Carolina

THE EFFECT OF THYMIDYLATE SYNTHASE INHIBITORS ON BONE MARROW DERIVED CELLS IN THE INTESTINAL TUMOR MICROENVIRONMENT

by

GRISHMA ACHARYA

BACHELOR OF TECHNOLOGY
INSTITUTE OF CHARTERED FINANCIAL ANALYSTS OF INDIA, 2007

Submitted in Partial Fulfillment of the Requirements

For the Degree of Doctor of Philosophy in

Biological Sciences

College of Arts and Sciences

University of South Carolina

2013

Accepted by:

Franklin G. Berger, Major Professor

Maria Marjorette O. Pena, Major Professor

Hexin Chen, Committee Chair

Minsub Shim, Committee Member

Robert Price, Committee Member

Lacy Ford, Vice Provost and Dean of Graduate Studies

DEDICATION

I dedicate my thesis to my late father Mr. Debendra Nath Acharya who showed unwavering trust and faith in my abilities throughout his life. I wish to make him proud through my endeavors to contribute to the world of science.

ACKNOWLEDGEMENTS

This has been quite a journey. The work that I present through my thesis is only a part of this experience, as it does not include the trials, tribulations, standardizations, and occasional frustrations omnipresent during the PhD process. I would thus like to acknowledge all those who have encouraged, supported, assisted me, and made invisible yet significant contributions to this thesis. To begin, I would like to thank my father, mother, Uncle Suresh, Aunt Alpana, my mother in law, my father-in-law, my grandfather Aja, my Aai, and the rest of my family who have always encouraged me to pursue my dreams and always made enormous efforts towards understanding my passion towards research. I would like to thank Anmiv S Prabhu for being a pillar of endless emotional and professional support during these years of graduate studies.

I am very grateful to my advisor Dr. Maria Marjorette Peña, under whose able guidance I have learned a lot, both professionally and personally. I would like to thank my amazing lab mates, who are more like friends than colleagues and have made the long hours in the lab more enjoyable – Nikeya, Tia, Yu, Daniel, Sapana, and John. I would like to acknowledge my committee members Dr. Frank Berger, Dr. Dan Dixon, Dr. Robert Price, Dr. Hexin Chen, and Dr. Minsub Shim for being a very approachable and encouraging committee. I extend my thanks to Dr. Berger's lab members Karen, Ufuk, Sarah, Yang Yang, and Sandra who have been a part of my lab family.

I'd like to take the opportunity to acknowledge my supportive friends who have

been like an extended family to me - Mouna, Aditi, Swati, Rupa, Anindita, Ronak, and Atishi. They have shared the joys and trials of research with me, patiently and uncomplainingly, never once failing to be there for me.

ABSTRACT

Tumors have come to be known as independently functioning complex organs consisting of cancer cells coexisting with a heterogeneous mixture of host-derived non-neoplastic cells that form the tumor stroma. Tumor survival, progression, and metastasis depend on multiple close interactions between the cancer cells and the tumor stromal cells. These tumor stromal cells are mainly bone marrow derived cells (BMDCs) that are recruited to the primary tumor and sites of metastasis by a variety of signals secreted by the cancer cells. Because of the close interaction between the tumor and the tumor stroma, we propose that tumor stromal cells play an important role in tumor response to systemic treatment with chemotherapeutic agents and that tumor response to therapy will reflect that of the tumor stroma. By also targeting the tumor stroma with chemotherapy, we can potentially enhance drug efficacy and specificity. In this study, we used *Apc*$^{Min/+}$ mice that are predisposed to the development of spontaneous adenomatous tumors in the small intestine and colon, and a Balb/cByJ ectopic mouse model that were subcutaneously implanted with CT26 colon carcinoma cells. Using these murine models, we identified and quantitated the myeloid derived suppressor cells (MDSCs), mast cells, and T-regulatory cells (T-regs) in the intestinal tumor stromal compartment. We then determined if these BMDCs were direct cellular targets of thymidylate synthase (TS) inhibitors in the tumor stroma by studying the kinetics of their response to the drug 5-fluorouracil (5-FU). We validated the impact of TS inhibitors on these target cells in chimeric *Apc*$^{Min/+}$ mice that were generated by transplanting genetically modified bone

marrow cells, such that the sensitivity of tumor stromal cells to systemic drug treatment was distinct from that of the tumor cells. The results showed that MDSCs are selectively sensitive and are direct targets of 5-FU, mast cells are resistant and are recruited the tumor bed in response to 5-FU, while T-regs are not prominently affected by 5-FU. We examined the mechanisms underlying the differential effects of 5-FU on MDSCs, mast cells, and T-regs. The results will lay the foundation for our ultimate goal of developing a strategy to target TS specifically in the tumor and tumor associated stromal cells using a single agent while protecting normal, healthy actively dividing cells from the detrimental effects of these inhibitors.

TABLE OF CONTENTS

Dedication iii

Acknowledgements iv

Abstract vi

List of tables xi

List of figures xii

Dedication iii

Acknowledgements iv

Chapter 1- Introduction: a paradigm shift 1

1.1 Hallmarks of cancer, traditionally 1

1.2 Tumor and the friendly neighborhood microenvironment 2

1.3 Tumor microenvironment and response to anti-cancer therapy 5

1.4 Colorectal cancer: facts, therapies, and challenges 7

1.5 Thymidylate synthase 8

1.6 Animal model for colorectal cancer studies: the *Apc*$^{Min/+}$ mouse 11

1.7 Animal model for colorectal cancer studies: CT26-derived subcutaneous tumor implantation model in Balb/cByJ mice 12

1.8 Overall goal of this project 13

1.9 Innovation of the research 14

1.10 Engraftment of hematopoietic derived cells in the *Apc*$^{Min/+}$ recipient mice...15

1.11 Preliminary studies.....18

1.12 Cellular constituents of the inflammatory microenvironment of intestinal tumor stroma 20

Chapter 2 – Quantitation and localization of bone marrow derived cells infiltrating the tumor stroma 29

2.1 Introduction.....29

2.2 Materials and methods 33

2.3 Results.....38

2.3.1(a): Quantitation of target cell types in the spleen, bone marrow and tumor beds of *Apc*$^{Min/+}$ mice and age-matched C57BL/6J mice by flow cytometry 38

2.3.1 (b): Quantitate the target cell types in the spleen, bone marrow and tumor in a Balb/cByJ based CT26 colon carcinoma model 40

2.3.2: Localization of MDSCs, mast cells and T-regs in the tumor stroma.....43

2.4 Discussion 47

Chapter 3 – Determine the impact and kinetics of response to TS inhibitors on MDSCs, mast and T-regulatory cells....52

3.1 Introduction....52

3.2 Materials and methods....54

3.3 Results....58

3.3.1 (a) Effect of 5-FU on target cell types in *Apc*$^{Min/+}$ mice....58

3.3.1(b) Effect of 5-FU on MDSCs, Mast cells and T-regs in the tumor beds of ectopic Balb/cByJ - CT26 mouse model....61

3.3.2 Determine the kinetics of 5-FU in mice transplanted with TS overexpressing chemo-resistant marrow....64

3.4 Discussion....69

Chapter 4 – Mechanisms underlying the impact of TS inhibitors on MDSCs, mast cells and T-regulatory cells....74

4.1 Introduction....74

4.2 Materials and methods....76

4.3 Results....79

4.3.1 Apoptotic status of the target cell-types post administration of 5-FU....79

4.3.2 Proliferative index of the target cells pre- and post- 5-FU administration....86

4.4 Discussion....93

Chapter 5 – Conclusions and future directions 96

5.1 Conclusions 96

5.2 Future directions 97

References 99

LIST OF TABLES

Table 1.1. Potential cellular constituents of tumor stroma 21

Table 4.1. Apoptosis induced in monocytes 5 days after 5-FU administration.....81

Table1 4.2. Apoptosis induced in granulocytes 5 days after 5-FU administration.....83

Table1 4.3. Apoptosis induced in mast cells 5 days after 5-FU administration 85

Table 4.4. Reduction in the level of proliferation of monocytes 5 days after 5-FU administration 88

Table 4.5. Reduction in the level of proliferation of granulocytes 5 days after 5-FU administration 89

Table 4.6. Reduction in the level of proliferation of mast cells 5 days after 5-FU administration 92

LIST OF FIGURES

Figure 1.1. Colorectal cancer progression 8

Figure 1.2. Thymidylate synthase 9

Figure 1.3. Schematic of bone marrow transplantation 15

Figure 1.4. Localization of eGFP expressing BMDCs in intestinal tumor stroma 17

Figure 1.5. Bone marrow engraftment in recipient organs 18

Figure 1.6. Schematic of overall strategy 19

Figure 1.7. Interaction between tumor stromal cells.....28

Figure 2.1. Quantitation of MDSCs, Mast cells and T-regs in the spleen, bone marrow and tumor of (A) C57BL/6J control mice and (B) *Apc*$^{Min/+}$ mice by flow cytometry 39

Figure 2.2. Quantitation of MDSCs, Mast cells and T-regs in the spleen, bone marrow and tumor of (A) Balb/cByJ control mice and (B) CT26 tumor bearing Balb/cByJ mice by flow cytometry 42

Figure 2.3. Localization of Monocytes, Granulocytes, Mast cells and T-regs in the intestinal tumor stroma of *Apc*$^{Min/+}$ mice by confocal microscopy 45

Figure 2.4. Localization of Monocytes, Granulocytes, Mast cells and T-regs in the CT26-derived tumors in Balb/cByJ mice, an ectopic model of colorectal carcinoma.....46

Figure 3.1. Schedule of drug administration and time points for cell analyses 56

Figure 3.2. Effect of 5-FU on MDSCs, Mast cells, T-regs in tumor beds of *Apc*$^{Min/+}$ mice.....59

Figure 3.3. Effect of 5-FU on MDSCs, Mast cells, T-regs in the spleens of *Apc*$^{Min/+}$ mice.....60

Figure 3.4. Effect of 5-FU on MDSCs, Mast cells, T-regs in the bone marrow of *Apc*$^{Min/+}$ mice.....60

Figure 3.5. Effect of 5-FU on MDSCs, Mast cells, and T-regs in tumor beds of Balb/cByJ mice implanted with CT26 cells.....63

Figure 3.6. Effect of 5-FU on MDSCs, mast cells, and T-regs in spleens of tumor bearing Balb/cByJ mice.....63

Figure 3.7. Effect of 5-FU on MDSCs, mast cells, and T-regs in the bone marrow of tumor bearing Balb/cByJ mice.....64

Figure 3.8. Comparison of the effect of 5-FU on MDSCs, Mast cells, and T-regs in the tumor beds of *Apc*$^{Min/+}$ mice that were non-transplanted or transplanted with non-transduced chemosensitive or ecTS-transduced chemoresistant bone marrow.....67

Figure 3.9. Comparison of the effect of 5-FU on MDSCs, Mast cells, and T-regs in the spleens of *Apc*$^{Min/+}$ mice that were non-transplanted or transplanted with non-transduced chemosensitive or ecTS-transduced chemoresistant bone marrow.....68

Figure 3.10. Comparison of the effect of 5-FU on MDSCs, Mast cells, and T-regs in the bone marrow of *Apc*$^{Min/+}$ mice that were non-transplanted or transplanted with non-transduced chemosensitive or ecTS-transduced chemoresistant bone marrow.....69

Figure 4.1. Apoptosis induced in monocytes at 5 days after 5-FU administration.....80

Figure 4.2. Box plots of the number of apoptotic monocytes in PBS versus 5-FU treated mice at 5 days post treatment.....81

Figure 4.3. Apoptosis induced in granulocytes at 5 days after 5-FU administration.....82

Figure 4.4. Box plots of the number of apoptotic granulocytes in PBS versus 5-FU treated mice at 5 days post treatment.....83

Figure 4.5. Apoptosis induced in mast cells at 5 days after 5-FU administration.....84

Figure 4.6. Box plots of the number of apoptotic mast cells in PBS versus 5-FU treated mice at 5 days post treatment.....85

Figure 4.7. Proliferation levels of monocytes at 5 days after 5-FU administration.....87

Figure 4.8. Box plots of the number of proliferating monocytes in PBS versus 5-FU treated mice at 5 days post treatment.....88

Figure 4.9. Proliferation levels of granulocytes at 5 days after 5-FU administration89

Figure 4.10. Box plots of the number of proliferating granulocytes in PBS versus 5-FU treated mice at 5 days post treatment.....90

Figure 4.11. Proliferation levels of mast cells at 5 days after 5-FU administration 91

Figure 4.12. Box plots of the number of proliferating mast cells in PBS versus 5-FU treated mice at 5 days post treatment.....92

Figure 5.1. Schematic of conclusion.....97

CHAPTER 1

INTRODUCTION: A PARADIGM SHIFT

1.1 Hallmarks of cancer, traditionally

The hallmarks of cancer postulated a list of underlying principal properties that collectively characterize a variety of cancers based on their typical phenotypic behavior during cancer progression (Hanahan and Weinberg 2000; Hanahan and Weinberg 2011). These underlying principal traits govern the transformation of normal cells into cancerous cells. These hallmark properties include the following: (1) cancer cells can stimulate their own growth, (2) they resist inhibitory signals that might otherwise stop their growth, (3) they resist programmed cell death (apoptosis), (4) they stimulate the growth of blood vessels to supply nutrients to tumors (angiogenesis), (5) they can multiply indefinitely, and (6) for some cells, they can invade local tissue and spread to distant sites (metastasis). For a long time, it was believed that understanding the biology of just the cancer cells themselves could explain the complete functioning of a tumor (Kerkar and Restifo 2012). Because of this, most anti-cancer pharmaco-therapeutic strategies were traditionally designed to specifically target the cancer cells themselves. Various anti-cancer therapies include surgical removal of the neoplastic region and are often accompanied by chemotherapy or radiation therapy targeted directly at the cancer, either alone or in combination. Even with the variety of available options, traditional anti-cancer treatment is usually accompanied by detrimental side-effects, such as drug-

induced toxicity to normal cells resulting in hematopoietic and gastrointestinal damage, and gradual resistance to the chemotherapy (Love, Leventhal et al. 1989; Attar, Ervin et al. 2000; Burstein 2000; Partridge, Burstein et al. 2001; McKnight 2003). Most therapies are moderately effective for a short time but are typically followed by accelerated repopulation of the tumor and a relapse of the disease in most patients. Such challenges and the failure to conquer the disease have instigated intense research on tumors and their microenvironment, and new effective therapies are needed while minimizing the toxic side effects (Ohtsu 2003; Omura 2008; Fujii, Kochi et al. 2010).

1.2 Tumor and the friendly neighborhood microenvironment

In recent years, further research has revealed that cancer cells do not exist as isolated entities but are in continuous communication with the normal non-neoplastic cells that are recruited and infiltrate into their surrounding environment. These non-neoplastic "normal" cells, along with the extracellular matrix in which the tumor is embedded, the blood vessels, connective tissue, and secreted molecules collectively make up the tumor microenvironment or the tumor stroma and provide a platform where the tumor can interact closely with the surrounding stromal cells. This concept was derived from previous studies by Harold Dvorak in his hypothesis that 'tumors are wounds that do not heal' (Dvorak 1986). Under normal homeostatic conditions, a mutated or aberrantly functional cell is usually eliminated by the body's defense mechanism of inflammatory cells to restore normal homeostasis such as that in the process of wound healing. However cancer can be considered as a state of continuous disruption of normal homeostasis, a state that can be viewed as a wound that does not heal, despite the best

efforts of normal functional cells to try to eliminate it. In this disease state, the normal cells surrounding the neoplastic cells are confounded by the cancer cells into ignoring the wound healing process thereby aiding in the survival and replication of the malfunctioning cancer cells (Dvorak 1986).

Because of the complexity of its structure and composition, tumors have begun to be viewed as independently functional organs that are comprised of aggressively proliferating cancer cells coexisting with a heterogeneous mixture of non-neoplastic cells that provide nourishment and support and create a conducive environment for cancer cell survival and proliferation (Hanahan and Weinberg 2011; Swartz, Iida et al. 2012). The composition and proportion of the stroma varies depending on the type and location of the cancer and depends on the tumor malignancy (Mueller and Fusenig 2004; Sebens and Schafer 2012).

A major contributor to the tumor microenvironment has been found to be inflammation and inflammatory mediators. In most cases, tumors generally circumvent the immune system and evade their intervention by exploiting the inflammatory cells for pro-survival strategies. These inflammatory cells are predominantly derived from the hematopoietic system and are thus very varied in their character as well as functions within the tumor stroma. For example, connective tissue mast cells have been implicated in tumor progression because they concentrate around tumors prior to the formation of new blood vessels (Reed, McNutt et al. 1996). Mast cells are also known to be instrumental in polyp formation resulting in colorectal carcinogenesis (Gounaris, Erdman et al. 2007). Recruitment of macrophages and mast cells has been observed in the development of the cervical intraepithelial neoplasia (Utrera-Barillas, Castro-Manrreza et

al. 2010). T-regulatory cells (T-regs) have been found to suppress protective anti-tumor immune responses (Gounaris, Blatner et al. 2009). Tumor associated myeloid derived suppressor cells (MDSCs) have been found to suppress both antigen-specific and nonspecific T cell activity (Corzo, Condamine et al. 2010) and have been found to infiltrate tumors that are ectopically implanted in C57BL/6J mice such as MC38 colon cancers, 3LL (lung carcinomas), B16 melanoma or CT26 tumors in Balb/c mice (Ostrand-Rosenberg and Sinha 2009). These studies show that inflammatory cells are highly abundant and in close contact with the cancer cells in the tumor microenvironment.

The hematopoietic system is a rich source of immature cells from which inflammatory cells are derived from. Due to its close proximity, molecular signals secreted by tumor cells can lead to the recruitment of a variety of host-derived cells that originate from the bone marrow. For example, Udagawa et al. demonstrated that $CD31^+$ cells are recruited from the nearby GFP^+ tissue in murine syngeneic lung carcinoma or a xenogeneic osteosarcoma model to create blood vessels within the tumor (Udagawa, Puder et al. 2006). Marini et al. and Pittet et al. have shown that tumor associated fibroblasts, macrophages and neutrophils are derived from the bone marrow (Cortez-Retamozo, Etzrodt et al. 2012). Recruited bone marrow derived cells (BMDCs) enhanced tumor progression through paracrine Wnt signaling in the prostrate epithelia of an orthotopic C4-2B xenograft model (Placencio, Li et al. 2010; Kidd, Spaeth et al. 2012). Various studies, thus, support the theory that BMDCs actively participate in colonizing the tumor stroma, and that they are recruited by the cancer cells through a variety of signaling chemokines (Chantrain, Feron et al. 2008). Tumor infiltrating, bone marrow

derived inflammatory cells and inflammatory signals have been shown contribute to cancer growth and spread, and to the immunosuppression associated with malignant disease, promoting inflammation and vascularization within the tumor (Balkwill and Mantovani 2001). Because of these, it is important to characterize and understand the tumor microenvironment particularly with respect to their role in determining the clinical efficacy of anti-tumor therapy.

1.3 Tumor microenvironment and response to anti-cancer therapy

The close proximity and the complex cross-talk that exists between stromal cells and cancer cells within the tumor suggest that stromal cells may play a highly influential role in dictating the tumor's response to therapy. Recent studies have shown that the intricate involvement of tumor stromal cells can define the manner in which cancer cells respond to different anti-cancer therapies. For example, it has been shown in a rat colon cancer model that administration of cyclophosphamide delayed the outgrowth of tumors by depleting T-regs (Ghiringhelli, Larmonier et al. 2004). Tumor response to radiation therapy was found to be dependent on the apoptotic capacity of infiltrating, hematopoietic derived endothelial cells (Garcia-Barros *et al*). Addition of pro-inflammatory cytokines to bolster cytotoxic T cell response has been found to enhance the efficacy of radiation therapy (Shiao and Coussens 2010). Tumor infiltration by lymphocytes has been shown to predict the efficacy of neo-adjuvant chemotherapy (Denkert, Loibl et al. 2010). Therapeutic interventions with the generation of tumor-associated-macrophages are known to enhance existing anti-cancer therapies in several different trials (Gerard and Rollins 2001; Duluc, Delneste et al. 2007; Porta, Subhra

Kumar et al. 2007). Thus, it is critical to identify the key players in the tumor microenvironment, to elucidate their specific role in cancer progression, and to target them, along with the cancer cells, to potentially enhance the efficacy of anti-cancer therapies.

Since the majority of tumor stromal cells are derived from the hematopoietic system, BMDCs are excellent candidates as targets or as carriers for the systemic delivery of therapeutic agents and factors that might enhance the efficacy of anti-cancer therapies (Doering, Archer et al. 2010). Exploiting BMDCs for anti-cancer therapy, therefore, is the subject of active research in the development of new anti-cancer therapies. The close synergistic interaction between the cancer cells and the tumor-stromal cells can be exploited for the effective therapeutic targeting of tumor. BMDCs can be strategically utilized for systemic delivery of anti-cancer therapeutics (Doering, Archer et al. 2010). Since an aggressive tumor participates in active recruitment of BMDCs, these BMDCs can be modified to function as a delivery system. The main advantage of exploiting BMDCs for enhancing therapeutic efficacy is that they can be conveniently genetically manipulated *ex vivo* and then transplanted back into pre-clinical models to systemically deliver genes that might enhance therapeutic efficacy. For example, bone marrow-derived mesenchymal stem cells have been used as vehicles to deliver IFN-β to inhibit the growth of malignant cells in a melanoma model (Studeny, Marini et al. 2002). The pancreatic tumor stroma has been targeted by transplantation of genetically manipulated mesenchymal stem cells carrying thymidine kinase resulting in the reduction of tumor size in an orthotopic model of pancreatic carcinoma (Zischek, Niess et al. 2009). Engineered BMDCs have been used to selectively eliminate Tie-2 expressing

mononuclear cells to inhibit angiogenesis in mouse models of mammary carcinoma and lewis lung carcinoma (De Palma, Venneri et al. 2003). Garcia-Barros et al showed that apoptosis of cancer cells in response to radiation therapy is dependent on the apoptotic capacity of the infiltrating hematopoietic cells (Garcia-Barros, Paris et al. 2003). Other studies have shown that specific targeting of tumor stroma aids in tumor regression and treatment. Willhauck et al, showed that tumor vascularization and invasion can be greatly diminished by altering the tumor stroma in squamous cell carcinoma using biodegradable scaffolds (Willhauck, Mirancea et al. 2007). Mesenchymal stem cells derived from the bone marrow can be genetically modified to overexpress thymidine kinase and then utilized in combination with ganciclovir to enhance the reduction of pancreatic tumor growth and the incidence of metastases significantly (Zischek, Niess et al. 2009). These studies showed that BMDCs in the microenvironment can have a significant impact on tumor response to therapy.

1.4 Colorectal cancer: Facts, therapies, and challenges

The role of inflammatory cells in gastrointestinal carcinogenesis has long been established epidemiologically (Taketo 2009); (Balkwill and Mantovani 2001). It is estimated that 60-90% of the mass of gastrointestinal tumors is occupied by stroma. Colorectal cancer is a malignant tumor arising from the inner wall of the large intestine. It is the third most frequent cancer in males and fourth in females in the United States. Colorectal cancer is the second leading cause of cancer related mortality (Whitlock, Lin et al. 2008; Peddareddigari, Wang et al. 2010). Figure 1.1 shows the different stages of colorectal cancer progression from the development of adenomatous polyps to

carcinomas and eventually, the initiation of metastasis. In our studies, we will utilize murine models of colorectal cancer that pertain to different stages of cancer progression. In human patients, the majority of colorectal cancers are adenocarcinomas, which are tumors arising from colonic mucosal cells. While most adenocarcinomas are well or moderately differentiated, approximately 15% are poorly or undifferentiated tumors. These tumors are typically associated with a poorer prognosis.

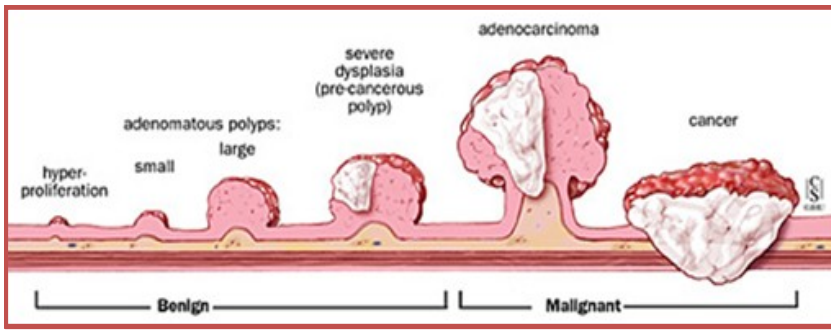

Figure 1.1. Colorectal cancer progression. Depicts the progression of colorectal cancer, from the polyp stage to the malignant cancer stage (Adapted from Johns Hopkins Medicine, Sidney Kimmel Comprehensive Cancer Center).

1.5 Thymidylate Synthase

There are several available therapies for the clinical management of colorectal cancer, including surgical removal of the tumor, chemotherapy commonly involving drug combinations like FOLFOX (leucovorin, 5-FU, and oxaliplatin) or FOLFIRI (leucovorin, 5-FU, and irinotecan), cryosurgery, radiation therapy and targeted therapy (Dwight, Higgins et al. 1972; Fong, Kemeny et al. 1996; de Gramont, Figer et al. 2000; Bokemeyer, Bondarenko et al. 2009). Among the most commonly used chemotherapeutic agents are the inhibitors of the S-phase enzyme thymidylate synthase (TS). TS catalyzes

the reductive methylation of 2'-deoxyuridine-5'monophophate (dUMP) to 2'-deoxythymidine-5'monophosphate (dTMP) using 5,10-methylenetetrahydrofolate as a methyl source, (Figure 1.2) (Rose, Farrell et al. 2002; Costi, Ferrari et al. 2005). Subsequently, dTMP is phosphorylated to 2'deoxythymidine-5'-triphosphate (dTTP) which is used for DNA synthesis in actively dividing cells (Rose, Farrell et al. 2002; Costi, Ferrari et al. 2005). This reaction is the sole *de novo* source of dTTP within the cell, making TS an important target of anti-cancer agents. Inhibition of the TS enzyme leads to depletion of thymidine pools, elevation of dUTP pools resulting in mis-incorporation of uracil into DNA causing DNA damage and ultimately, cellular apoptosis (Danenberg, Malli et al. 1999; Gmeiner 2005).

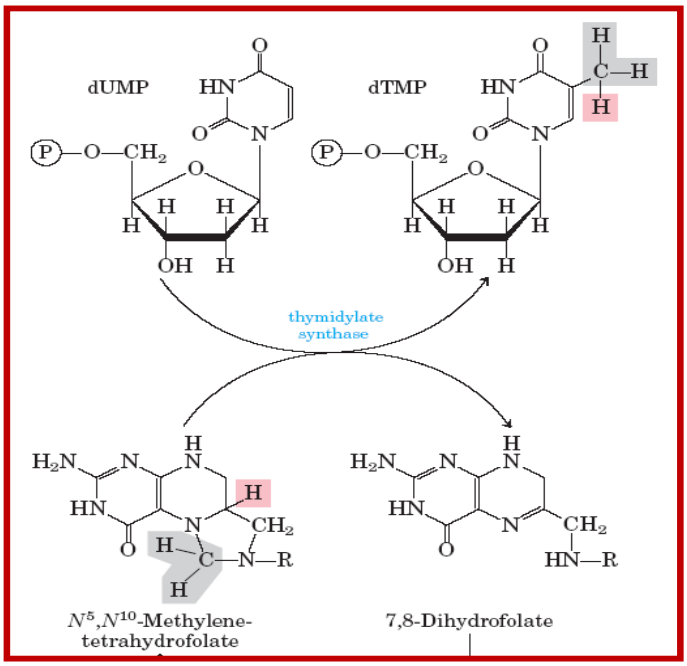

Figure 1.2. Thymidylate synthase. Pathway depicting reductive methylation of dUMP to dTMP by thymidylate synthase (Adapted from (Rose, Farrell et al. 2002; Costi, Ferrari et al. 2005).

Studies have shown that tumors in general express 2 to 10-fold higher levels of TS as compared to normal tissues (Parise, Janot et al. 1994; Findlay, Cunningham et al. 1997; Farrugia, Ford et al. 2003; Mauritz, Giovannetti et al. 2009). Among the earliest classes of drugs used clinically for TS inhibition are the fluoropyrimidines. A good example is 5-fluorouracil (5-FU) which has been used for many decades in the clinical management of colon and other cancers. In 1957, Heidelberger and his colleagues observed that rat hepatoma tumors had a higher rate of uracil incorporation into DNA as compared to the corresponding normal tissue. This research lead to the development of 5-FU, one of the first class of chemically modified molecules developed as a TS inhibitor anti-neoplastic drug that are analogs of the TS substrate dUMP (Heidelberger, Chaudhuri et al. 1957). A fluorine atom was substituted for hydrogen atom at the carbon-5 position of the pyrimidine ring to create 5-FU which is a competitive inhibitor of TS (Chu, Callender et al. 2003; Showalter, Showalter et al. 2008). Upon administration, inactive 5-FU is transported into the cell by facilitated transport using the uracil transporter protein and then converted into the powerful TS inhibitor 5-fluoro-2'-deoxyuridine-5'-monophosphate (FdUMP) that is covalently bound to TS. In addition to TS inhibition, 5-FU can also be incorporated into both cytoplasmic and nuclear RNA molecules (Rose, Farrell et al. 2002). It can also be mis-incorporated into DNA during DNA biosynthesis in cancer cells resulting in DNA strand breaks leading to apoptosis. Thus, while induction of cell death generally involves DNA directed events, 5-FU mediated induction of apoptosis could also be a consequence of mis-incorporation into RNA.

Although widely used in the clinical management of many cancers, the use of TS inhibitors is accompanied by severe side effects due its lack of specificity for cancer

cells. TS inhibitors primarily target rapidly proliferating cells and do not discriminate between actively dividing cancer cells or normal cells (Grem 2000; Rose, Farrell et al. 2002). Thus actively dividing normal cells such as those in the intestinal tract, the hematopoietic system, optical system, or hair follicles are equally targeted resulting in gastrointestinal epithelial ulceration, myelosuppression, ocular toxicity, and harmful effects on hair follicles or hair loss (Grem 2000; Chu, Callender et al. 2003). Prolonged administration of TS inhibitors to cancer patients can also gradually induce apoptotic resistance in cancer cells (Grem 2000).

In order to increase the clinical utility of TS inhibitors, it is necessary to develop strategies and combination therapies to enhance its cytotoxicity to cancer cells while minimizing its toxic effects on normal cells. While the impact of TS inhibitors on cancer cells has been assessed based on tumor burden, their impact on tumor associated stromal cells is less known. In this study, we examined the effect of TS inhibitors on tumor associated stromal cells in order to develop novel strategies to enhance their anti-tumor efficacy and the specificity for cancer cells of these inhibitors.

1.6 Animal model for colorectal cancer studies: the $Apc^{Min/+}$ mouse

A number of animal models have been used to study colon carcinogenesis, the mechanisms of its pathogenesis and have been used to establish therapeutic and preventive treatments (Taketo and Edelmann 2009). One of the most widely used genetic mouse model for studying the initiation and progression of intestinal tumors is the $Apc^{Min/+}$ mouse. This mouse has a germ-line mutation in the adenomatous polyposis coli

(APC) gene that is similar to that found in approximately 80% of sporadic colon cancer in humans (Dove, Gould et al. 1995). Tumor development mimics that in patients with Familial Adenomatous Polyposis (FAP), an inherited form of colon cancer which is also caused by a mutation in the APC gene (Shoemaker, Gould et al. 1997). The multiple intestinal neoplasia (Min) is a mutant allele of the murine APC locus, encoding a nonsense mutation at codon 850. It has a transversion point mutation that alters nucleotide 2549 from a T to an A that converts codon 850 from one encoding a leucine to a stop codon resulting in a truncated polypeptide. These mice are predisposed to the spontaneous development of multiple adenomas predominantly in the small intestine with a few in the colon (Shoemaker, Gould et al. 1997). The animals typically die within four to six months due to severe anemia and intestinal blockage by tumors. These mice provide a convenient model to test the effect of a drug therapy and their modulations because their impact can be readily measured by counting intestinal tumors and measuring their size in the mouse pre- and post- treatment. Also, it is known that the intestinal stroma of *Apc*$^{Min/+}$ mice is highly infiltrated by hematopoietic derived cells (Erdman and Poutahidis 2010; Davis, Price et al. 2011). Nevertheless, the exact cellular constitution of the *Apc*$^{Min/+}$ mouse intestinal tumor stroma as well as the functional role of each cell type in modulating the response of cancer cells towards therapy using TS inhibitors, has not been elucidated. Thus the *Apc*$^{Min/+}$ mouse has facilitated our study of stromal cell populations and their response to TS inhibitors.

1.7 Animal model for colorectal cancer studies: CT26-derived subcutaneous tumor implantation model in Balb/cByJ mice

Balb/cByJ mice have been used as immune-competent hosts for the subcutaneous

implantation of syngeneic immortalized cell lines. In this study we used eight-week old Balb/cByJ mice for subcutaneous implantation of the mouse CT26 colon carcinoma cell line as a model to study more advanced stage of cancer as compared to adenomas in *Apc*$^{Min/+}$ mice. CT26 is an undifferentiated murine colon carcinoma cell line derived from Balb/cByJ mice after treatment with N-nitroso-N-methylurethane, a chemical mutagen. CT26 cells proliferate like malignant tumors when injected subcutaneously or orthotopically into the cecum of Balb/cByJ mice. These cells have been used to test immunotherapy protocols and in several studies examining host immune responses.

Two weeks post injection of 1 million CT26 cells into the flank; the Balb/cByJ mice develop tumors with 9-11 mm diameter, that can be excised, de-bulked, and the resulting single cell suspension used for various analyses. This model provides a good platform for cancers that mimic the aggressiveness and disease morphology of human colorectal carcinoma. Furthermore, these cells can give rise to liver metastases when injected into the cecum providing an opportunity to study colon cancer progression at various stages of the disease. For the purpose of this research, both of these animal models have provided a convenient means to test our hypothesis.

1.8 Overall goal of this project

The overall goal of this study was to test the hypothesis that tumor response to systemic treatment using TS inhibitors is determined by the chemo-sensitivity of tumor infiltrating hematopoietic-derived stromal cells. Previous data had shown that, when transplanted with bone marrow overexpressing *e.coli.*TS, *Apc*$^{Min/+}$ mice were capable of refracting a

combination therapy of 5-FU and Raltitrexed drugs, suggesting the possible presence of BMDCs in the intestinal tumor stroma influencing tumor response to chemotherapy. Thus specifically, our objectives were: 1) to identify the bone marrow derived cellular components of the intestinal tumor microenvironment; 2) to identify the cells that might be the direct targets of TS inhibitors; and 3) to analyze the effect of TS inhibitors on various hematopoietic derived tumor stromal cells. Our ultimate goal is to enhance the efficacy and tumor specificity of TS inhibitors by simultaneously targeting the tumor and tumor-associated stromal cells with chemotherapy using TS inhibitors without affecting the normal healthy non-cancerous cells.

1.9 Innovation of the research

Research regarding cancer cell dependency on tumor stroma would alter the general perspective for the chemotherapeutic targeting of tumor cells. A paradigm shift towards targeting specific pro-tumorigenic non-neoplastic cells in the tumor periphery along with directly attacking the cancer cells would ensure a better killing of cancer cells and prevent relapse, thereby increasing patient survival. In this study, we localized and quantitated a variety of hematopoietic derived cells in the intestinal tumor microenvironment including MDSCs, mast cells, and T-regs. We then examined the effect of 5-FU on these cells and studied the underlying mechanisms of the manner in which 5-FU affects these cells. Understanding the effect and kinetics of 5-FU on different BMDCs in the intestinal tumor stroma, can be exploited to develop a strategy to target TS specifically in both tumor and tumor stromal cells only using a single agent while causing negligible distress to normal, healthy actively dividing cells.

1.10 Engraftment of hematopoietic derived cells in the Apc$^{Min/+}$ recipient mice

In previous studies, the contribution of BMDCs to the intestinal tumor microenvironment was determined by transplanting bone marrow cells from transgenic mice expressing eGFP into recipient *Apc*$^{Min/+}$ mice (Davis, Price et al. 2011). Donor marrow from C57BL/6-UB1-GFP mice, expressing eGFP under the control of the human ubiquitin promoter was isolated from the femur and tibia. The eGFP-expressing bone marrow cells were then transplanted via tail vein injection into age-matched, lethally-irradiated (950 rads) *Apc*$^{Min/+}$ mice (Figure 1.3).

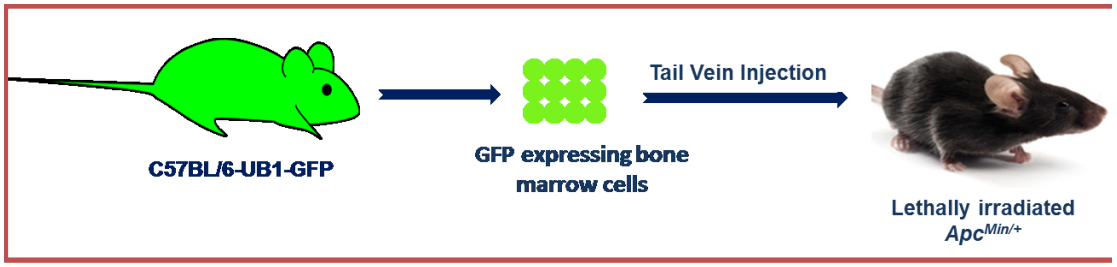

Figure 1.3. Schematic of bone marrow transplantation. eGFP expressing bone marrow cells were isolated by flushing the femur and tibia of 4-weeks old C57BL/6-UB1-GFP transgenic mice and transplanted into a lethally irradiated, age-matched *Apc*$^{Min/+}$ mice by tail vein injection. (Please see text for details)

To determine the distribution of BMDCs in the intestinal tract, intestinal tumor microenvironment, and in other organs, sections from these various organs were obtained from the transplanted *Apc*$^{Min/+}$ mice and analyzed by confocal microscopy. Eight weeks after transplantation, intestines, spleen, and liver were excised from the recipient mice, fixed in 4% paraformaldehyde and then sectioned for analyses by immuno-fluorescence microscopy. The sections were stained with phalloidin conjugated to Alexa 633 (for tissue morphology) and imaged using a Zeiss LSM510 META confocal laser scanning microscope. Figure 1.4 shows that the transplanted eGFP expressing marrow successfully

engrafted into the gastrointestinal tract of recipient *Apc*$^{Min/+}$ mice. eGFP expressing BMDCs were found abundantly in the small intestine sections, infiltrating both the tumor and the surrounding normal villi. On the other hand, in the colon sections from the transplanted mice, BMDCs appear to preferentially infiltrate the tumors, as compared to the surrounding normal areas (Davis, Price et al. 2011). As a control, sections taken from untransplanted C57BL/6J wild type mice and untransplanted *Apc*$^{Min/+}$ mouse intestines were also analyzed. Engraftment of eGFP expressing bone marrow derived cells in the intestine was shown to occur in a gradient fashion, with greater infiltration in the proximal regions as compared to that in the distal intestinal region and the colon (Davis, Price et al. 2011). This was observed in both *Apc*$^{Min/+}$ and wild type C57BL/6J control mice and is therefore independent of the *Apc*$^{Min/+}$ allele (Davis, Price et al. 2011). These data showed that indeed, BMDCs are a major component of the cells that make up the intestinal tumor microenvironment in the *Apc*$^{Min/+}$ mouse.

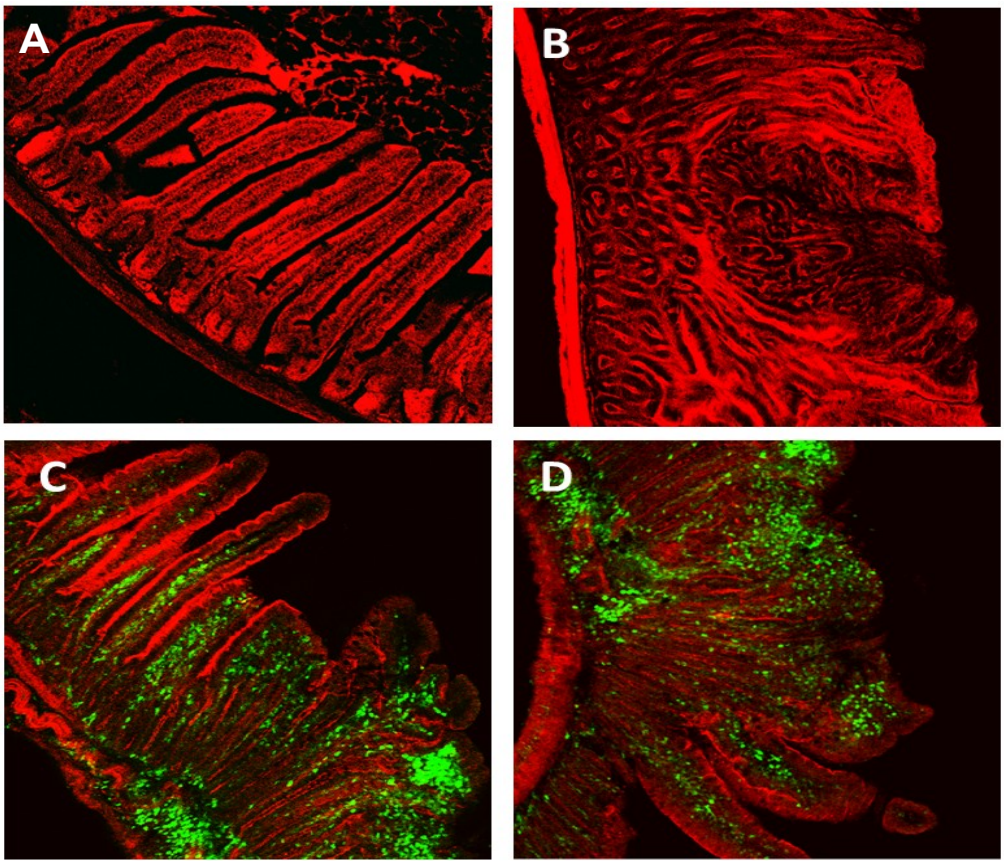

Figure 1.4. Localization of eGFP expressing BMDCs in the intestinal tumor stroma. Intestinal sections from *Apc*$^{Min/+}$ mice transplanted with eGFP expressing marrow were stained with phalloidin conjugated to Alexa-633 and analyzed by confocal microscopy. Donor-derived BMDCs efficiently repopulated and infiltrated both normal and tumor areas in the small intestine. A. Section from small intestine of untransplanted C57BL/6J control mouse (10x magnification), B. Small intestine section containing a tumor from untransplanted *Apc*$^{Min/+}$ mouse (10x magnification) C, D. Intestinal adenoma and surrounding areas of *Apc*$^{Min/+}$mice transplanted with eGFP expressing bone marrow. Red = Phalloidin for actin, Green = GFP.

Examination of other organs showed that there was an extensive engraftment of eGFP^{+} BMDCs in the hematopoietic organs like spleen and lung. As compared to that, there is a significantly low level engraftment of BMDCs expressing eGFP in other organs like the heart, soleus muscle, kidney and liver in the recipient *Apc*$^{Min/+}$ mice (Davis, Price et al. 2011).

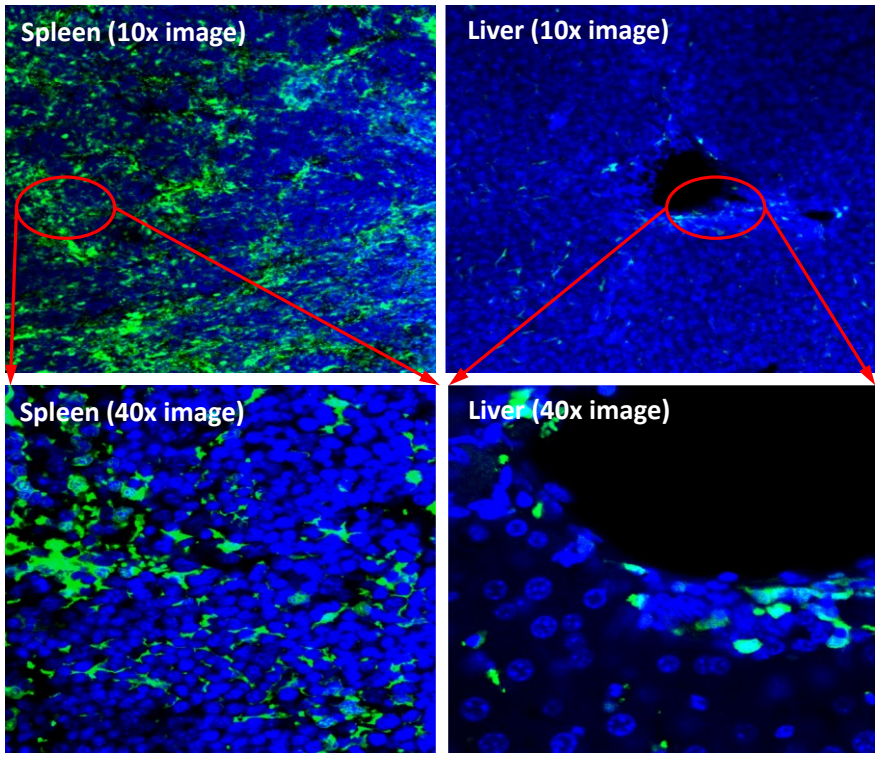

Figure 1.5. Bone marrow engraftment in recipient organs. Engraftment of donor-derived GFP^+ BMDCs in the spleen and liver of the recipient $Apc^{Min/+}$ mice. Blue = DAPI, Green = GFP. Spleen being a hematopoietic organ has a much higher level of $eGFP^+$ BMDCs as compared to their sporadic presence in the liver.

1.11 Preliminary studies

To assess the role of tumor stromal BMDCs in tumor response to therapy, previous studies were carried out wherein BMDCs in the tumor microenvironment were made resistant to TS inhibitors while keeping tumor cells sensitive to the therapy (Pena *et. al*., unpublished data). The overall strategy used in the study is outlined in Figure 1.6. Briefly, bone marrow from transgenic donor mice expressing the enhanced green fluorescent protein eGFP were genetically modified by transduction with the E. coli TS gene that conferred enhanced resistance to TS inhibitors as compared to non-transduced

cells. These were transplanted into lethally irradiated *Apc*$^{Min/+}$ mice and resulted in the creation of chimeric mice wherein the sensitivity of the tumor stromal cells was different from that of the tumor cells. After full engraftment of the transplanted marrow, the chimeric mice were subjected to systemic drug therapy using a combination of TS inhibitors. This therapeutic schedule had previously been shown to decrease tumor burden in *Apc*$^{Min/+}$ mice by 80% (Murphy, Tucker et al. 2004). As controls, *Apc*$^{Min/+}$ mice transplanted with non-transduced, chemosensitive marrow were also subjected to the same systemic therapy.

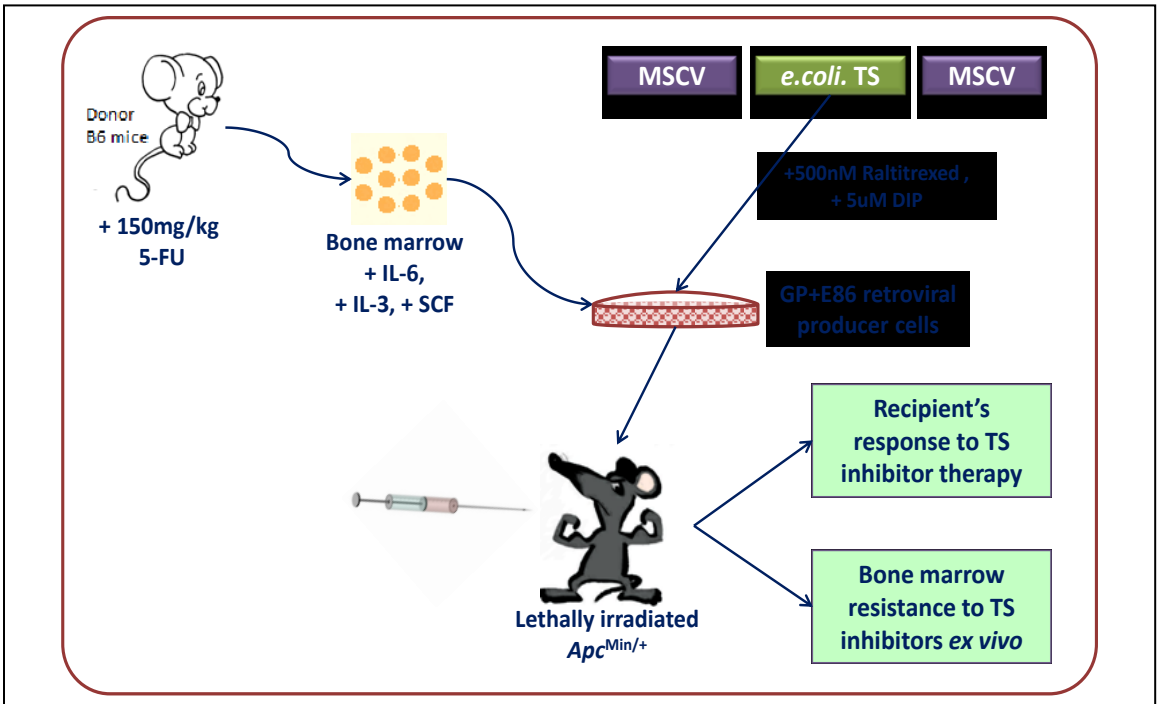

Figure 1.6. Schematic of overall strategy. This schematic outlines the method for isolating bone marrow from a donor C57BL/6J mouse, then co-culturing them with retroviral producer cells carrying the expression of *e.coli.* TS and subsequently transplanting the genetically modified BMDCs into lethally irradiated *Apc*$^{Min/+}$ mice. Using this protocol in the previous studies, chimeric mice were genetically engineered to have tumors whose response to chemotherapy is different from that of the tumor infiltrating BMDCs and the effect of TS inhibitors was studied on the tumor response to chemotherapy in these mice (Please see text for details.)

The results showed that when subjected to a combination of the TS inhibitors Raltitrexed and 5-FU, tumors in the chimeric mice were refractile to the therapy. On the other hand, age-matched control *Apc*$^{Min/+}$ mice transplanted with non-transduced marrow showed an 80% reduction in tumor burden similar to that in untransplanted *Apc*$^{Min/+}$ mice when subjected to the same chemotherapy regime. The results from these studies provided the basis for further investigations carried out in the following sections.

1.12 Cellular constituents of the inflammatory microenvironment of intestinal tumor stroma

There are numerous types of BMDCs that can potentially be found in the intestinal tumor microenvironment. These cells are listed in Table 1.1 together with the specific cell surface markers that can be used to identify them. In this study, we focused our efforts to understand the impact of TS inhibitors on three major cell types that have been shown in previous studies to play important roles in polyp development and tumor progression in *Apc*$^{Min/+}$ mice and also have been shown to interact with each another for survival within the tumor microenvironment and for promoting tumor development. These host-derived BMDCs include the myeloid derived suppressor cells (MDSCs), mast cells, and T-regs.

Table 1.1. Potential cellular constituents of tumor stroma.

Cell Types and Associated Surface Markers	
Cell Type	**Specific Biomarkers**
T-Cells	CD3
Helper T-Cells	CD4
Killer T-Cells	CD8
Activated T-Cells	CD69
NK T-Cells	CD16, CD56
B-Cells	CD5, CD19, CD27, CD45, B220
Macrophages	CD204, CD11b, Mac1
Neutrophils, Eosinophils, Granulocytes	CD66b, CD67, CD87, CD35, HNL
Fibroblasts	DDR2
Endothelial Cells	CD34, Flk-1, Tie-1, Tie-2, Vwf1
Epithelial Cells	Cytokeratin
Myeloid Derived Suppressor Cells	CD11b, Gr1
Mast Cells	CD34, CD117, MCT1
T-regulatory Cells	CD4, CD25, FOXP3

This is a list of a variety of immune cells that are potential components of the tumor microenvironment. The table outlines different immune-derived cells in the tumor microenvironment, as well as the respective cell-specific biomarkers used for their identification.

Myeloid Derived Suppressor Cells: The term myeloid derived suppressor cells, is used to define a heterogeneous population of immature myeloid cells derived from bone marrow hematopoietic precursors in mice. They remain undifferentiated under chronic inflammatory condition altering myelopoiesis that is typical of the tumor stroma (Baniyash 2006; Ostrand-Rosenberg and Sinha 2009; Umansky and Sevko 2012; Wu, Yan et al. 2012). MDSCs have been found to accumulate in human patients as well as in mice with cancer. MDSCs in tumor-bearing mice express the cell surface markers CD11b and Gr-1 antigens and have the potential to suppress immune responses of T-lymphocytes *in vitro* and *in vivo* (Gabrilovich, Bronte et al. 2007; Marigo, Dolcetti et al. 2008; Murdoch, Muthana et al. 2008; Gabrilovich and Nagaraj 2009; Peranzoni, Zilio et al. 2010). They are recruited by the tumor cells and host tumor stromal cells into the tumor

stroma and they have also been shown to accumulate after bacterial attack, parasitic infection, chemotherapy, and stress. Their accumulation leads to immune dysfunction in cancer patients due to their immunosuppressive functions (Jutila, Kroese et al. 1988; Nagendra and Schlueter 2004; Sunderkotter, Nikolic et al. 2004; Dolcetti, Marigo et al. 2008; Huang, Lei et al. 2008; Movahedi, Guilliams et al. 2008; Youn, Nagaraj et al. 2008; Abbitt, Cotter et al. 2009; Ostrand-Rosenberg and Sinha 2009; Ribechini, Leenen et al. 2009; Dolcetti, Peranzoni et al. 2010). In the tumor microenvironment, they are known to secrete various immunosuppressive molecules in variable quantities (depending on their location) such as arginase, inducible nitric oxide synthase, and reactive oxygen species. They also assist tumors in developing resistance to chemotherapy by secreting nitric oxide allowing them to avoid the caspase mediated apoptotic cascade (Bronte, Serafini et al. 2003; Bronte, Serafini et al. 2003; Kusmartsev and Gabrilovich 2003; Kusmartsev, Nefedova et al. 2004; Sinha, Clements et al. 2007; Sebens and Schafer 2012; Umansky and Sevko 2012). Their accumulation has been documented in the bone marrow, spleen, and peripheral blood of most patients and mice with cancer, where they are induced by various factors produced by tumor cells and/or by host cells in the tumor microenvironment (Almand, Clark et al. 2001; Pflugh, Maher et al. 2002; Gabrilovich 2004; Serafini, Carbley et al. 2004; Kusmartsev, Nagaraj et al. 2005; Sica and Bronte 2007; Dolcetti, Marigo et al. 2008; Haile, von Wasielewski et al. 2008; Marigo, Dolcetti et al. 2008; Markiewski, DeAngelis et al. 2008; Sinha, Okoro et al. 2008; Umemura, Saio et al. 2008; Youn, Nagaraj et al. 2008; Abbitt, Cotter et al. 2009; Diaz-Montero, Salem et al. 2009; Greifenberg, Ribechini et al. 2009).

MDSCs are mainly influenced by either tumor derived factors or by factors

released by activated T cells and other tumor stromal cells. Tumor derived factors help to stimulate myelopoiesis and assist myeloid cells in remaining undifferentiated. On the other hand, activated T cells and tumor stromal cells act by directly activating MDSCs through stimulating factors like Interferon-γ (IFN-ɤ), Toll like receptors, Interleukins 3 and 4, and Transforming growth factor β (TGF-β). These activated MDSCs in return release iNOS, arginase I, TGFβ, Cyclin D1, Myc and Survivin (Marigo, Dolcetti et al. 2008; Gabrilovich and Nagaraj 2009; Condamine and Gabrilovich 2011; Sonda, Chioda et al. 2011). They express low levels of the major histocompatibility complex (MHC) class II and CD80, a co-stimulatory signal necessary for T-cell activation and survival. MDSCs also have the ability to induce T-regs expansion and function synergistically with them to promote the suppression of T-cell activation and down regulate cell-mediated immunity (Peranzoni, Zilio et al. 2010).

T-regulatory cells: T-regs have been identified as the primary mediators of peripheral tolerance (Ling, Pratap et al. 2007). Stromal infiltration of T-regs has been found to be elevated in colorectal cancer patients. They are known to suppress tumor-specific immunity by suppressing $CD4^+$ T cells in part by competing for IL-2, rendering $CD8^+$ T cells inactive via cell contact and by TGF-β (Gounaris, Erdman et al. 2007; Mougiakakos, Choudhury et al. 2010). Adoptive transfer of anti-inflammatory T-regs has previously been shown to suppress polyposis in $Apc^{Min/+}$ mice in an IL-10 dependent manner (Gounaris, Blatner et al. 2009). However, under the influence of strong inflammatory stimuli within the polyp microenvironment, they can convert into pro-inflammatory IL-17 producing cells (Th17) that help promote colorectal cancer progression (Colombo and Piconese 2007). Many murine tumor model studies have

shown that targeting T-regs by depletion might help enhance anti-tumor response (Yang, Zhang et al. 2010). Studies on the role of T-regs in inflammation associated cancer have presented a lot of conflicting and paradoxical data. T-regs are a well-known subtype of immunosuppressive cells that are recruited to the tumor sites by colon cancer cells producing the chemokine CCL5, to suppress anti-tumor cytotoxic responses (Woo, Chu et al. 2001; Wolf, Wolf et al. 2003; Okita, Saeki et al. 2005; Bettelli, Carrier et al. 2006; Ling, Pratap et al. 2007; Siddiqui, Frigola et al. 2007; Clark, Huang et al. 2008; Giannopoulos, Schmitt et al. 2008; Soria and Ben-Baruch 2008; Sugasawa, Ichikura et al. 2008; Cambien, Karimdjee et al. 2009; Erdman and Poutahidis 2010; Lin, Mahalingam et al. 2013); and to control self-antigen specific responses in the periphery (Clarke, Betts et al. 2006). Also, their numbers have been found to be highly inflated in draining lymph nodes and in peripheral blood in most human cancers (Loddenkemper, Schernus et al. 2006; Ling, Pratap et al. 2007). Expression of the integrin CD103 surface molecule in effector $CD4^{+}Foxp3^{hi}CD45RA^{-}$ T-regs guides them to an inflamed site of activation and they accumulate in chronic inflammation, graft-vs-host disease, as well as cancer to enable the loss of immune-surveillance and enhance tumor-immunosuppression (Kettunen, Kettunen et al. 2003; Hall, Fortney et al. 2004; Jin, Shido et al. 2006; Hofmeister, Schrama et al. 2008; Hanna, Quick et al. 2009; Jenq and van den Brink 2010). In humans, T-regs are known to secrete various cytokines such as IL-10 and TGFB, or IL-17 to suppress the expansion of effector T cells or anti-tumoral peripheral $CD8^{+}$ T cells for cancer development (Levings, Bacchetta et al. 2002; Ma and Dong 2011). Depletion of T-regs by different mechanisms has been shown to be a successful anti-cancer therapy by a variety of studies (Schabowsky, Madireddi et al. 2007).

Cytotoxic drugs like cyclophosphamide, 5-FU, gemcitabine, and/or oxaliplatin have been used in preclinical models to deplete T-regs and have been found to correlate with a better response to treatment (Ghiringhelli, Larmonier et al. 2004; Lutsiak, Semnani et al. 2005; Correale, Rotundo et al. 2010).

There is approximately a 20-fold increase in the numbers of T-regs infiltrating colorectal tumor stroma as compared to the healthy normal colonic mucosa or colonic lamina propia (Lin, Mahalingam et al. 2013). In colorectal cancer, specifically, the expression of Foxp3, a member of the fork head and winged helix family of transcriptional regulators, is essential for the tumor stroma infiltrating $CD4^+CD25^+$ T-regs (Ziegler 2006). Foxp3 is also crucial for the ability of T-reg cells to actively suppress a variety of immune cells such as dendritic cells, natural killer T cells, $CD8^+$ T cells, $CD4^+CD25^-$ T and B cells (Beyer and Schultze 2006). $Foxp3^+$ T-regs with a deletion of IL-10 are in fact known to contribute to colonic disease and IL-10 producing $Foxp3^+$ T-regs are enriched within the colon during murine colitis (Li, Hsieh et al. 2009; Kaler, Galea et al. 2010). During active inflammation, circulating T-regs migrate into the lamina propia to maintain homeostasis (Muzes, Molnar et al. 2012). The vastly utilized animal model to study colorectal cancer, $Apc^{Min/+}$ mice, in fact have a higher serum levels of IL-6, TNF-α and IL-17 as compared to their age matched C57BL/6J counterparts (Erdman and Poutahidis 2010). Thus, studying the interaction of pro-inflammatory T-regs with other bone marrow derived immune cells, is crucial to understanding the mechanisms underlying the tumor response to anti-cancer therapies.

In the context of interacting with other cell-types, specifically in colorectal cancer, T-regs have been found to interact with mast cells very closely in the tumor

stroma. This interaction, combined with other tumor-generated inflammatory cytokines induces the T-regs to switch into a pro-tumorigenic suppressive characteristic, in an IL-6 and IL-17 dependent manner (Blatner, Bonertz et al. 2010). T-regs show pro-tumorigenic activity in the colorectal tumor stroma by maintaining mast cell activation to promote polyposis by secreting IL-17 and by being IL-10 deficient.

Mast cells: Mast cells have been studied widely in adenomatous polyp initiation in $Apc^{Min/+}$ mice and have been found to be required for tumor initiation and development (Shinar, Milo et al. 2007). They are derived from bone-marrow hematopoietic progenitors but migrate, while still immature, from vascular to peripheral tissues and participate in stroma re-modeling (Yang, Zhang et al. 2010; Liu, Zhang et al. 2011). Mast cells are known to infiltrate the tumor stroma aggressively in the early stages of tumor development. While still immature, these hematopoietic derived mast cell progenitors tend to travel from the vascular to peripheral tissues in a sialomucin dependent manner, into areas where they can mature and reside. Under normal conditions, mast cells are known to locate themselves in areas where they can ward off external attacks as quickly as possible, such as blood vessels, nerves, mucosal surface, skin, respiratory tract, and the gastro-intestinal tract (Bauer and Razin 2000; Heib, Becker et al. 2008; Liu, Zhang et al. 2011). Although their specific role in tumor stroma remodeling and malignant transformation is yet unclear, they have been suspected to participate in angiogenesis and tumor initiation in adenomatous polyps, skin dysplasia, malignant melanoma, breast carcinoma, and colorectal cancer (Maltby, Khazaie et al. 2009; Liu, Zhang et al. 2011). Tumor cells are speculated to recruit mast cells to the tumor sites by secretion of stem cell factors that eventually binds to its receptor c-kit on mast cells. There is also a

possibility that in a dysregulated tumor stroma, mast cells reprogram tumor cells to obtain c-kit signaling by transferring the receptor through autocrine or paracrine secretion (Kitamura and Fujita 1989; Huang, Lei et al. 2008; Liu, Zhang et al. 2011). Post-recruitment, mast cells have been shown to survive in the tumor stroma using the cytokine IL-9 which is secreted by pro-inflammatory $FOXP3^{+}IL\text{-}10^{-}IL\text{-}17^{+}$ T-regs, thus feeding into the interconnected network among the mast cells, T-regs, and MDSCs.

In their activated form, mast cells release several mediators that are pre-formed in the cells and stored as granules. These preformed mediators range from histamine granules to *de novo* synthesized lipid mediators, cytokines, and chemokines, and they are released when mast cells face direct injury, cross-linking of IgE receptors, or complement activation (Prussin and Metcalfe 2003; Dawicki and Marshall 2007; Sanchez-Munoz, Dominguez-Lopez et al. 2008).

MDSCs, mast cells, T-regulatory cells form a closely knit network of cells that function synergistically and are crucially involved in various aspects of colorectal carcinogenesis (Figure 1.7).

Although different aspects pertaining to these cell-types have been studied, the impact of TS inhibitors on these cells, particularly in a model of colorectal cancer has not yet been studied or elucidated. This study examines the effect of 5-FU, a therapeutic agent that has been used for decades, on MDSCs, mast cells and T-regs in the intestinal tumor stroma as well as in the stroma of an ectopic model of murine colorectal carcinoma. In the subsequent sections, we have localized and quantitated these specific BMDCs and we have also studied the kinetics of the effect of a single dose of

systemically administered 5-FU on these cells in the tumor beds and in the hematopoietic organs. The results suggest that due to their higher rate of proliferation, MDSCs are more sensitive to 5-FU as compared to the mast cells in the tumor stroma.

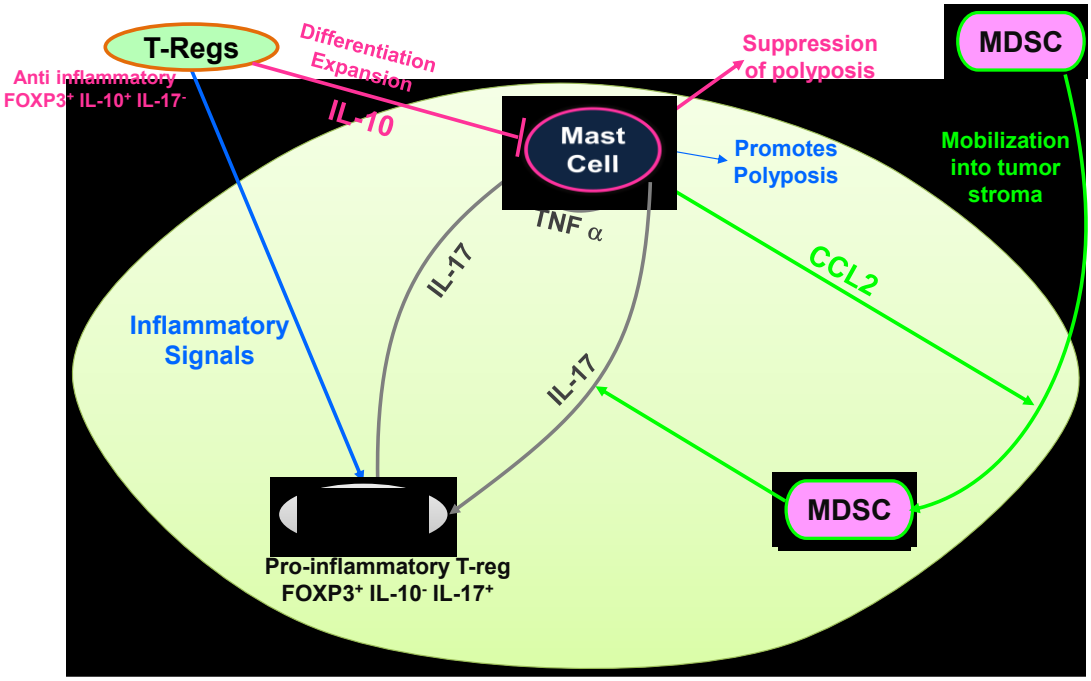

Figure 1.7. Interactions between tumor stromal cells. Close interaction network of myeloid derived suppressor cells, T-regulatory cells, and mast cells in the intestinal tumor microenvironment. (See text for details).

CHAPTER 2

QUANTITATION AND LOCALIZATION OF BONE MARROW DERIVED CELLS INFILTRATING THE TUMOR STROMA

2.1 Introduction

Colorectal cancer is the second leading cause of cancer-related mortality in the United States. Despite advances in available techniques for treating colorectal cancer at various stages of the disease, the majority of patients remain incurable and existing therapies are only of limited effectiveness due to accompanying limitations. Many of the treatment options used in the clinical management of the disease include a combination of chemotherapy with targeted therapy; however, not much has been studied with respect to the effect of these therapies on the tumor stromal cells in colorectal cancer microenvironment.

Several studies have been reported attempting to characterize the microenvironment of a variety of gastrointestinal tumors. Patient prognosis is reportedly impacted by the density, type and location of inflammatory activity within the colorectal tumor microenvironment (Galon, Costes et al. 2006; McLean, Murray et al. 2011). Preclinical studies have also demonstrated increased effectiveness of chemotherapy by combining it with the targeting of a variety of tumor stromal cells. For example, follicular dendritic cells inhibited apoptotic response of transformed B-cells to etoposide,

cyclophosphamide, busulfan (Schwarz, Yang et al. 1999). Tumor response to radiation therapy was shown to be dependent on apoptotic capacity of hematopoietic derived stromal endothelial cells and cytotoxic T cells (Garcia-Barros, Paris et al. 2003; DeNardo, Brennan et al. 2011). Thus, in order to understand colorectal carcinogenesis and develop effective therapeutic strategies, it is important to identify the key cellular players within the intestinal tumor stroma that are involved in initiating and maintaining the elevated inflammatory level to promote a pro-tumorigenic environment. With better characterization of infiltrating immune cells, the precise role of inflammation in the tumor stroma can be understood and exploited to enhance tumor sensitivity to therapy. Tumor progression and sustenance depend heavily on a receptive microenvironment. In colorectal cancer, this tumor-supportive microenvironment includes the co-dependent existence and functioning of the MDSCs, mast cells, and T-regs interacting closely at various stages from polyposis and progression to adenoma, to carcinoma, and ultimately metastasis.

Mast cells are thought to play a tumor-protective role in intestinal immune-surveillance. Activated mast cells in the colorectal tumor stroma secrete various pro-inflammatory mediators, small molecules, and cytokines involved in leukocyte recruitment and activation, vasodilation, angiogenesis, and mitogenesis (Frankenstein, Alon et al. 2006; Bischoff and Kramer 2007; Theoharides, Kempuraj et al. 2007; Sinnamon, Carter et al. 2008). Activated mast cells also have an immense ability to recruit cells by secreting cytokines such as, CCL2, IL-10 and IL-13, that result in the recruitment of immune-suppressive $CCR2^{+}$ cells such as, MDSCs. The MDSCs that are mobilized into the colorectal tumor stroma function effectively by remodeling the stromal

architecture making it more immune-suppressive and less anti-tumorigenic, permitting the further development of aggressive polyps (Yang, Zhang et al. 2010). Once in the tumor stroma, MDSCs also produce massive amounts of pro-inflammatory IL-17 that in-turn contributes to the maintenance of activated mast cells. MDSCs also promote the migration and development of other immune-suppressive cells such as pro-inflammatory IL-10^{-}IL-17^{+}FOXP3^{+} T-regs by secreting cytokines like IL-17 and IFN-γ (Colombo and Piconese 2009; Gounaris, Blatner et al. 2009).

The anti-inflammatory and tumor reprogrammed IL-10^{-}IL-17^{+} T-regs play a role in tumor maintenance and progression by secreting cytokines such as IL-17 mainly to aid in the recruitment of pro-tumorigenic mast cells (Colombo and Piconese 2009; Gounaris, Blatner et al. 2009). Although, normal T-regs are known to inhibit histamine release by mast cells, they act in a pro-tumorigenic polyp initiating manner by promoting the mast cell mediated release of TNF-α in the tumor stroma (Colombo and Piconese 2009). They are also thought to recruit and expand mast cell proliferation in an IL-9 dependent manner (Gounaris, Blatner et al. 2009).

In this study, we localized and quantitated the MDSCs, mast cells, and T-regs in intestinal tumor microenvironment using two animal models of colorectal cancer. The *Apc*$^{Min/+}$ mouse, a genetic model of colon carcinogenesis, and an ectopic model of colon carcinoma using Balb/cByJ mice. *Apc*$^{Min/+}$ mice are predisposed to the spontaneous development of multiple adenomas mostly in the small intestine with a few in the colon, however these tumors never progress to the carcinoma stage or metastasize to distant organs. In the ectopic model, Balb/cByJ mice are used as immune-competent hosts for the subcutaneous implantation of syngeneic immortalized murine cancer cell lines. We

used eight-week old Balb/cByJ mice for subcutaneous implantation of CT26 mouse colon adenocarcinoma cells as a model to study a more advanced stage of cancer as compared to the adenomas in *Apc*$^{Min/+}$ mice. CT26 proliferate as malignant tumors when injected subcutaneously or into the cecum of Balb/cByJ mice. Two weeks post-injection, the mice develop a large tumor that can be excised and the cells utilized for further analyses by confocal microscopy or flow cytometry. Furthermore, when injected into the cecum, they spontaneously give rise to liver metastases, providing an opportunity to study colon cancer progression at various stages of the disease. The ectopic model progresses much faster than tumor development in the *Apc*$^{Min/+}$ mice, thus providing an alternative model where we can examine the role of BMDCs in tumorigenesis and tumor response to TS inhibitors within a defined time frame.

To develop therapies targeting the tumor and cells in the tumor stroma, it is crucial to confirm that the target cells indeed reside within the tumor and are localized to the microenvironment of intestinal tumors. These localization studies will confirm the infiltration of bone marrow derived MDSCs (Monocytes and Granulocytes), mast cells, and T-regs in the adenomas and carcinomas of both mouse models. The distribution of the cell types within the tumor microenvironment were established by confocal microscopy, while the abundance of each cell type was determined by flow cytometry.

The results from these studies will provide a baseline measurement for (a) comparing the tumor dependent immune cell recruitment to tumor stroma, and (b) measuring the quantitative effect of TS inhibitors on these BMDCs. The abundance of these host-derived immune-cells were simultaneously quantitated in the tumor beds as well as hematopoietic organs of tumor-bearing mice and compared to that in normal non-

inflamed hematopoietic organs of age-matched non-tumor bearing C57BL/6J and Balb/cByJ mice.

2.2 Material and Methods

Cell Culture: CT26 cells are derived from Balb/cByJ mice by mutagenesis using N-nitroso-N-methylurethane-(NNMU). They were purchased from the American Type Culture Collection (ATCC), and grown in monolayer in Dulbecco's Modified Eagle Medium (DMEM) supplemented with 10% heat inactivated Fetal Bovine Serum (FBS) (Atlanta Biologicals, Lawrenceville, GA), 2 mmol/L L-glutamine, and 1× penicillin/streptomycin (Mediatech, Manassas, VA) at 37^{o}C and 5% CO_2 in a humidified atmosphere, until they reached 90% confluence. They were trypsinized with 0.25% trypsin in 2.21 mM EDTA (Mediatech, Manassas, VA) for 5 minutes. 5 ml of DMEM supplemented with 10% heat inactivated FBS was then added to the trypsinized cells to inactivate the trypsin. The cells were then centrifuged at 3000 rpm for 5 minutes. Upon centrifugation, the supernatant was discarded and the pellet disintegrated with 5 ml of sterile phosphate buffered saline (PBS) used as wash buffer, to remove traces of FBS from the cell preparation. The mixture was the centrifuged for 5 minutes at 3000 rpm and the pellet thus obtained is re-suspended in 1 ml PBS. The harvested CT26 cells suspended in sterile PBS are then ready for subcutaneous implantation.

Mice: Balb/cByJ mice, C57BL/6J-*Apc*^{Min}*/J mice (Apc*$^{Min/+}$) and C57BL/6J mice were purchased from the Jackson Laboratories (Bar Harbor, ME, USA) but were bred and maintained at the Mouse Experimentation Core Facility of the Center for Colon Cancer

Research at the University of South Carolina (USC), Columbia, SC. All aspects of the animal experiments were conducted in accordance with the guidelines and approval of the USC Institutional Animal Care and Use Committee.

Subcutaneous injection into Balb/c mice: One million CT26 cells were injected with subcutaneously into the flank of eight-week old Balb/cByJ mice. After 1 week, tumors were measured daily and excised when they reached a diameter of about 9-11 mm (about 10-14 days post implantation).

Isolation of single cell suspensions from tumors and other organs:

Balb/cByJ mice: Tumor bearing Balb/cByJ mice were humanely sacrificed and tumors excised. Tumors were sliced into smaller pieces using a sterile scalpel and then enzymatically digested with collagenase I (5mg/ml), collagenase IV (5mg/ml), hyaluronidase V (2.5mg/ml) and DNase I (1mg/ml). The tissue/enzyme mixture was placed in a 37^{o}C shaker for 30 minutes then filtered using 70-micron nylon filter. The flow-through was centrifuged at 2000 rpm for 5 minutes using an Eppendorf 5430R microcentrifuge at room temperature and the supernatant discarded. The pellet free of media and enzyme was then processed as described in the protocol for flow cytometry analysis in the following section.

Apc$^{Min/+}$ *mice:* 15-week old *Apc*$^{Min/+}$ mice were humanely sacrificed. Intestines and colon were isolated, connective tissue removed, and the small intestine divided into four sections with the colon as the fifth segment. Each section was flushed with PBS to remove fecal matter and then sliced longitudinally. Intestinal tumors were excised under a dissecting microscope. Tumors from intestines and colons from each group of mice,

PBS or 5-FU, were combined together for each time point. They were then mechanically disintegrated and passed through a 70-micron nylon filter to obtain a single cell suspension containing a mixture of tumor and stromal cells.

Spleen: Spleens were isolated from the mice. Spleens from the same treatment group, PBS or 5-FU, were combined and processed together by homogenization. 1ml of PBS containing 2% FBS solution was then added to the homogenized tissues. The mixture was then passed through a 70 micron nylon cell strainer to obtain a single cell suspension.

Bone marrow: Bone marrow was flushed from the femur and tibia of the mice using a 21 gauge syringe containing PBS with 2% FBS, and passed through the 70 micron nylon cell strainer to remove bone debris and other impurities. Bone marrow from 5 mice from each group, PBS or 5-FU, were combined for further analysis. The resulting single cell suspension was then prepared for analyses by flow cytometry as described below.

Analysis of cells by flow cytometry: The single cell suspensions obtained from the tumors and organs were incubated in ammonium chloride lysis buffer (150 mM NH_4Cl, 10 mM Na_2CO_3, 0.1 mM EDTA, pH 7.4) for 10 minutes on ice, in the dark, to lyse the red blood cells, followed by centrifugation at 2000 rpm for 5 minutes at room temperature and the supernatant discarded. Excess lysis buffer was removed by washing the pellet twice with cold PBS containing 2% FBS and then centrifuged at 2000 rpm for 5 minutes to obtain an enzyme free cell pellet of single cells consisting of tumor and stromal cells. The cells were counted using a hemocytometer and 1 million cells were stained with antibodies against cell specific cell-surface antigens. To identify and quantitate each cell type, at least two cell specific markers were used. A combination of antibodies was used to

quantitate MDSCs (FITC-conjugated α-CD11b, Clone M/170 and PE-conjugated α-GR-1, Clone RB68C5), mast cells (FITC-conjugated α-CD34, Clone RAM34 and APC-conjugated α-CD117, Clone 2B8) and T-regs (FITC-conjugated α-CD4, Clone RM 4-5 and PE-conjugated α-FOXP3, Clone MF23). All antibodies were purchased from iCyt Visionary Bioscience (Champaign, IL) and were used according to manufacturer instructions at 0.25 μg per 10^6 cells in a 100 μl volume.

To each tube containing one million suspended cells, two cell surface antigen-specific antibodies conjugated to two different fluorophores were added at 0.25 μg per 10^6 cells in 100 μl volume, and incubated in the dark at 4^oC for one hour. After incubation, 1 ml of PBS containing 2% FBS was added to the mixture and mixed well. Removal of excess antibody from the mixture was done by centrifuged at 2000 rpm for 5 minutes and the supernatant containing un-used antibody is discarded. This washing process was repeated twice. Antibody labeled cells were then re-suspended in 500 μl of PBS containing 2% FBS and analyzed for the various cell types using a Beckman Coulter FC-500 flow cytometer. As controls, we analyzed cells from the spleen, bone marrow, and intestines of non-tumor bearing, age-matched C57BL/6J and Balb/cByJ mice processed in a similar manner.

Preparation of Sections for analysis by Confocal Microscopy: 14 to 15-week old *Apc*$^{Min/+}$ mice were humanely sacrificed by cervical dislocation. Their intestines were isolated, flushed with phosphate buffer saline (PBS) and cut open longitudinally as described above. The tissues were fixed in 4% paraformaldehyde overnight. The fixed intestines were then swiss-rolled and embedded in paraffin cassettes and left to dry overnight. 3-5 micron thick sections were cut from the swiss-rolled intestines and mounted on standard

microscopy slides coated with poly-L-lysine.

CT26 tumor-bearing Balb/cByJ mice were sacrificed when the tumors reached 9-11 mm diameter. Their tumors were excised and washed with PBS to remove cell debris. After overnight fixation in 4% paraformaldehyde, a small section was excised from the tumor, embedded in paraffin. 3-5 micron thick sections were cut and mounted on microscopy slides.

Immunofluorescence: The sections were deparaffinized, rehydrated then incubated in a microwave oven at 95^0C with 0.01 M citrate buffer, pH 6.0 (Diagnostic Biosystem, Pleasanton, CA) for 10 minutes for antigen retrieval. The sections were then blocked with 5% normal goat serum (Invitrogen, Frederick, MD) diluted with 1% IgG-free Bovine serum albumin (BSA) in PBS for one hour. The sections were then incubated with antibodies against monocytes (anti-CD11b), granulocytes (anti-Gr-1), mast cells (anti-MCT1), or T-regs (anti-FOXP3). All antibodies were purchased from Abcam (Cambridge, MA) and used at 1:200 dilutions (in 1% BSA in PBS). Anti-Mouse Cy-3 secondary antibody (Invitrogen, Frederick, MD) raised in goat was used to detect the primary antibody targeted at each cell-type. The tissues were then stained with 4',6-diamidino-2-phenylindole (DAPI, Invitrogen, Frederick, MD), a fluorescent stain that binds strongly to A-T rich regions in DNA and is used to detect the nucleus. The slides were imaged using a Zeiss LSM 510 confocal microscope. All images were captured digitally at 40x magnification using filters for detecting emissions at 470 nm (DAPI) and 550 nm (Cy-3).

2.3 Results

2.3.1(a): Quantitation of MDSCs, mast cells, and T-regs in the spleen, bone marrow, and tumor beds of $Apc^{Min/+}$ mice and age-matched C57BL/6J mice by flow cytometry

In order to determine the effect of TS inhibitors on BMDCs in the tumor microenvironment, it is important to establish the baseline quantities of these cells in various organs and in tumor beds of the animal models that will be used in these studies. Therefore, we carried out flow cytometry based quantitative analyses of MDSCs, mast cells, and T-regs present in the tumor stroma, spleen, and bone marrow of 15-week old $Apc^{Min/+}$ mice and in age-matched wild type C57BL/6J mice. The results are shown in Figure 2.1(A). We found that MDSCs, mast cells and T-regs constitute 4%, 1.1%, and 0.7%,respectively, of the cells isolated from the spleen, while in the bone marrow the constitute 1.8% (MDSCs), 1.2% (mast cells), and 0.1% (T-regs) of the cell suspension, respectively.

In contrast, when tissues from tumor bearing $Apc^{Min/+}$mice were analyzed, much higher percentages of the BMDCs were found in both spleen and bone marrow. As shown Figure 2.1(B), the single cell suspensions contained 5% MDSCs, 4.8% Mast cells, and 1.5% T-regs in the spleen. This represents approximately 1.3-, 4.4- and 2- fold increases in MDSCs, mast cells and T-regs, respectively, as compared to that in the spleens from wild type control C57BL/6J mice. The bone marrow consisted of 35% MDSCs, 5% mast cells, and 0.6% T-regs. These indicated approximately 20-, 4.2- and 6-fold increases in MDSCs, mast cells, and T-regs, respectively, as compared to the percentages in wild type control bone marrow from C57BL/6J mice.

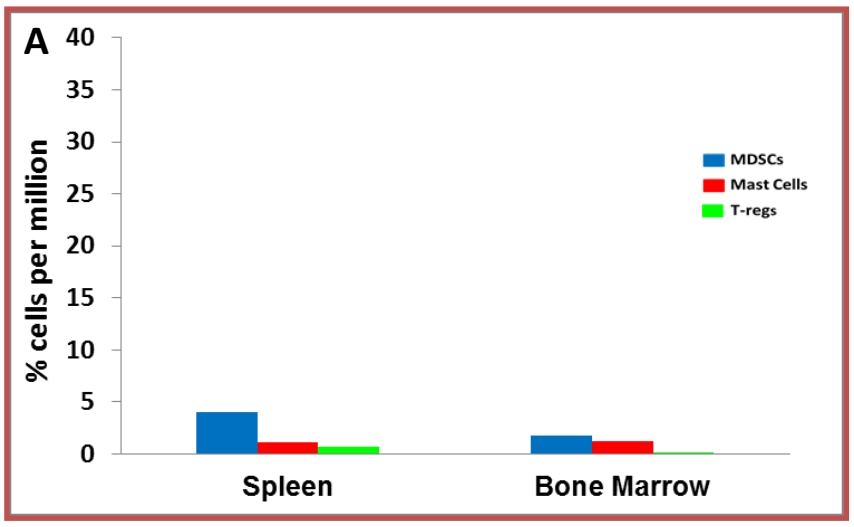

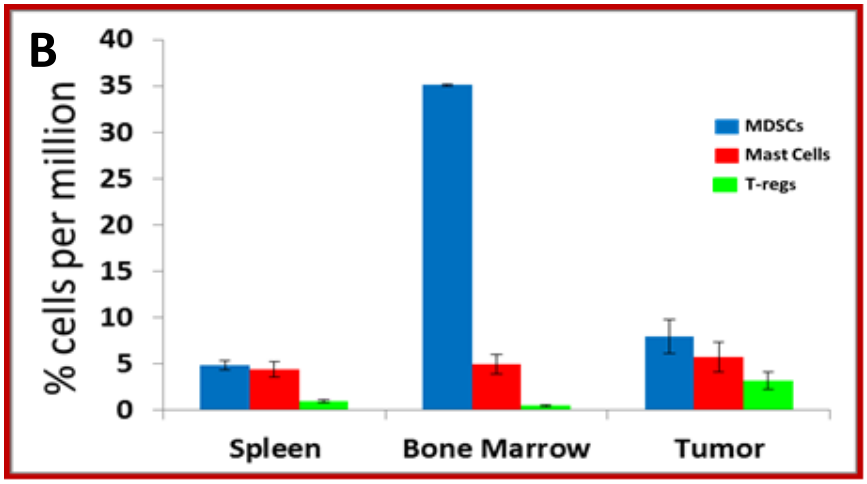

Figure 2.1. Quantitation of MDSCs, Mast cells and T-regs in the spleen, bone marrow and tumor of (A) C57BL/6J control mice and (B) *Apc*$^{Min/+}$ mice by flow cytometry. Spleen and bone marrow were extracted from 15-week old C57BL/6J mice and *Apc*$^{Min/+}$ mice and tumors were excised from *Apc*$^{Min/+}$ mice, stained with fluorochrome conjugated antibodies for MDSCs (α-CD11b-FITC and α-Gr-1-PE), Mast cells (α-CD34-FITC and α-CD117-APC) and T-regs (α-CD4-FITC and α-FOXP3-PE). Cells were then analyzed and quantitated by flow cytometry and plotted as percentage per million of the processed sample mixture. This graph shows the basal level quantities of the cell types in the bone marrow and spleen of the C57BL/6J control mice. Blue = MDSCs, Red = mast cells, Green = T-regs

These data indicate that the presence of intestinal tumors induces the aggressive generation of MDSCs in the bone marrow and subtle increase of the other cell types in

the hematopoietic organs. The single cell suspensions from tumors contained approximately 8% MDSCs, 6% mast cells and 3.8% T-regs. These data provided the basis for assessing the effects of chemotherapy on these cells in later studies.

2.3.1 (b): Quantitate the target cell types in the spleen, bone marrow, and tumor in an ectopic model by subcutaneous injection of CT26 cells into Balb/cByJ mice

To determine the extent of BMDC recruitment into tumor beds in a model with a more advanced carcinoma, and to ensure that the recruitment was independent of the Min allele, we analyzed the levels of BMDCs by quantitative flow cytometry of single cell suspensions from tumors, spleen, and bone marrow obtained from 10-week old Balb/cByJ mice bearing CT26 tumors. As controls, we compared these levels to that in tissues from age-matched tumor-free Balb/cByJ mice. Figure 2.2(A) shows that in non-tumor bearing Balb/cByJ mice, MDSCs, mast cells, and T-regs composed 1.3%, 0.7% and 0.1%, respectively, of the cells in the spleen, while in the bone marrow, they constituted 1.1%, 0.3%, and 0.2%, respectively, of the cell suspension.

Similar analyses conducted on age-matched Balb/cByJ mice bearing 9-11 mm diameter tumors in the flank, showed a huge increase in the immune cell populations in all the hematopoietic organs and in tumor beds, as shown in Figure 2.2(B). MDSCs, mast cells, and T-regs constituted 8%, 5.9%, and 2.1% of cell suspensions from the spleen. This indicated an increase in MDSCs, mast cells, and T-regs by approximately 6-, 8.5-, and 21- fold, respectively, in the spleen of tumor bearing Balb/cByJ mice as compared to that in the control tumor-free Balb/cByJ mice. MDSCs, mast cells and T-regs constituted

approximately 16.4%, 7.7%, and 1%, respectively, of the bone marrow cells in CT26 tumor-bearing Balb/cByJ mice. This represents about a 15-, 26-, and 5- fold increase in MDSCs, mast cells, and T-regs, respectively, in tumor bearing Balb/cByJ mice as compared to the control tumor-free Balb/cByJ mice. MDSCs, mast cells, and T-regs constituted approximately 13.2%, 3.6%, and 2.5% of the single cell suspension obtained from tumors excised from these mice.

Taken together, the data indicate that the presence of tumors in mice correlated with a large increase in the percentage of immune cells in various hematopoietic organs, suggesting that the signals from the tumors may induce an increase or recruitment bone marrow derived immune cells into both tumors and organs. The results indicate that recruitment of BMDCs into the tumor beds is not a consequence of the loss of the APC gene in the $Apc^{Min/+}$ mice but is dependent on the presence of neoplastic cells. The data from flow cytometric analyses further indicate that MDSCs, mast cells, and T-regs infiltrate the tumors in large numbers. In addition, these cells are also found at elevated levels in tissues such as the spleen and bone marrow in tumor bearing mice.

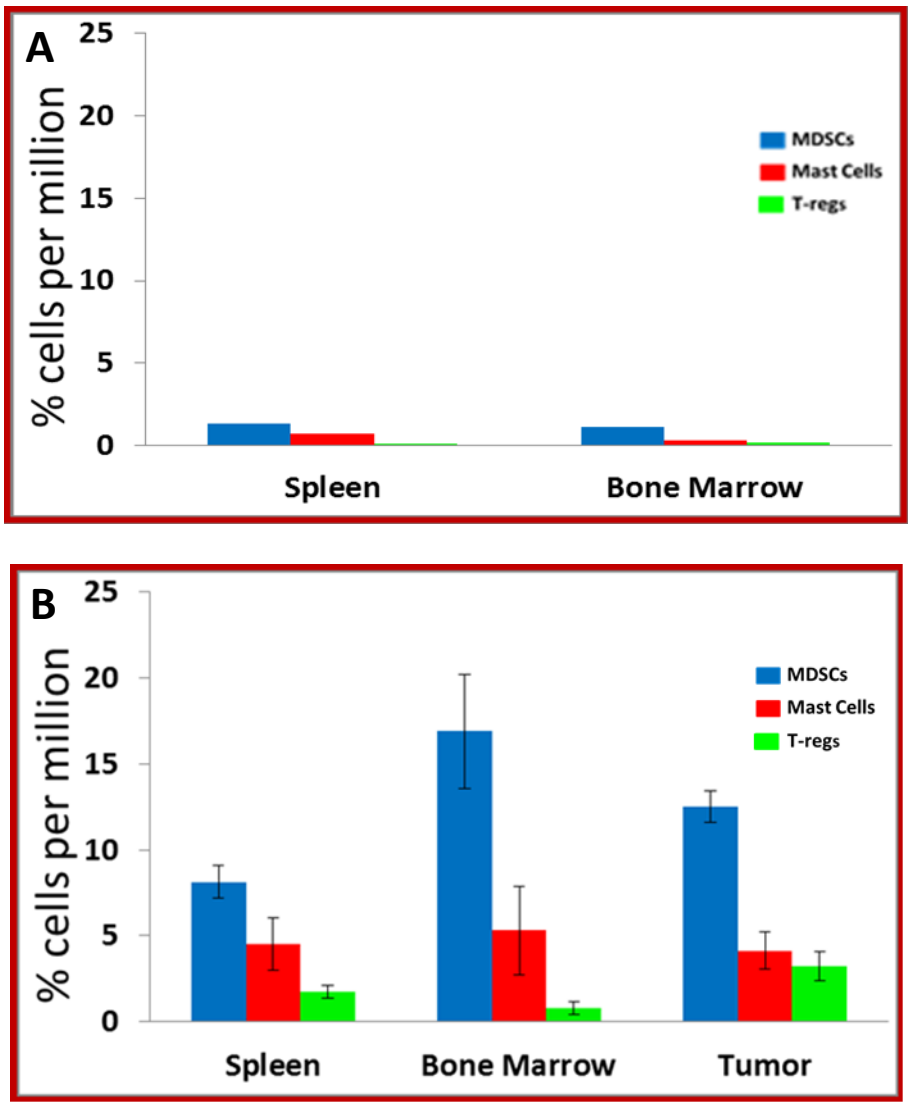

Figure 2.2. Quantitation of MDSCs, Mast cells and T-regs in the spleen, bone marrow and tumor of (A) Balb/cByJ control mice and (B) CT26 tumor bearing Balb/cByJ mice by flow cytometry. Spleen, bone marrow and tumors were extracted from 9-10 week old Balb/cByJ mice and CT26 tumor bearing Balb/cByJ mice and tumors, and 1 million cells were stained with fluorochrome conjugated antibodies to detect MDSCs (α-CD11b-FITC and α-Gr-1-PE), mast cells (α-CD34-FITC and α-CD117-APC), and T-regs (α-CD4-FITC and α-FOXP3-PE). Stained cells were analyzed and quantitated by flow cytometry and plotted as percentage per million of the processed sample mixture. This graph shows the quantities of the different cell types in the bone marrow and spleen of the Balb/cByJ control mice. Blue = MDSCs, Red = Mast cells, Green = T-regs

These data show that hematopoietic derived cells are a major component of the intestinal tumor microenvironment and support the notion that these cells can potentially be harnessed as targets to enhance tumor specific efficacy of existing therapies. They infiltrate into the tumor beds, and the presence of the tumors enhanced the level of inflammatory cells in the hematopoietic organs.

2.3.2: *Localization of MDSCs, mast cells and T-regs in the tumor stroma*

To further assess the infiltration of the target cells in the tumor stroma, we used confocal microscopy to localize the host-derived immune cells in the tumor bed. Tumor sections were processed and stained with fluorescently labeled antibodies against cell-specific cell surface markers. When imaged at 40x, we observed a massive infiltration by monocytes, granulocytes, and mast cells and a limited presence of T-reg cells of the intestinal tumor stroma in 15-week old *Apc*$^{Min/+}$ mice and in the CT26 tumors implanted in 10-week old Balb/cByJ mice. Figure 2.5 shows representative images of the intestinal tumor stroma analyzed by a confocal microscopy. To represent the MDSCs, we analyzed the infiltration of monocytes and granulocytes, two major sub-classes of MDSCs that are frequently studied separately by immunofluorescence analysis. As shown in Figure 2.5A, monocytes infiltrate the intestinal tumor stroma in high numbers and are distributed all over the tumor bed. Granulocyte (Figure 2.5B) and mast cells (Figure 2.5C) also infiltrate the intestinal tumors but are not as vastly distributed as monocytes. Tumor infiltrating T-regs on the other hand (Figure 2.4D), occupy very small regions of the tumor stroma and make up a very low percentage of the tumor infiltrating immune cells. These results are

consistent with the data obtained by flow cytometric shown in the previous section.

Tumors from the Balb/cByJ mice that were subcutaneously implanted with 1 million CT26 cells were processed and stained in a similar manner to localize monocytes, granulocytes, mast cells, and T-regs in the tumor beds. Figure 2.6 shows representative confocal images indicating the abundance of monocytes, granulocytes, and mast cells, as well as the small number of T-regs localized to the tumor beds. Visual examination of CT26 tumors indicate a more aggressive infiltration of monocytes and granulocytes as compared to tumors in the *Apc*$^{Min/+}$ mice (Figures 2.6 A and B vs Figures 2.5 A and B, respectively). In comparison, mast cells, although abundant, are lower in number as compared to monocytes and granulocytes (Figure 2.6C vs Figures 2.6A and B) in the CT26-derived tumors. T-regs are the lowest abundant cells in both the adenomas in *Apc*$^{Min/+}$ mice and CT26-derived tumors in Balb/cByJ mice (Figure 2.5D and Figure 2.6D.

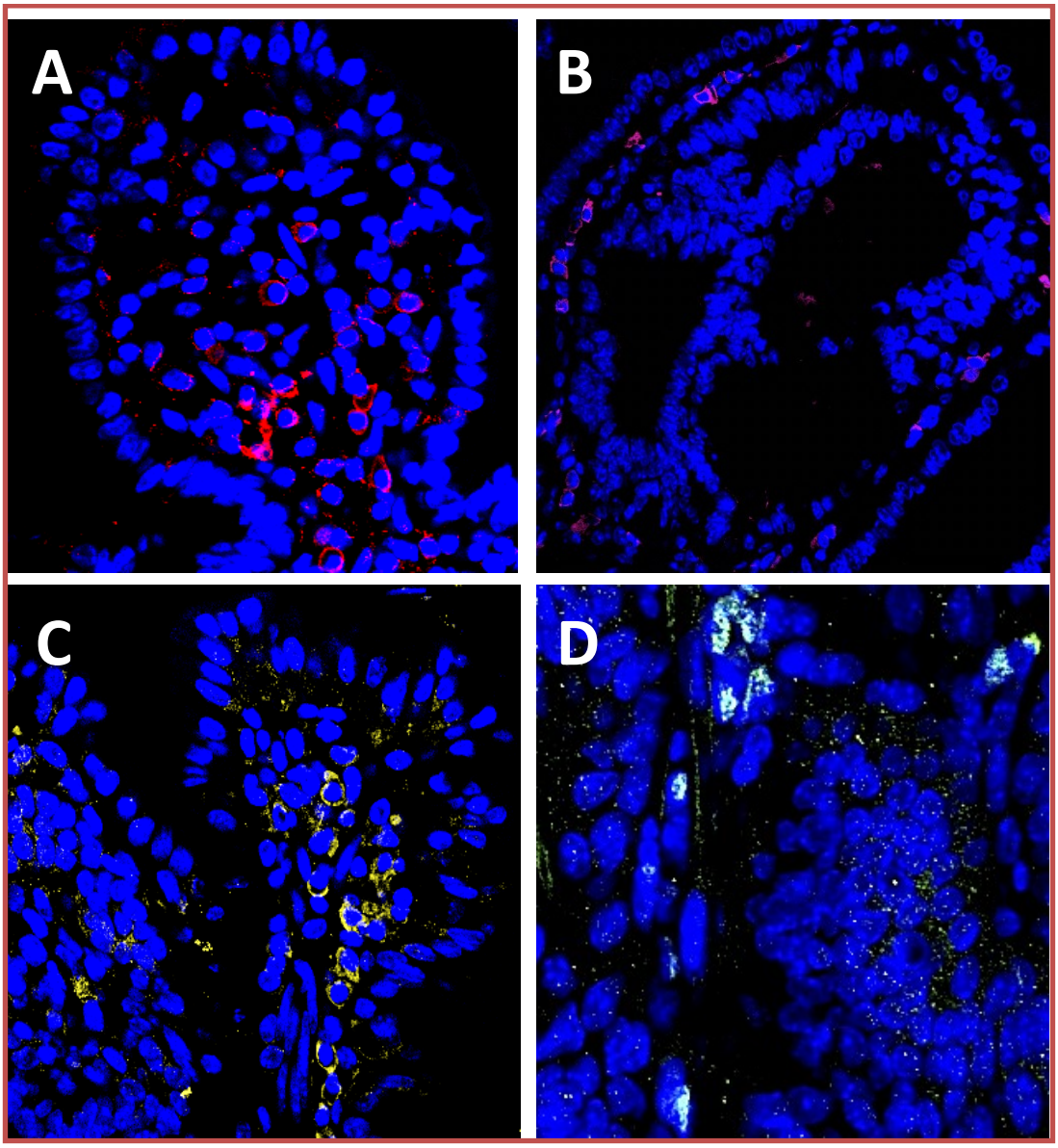

Figure 2.3. Localization of Monocytes, Granulocytes, Mast cells and T-regs in the intestinal tumor stroma of *Apc*$^{Min/+}$ mice by confocal microscopy. Intestinal sections were isolated from 15-week old *Apc*$^{Min/+}$ mice, flushed with PBS, fixed overnight in 4% paraformaldehyde, and embedded in paraffin cassettes. 3-5 micron thick sections were cut from the paraffin embedded intestines and stained with antibodies to detect monocytes (α-CD11b), granulocytes (α-Gr-1), mast cells (α-MCT1) and T-regs (α-FOXP3) The antibody-labeled samples were incubated with an anti-mouse secondary antibody conjugated to Cy-3, and then counter stained with DAPI to stain the nucleus. The slides were analyzed and imaged using a Zeiss LSM 510 confocal microscope to confirm cell localization in the intestinal tumor stroma A) Monocytes (CD11b - Red), B) Granulocytes (Gr-1 - Pink), C) Mast cells (MCT1 - Yellow), D) T-regulatory cells (FOXP3 - White). Blue = DAPI (nucleus).

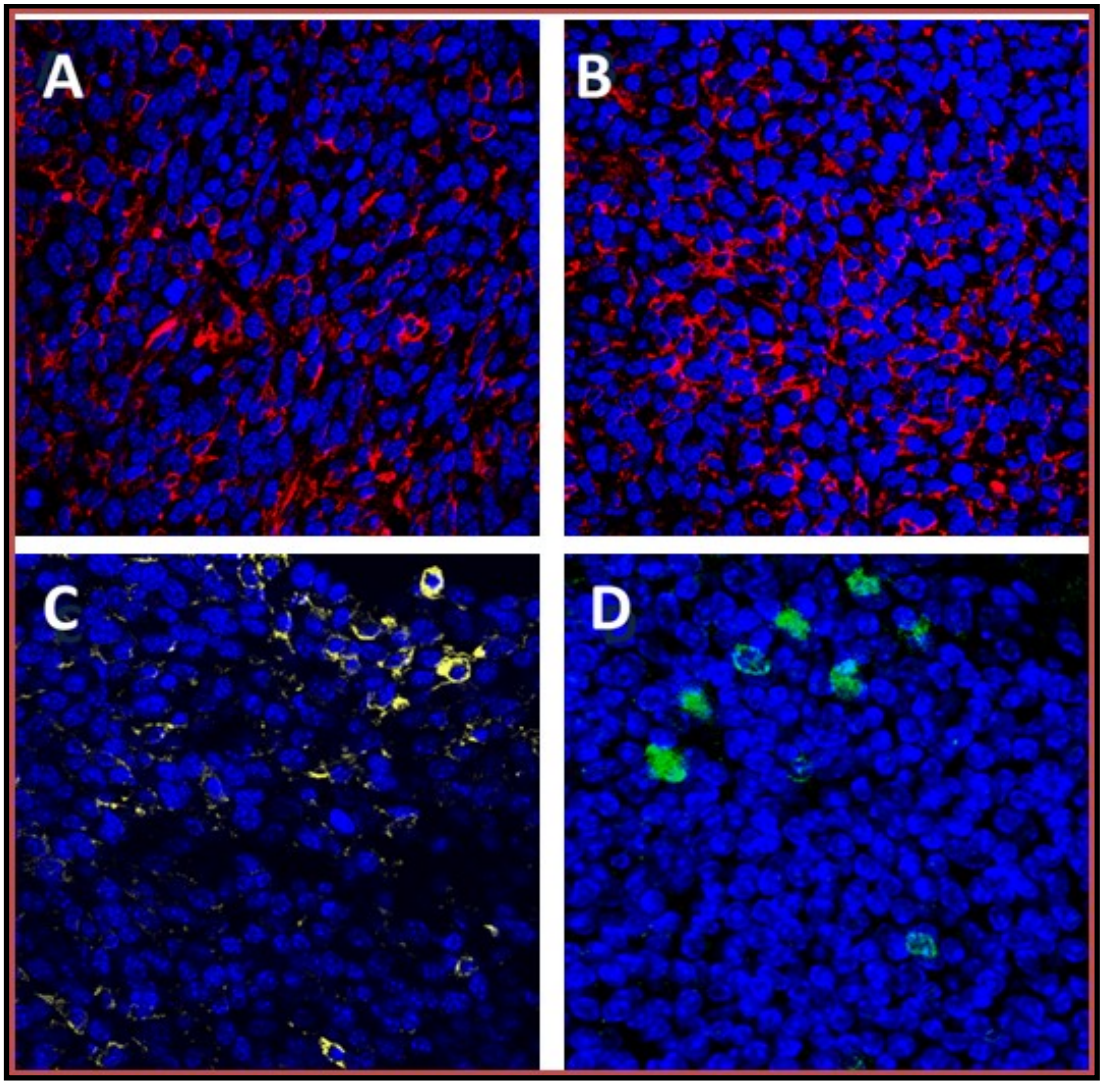

Figure 2.4. Localization of Monocytes, Granulocytes, Mast cells and T-regs in the CT26-derived tumors in Balb/cByJ mice, an ectopic model of colorectal carcinoma. Tumors derived from CT26 cells were excised from the flanks of Balb/cByJ mice, washed with saline solution, fixed overnight in 4% paraformaldehyde and smaller sections from the tumors were embedded in paraffin cassettes. 3-5 micron thick sections were cut from the embedded sections and stained with antibodies to detect monocytes (α-CD11b), granulocytes (α-Gr-1), mast cells (α-MCT1) and T-regs (α-FOXP3). The antibody-labeled samples were incubated with an anti-mouse secondary antibody conjugated to Cy-3 and then counter stained with DAPI to detect the nucleus. The cells were analyzed and imaged using a Zeiss LSM 510 confocal microscope imaged and their localization confirmed in the tumor stroma. A) Monocytes (CD11b - Red), B) Granulocytes (Gr-1 - Pink), C) Mast Cells (MCT1 - Yellow), D) T-regulatory cells (FOXP3 - White). Blue = DAPI (nucleus).

Collectively, the results showed that MDSCs, mast cells and T-reg cells are indeed abundant in the tumor beds at different stages of colorectal cancer, however, there seems to be a higher level of recruitment of BMDCs by the more advanced and invasive CT26-derived tumor in Balb/cByJ mice as compared to the early stage adenomas in $Apc^{Min/+}$ mice. This is supported by data from both flow cytometric and confocal microscopy analyses. It is possible that the stage of cancer progression might play an important role in the ability of the cancer cells to recruit stromal cells into their surrounding microenvironment. Thus the more advanced CT26 tumors can recruit monocytes and granulocytes more aggressively than adenomas in $Apc^{Min/+}$ mice.

2.4 Discussion

The tumor microenvironment consists of a variety of normal cells that behave differently due to their close interaction with aberrant cancer cells. Tumor epithelium is known to produce elevated levels of secreted molecules such as Chemokine (C-C motif) ligand 9 (CCL9) or Stromal Derived Factor 1 (SDF1) that actively recruit BMDCs to the tumor stroma (Galon, Costes et al. 2006; McLean, Murray et al. 2011). These recruited cells could function in different ways within the tumor stromal compartment, participating in different stages and aspects of tumorigenesis. Pro-tumorigenic cells in the tumor micro-environment could promote tumor progression in the following ways: (a) Produce cytokines that encourage survival and progression of tumor growth and recruitment of other immune cells; (b) Enhance the production of cytokines such as IFN-γ, IL-6 or TNF-α that promote a chronic inflammatory environment that supports tumor progression; (c)

confer immune-suppressive properties that enable tumors to escape the host immune-surveillance mechanisms; and (d) interact with cancer cells directly by cell to cell contact to provide them with pro-tumorigenic growth factors and cytokines.

Tumor-infiltrating stromal cells participate in one or more of these functions simultaneously to nurture the cancer cells. They can be immune-suppressive like the MDSCs and IL-17 secreting T-regs or they could be involved in tumor initiation or tumor progression such as the mast cells. Some cells can promote metastasis such as macrophage cells, or they could exist as undifferentiated monocytes that aid in tumor cell circulation or epithelial to mesenchymal transition. Bone marrow derived stromal cells are recruited by various molecular signals to the tumor microenvironment where they co-evolve with the cancer cells at each stage of cancer progression by synergistic activation of molecular pathways within both cells (Hanahan and Weinberg 2000; Hanahan and Weinberg 2011)

Colorectal adenomas in human patients have been shown to initiate the aggressive production of MDSCs in peripheral blood monocytes isolated from untreated, tumor bearing patients. Circulating levels of MDSCs have been shown to increase by 5-10% in patients diagnosed with stage III and IV advanced colorectal cancer (Kimura, McKolanis et al. 2013; Zhang, Wang et al. 2013). In murine models using CT26 colon carcinoma cell lines, $CD11b^{high}/GR\text{-}1^{intermediate}$ MDSCs secrete TGF-β upon stimulation with IL-13 resulting in reduced tumor immune-surveillance by cytotoxic T cells (Fichtner-Feigl, Terabe et al. 2008). They have further been shown to be instrumental in promoting peritoneal metastasis of colorectal cancer (Li, Wu et al. 2013). In another mouse model using MC38 colon cancer cell lines that were subcutaneously implanted onto the flanks

of C57BL/6J, there is a four-fold increase in the CD11b/Ly6G^{+} MDSC population in the spleens as compared to that in the age-matched naïve wild type controls. The same study showed that single cell preparations from tumors excised from these mice consisted of 50% MDSCs (Medina-Echeverz, Fioravanti et al. 2011). In an ectopic model using MC38 in C57BL/6J mice, MDSCs induced high activity levels of pro-tumorigenic pathways such as MAPK, NFkB, CXCL1, and CCL7 (Sinha, Okoro et al. 2008; Ichikawa, Williams et al. 2011).

The number of mast cells has been reported to increase in human patients as colon cancers progress from the adenoma to carcinoma stage. This quantitative value is neither a prognostic factor, nor a predictive index for patient survival. Nevertheless, mast cells are thought to participate in regulatory mechanisms that drive tumor progression (Xia, Ding et al. 2011). Gounaris and colleagues showed that mast cells in human colonic adenomas and adenocarcinomas are critical for epithelial tumorigenesis and tissue remodeling. Rodent mast cells associated with colorectal cancers have been studied more extensively as compare to human patients. Murine mast cells reside either in mucosal or connective tissues. Mucosal mast cells that populate the region around the epithelium of the gastrointestinal tract are of particular interest because these tumor educated mast cells play a variety of roles in the progression of colorectal cancer (Liu, Zhang et al. 2011). They localize to the colonic lesions induced in Crj: CD-1 (ICR) mice treated with colonic carcinogen azoxymethane, a model of inflammation associated colon carcinoma (Tanaka and Ishikawa 2013). Mast cells have also been shown to promote tumor growth by producing elevated levels of TNF-α in the tumor stroma, and by assisting in stromal remodeling and induction of angiogenesis (Colombo and Piconese 2009). Their

importance in intestinal adenoma has been established through many studies, however the roles that they play are highly contradictory and controversial (Sinnamon, Carter et al. 2008; Heijmans, Buller et al. 2012).

Early studies examining the role of T-regs in human colorectal cancer demonstrated that $CD4^+CD25^+$ T-regs in peripheral blood played an important role in heightened immune-suppression by inhibiting autologous HLA-A1 restricted $CD4^+$ cytotoxic T lymphocytes (Mougiakakos, Choudhury et al. 2010). The ratio of memory $CD8^+$ T cells to $FOXP3^+$ T-regs was found to be a predictive marker for patient survival in colorectal cancer cohorts (Correale, Rotundo et al. 2010; Suzuki, Chikazawa et al. 2010). $FOXP3^+$ cells abundantly infiltrate the mesenteric lymph nodes in mouse models of intestinal cancer and have been shown to promote immune tolerance to intestinal bacteria (Erdman and Poutahidis 2010). In the $Apc^{Min/+}$ mouse model of intestinal adenomas, cancer promoting pro-inflammatory T-regs constitute 3-5% of intestinal mononuclear preparations as analyzed by flow cytometry (Serebrennikova, Tsatsanis et al. 2012).

Our results provide a baseline quantitative estimation and specific localization of MDSCs, mast cells, and T-regs in the tumor stroma of adenomatous polyps of $Apc^{Min/+}$ mice and in colon cancer carcinomas in the ectopic model using Balb/cByJ mice. We highlighted the enhanced presence of MDSCs, mast cells, and T-regs in the hematopoietic organs of the tumor bearing mice, and high levels of infiltration into the tumor beds. These data suggest that the BMDCs respond to the presence of tumor cells in rodents by accumulating in hematopoietic organs and by aggressively infiltrating the tumor beds. It is possible that the immune cells respond to cancer cells as foreign agents

and infiltrate the tumor in an attempt to 'heal' the body of this foreign invasion. The baseline measurement of MDSCs, mast and T-regulatory cells within the tumor stromal location that we established in this section will provide the basis for further studies examining the impact of therapeutic agents on these cells.

CHAPTER 3

THE IMPACT AND KINETICS OF THYMIDYLATE SYNTHASE INHIBITORS ON MDSC, MAST, AND T-REGULATORY CELLS

3.1 Introduction

While the impact of TS inhibitors on tumor cells has been widely studied, their effect on the variety of BMDCs infiltrating the intestinal tumor is less well studied. The specific cells types that may be direct targets of TS inhibitors have yet to be enumerated. In this section, we focused our efforts in determining the effect of the TS inhibitor 5-FU on MDSCs, mast cells, and T-regs, and the kinetics of their response to 5-FU. These cells have been shown to interact with each other and to be critical for tumor initiation and progression in $Apc^{Min/+}$ mice (Clarke, Betts et al. 2006; Gounaris, Erdman et al. 2007; Ling, Pratap et al. 2007; Colombo and Piconese 2009; Gounaris, Blatner et al. 2009; Correale, Rotundo et al. 2010). 5-FU is thought to possess immunogenic properties that could affect these cells in the tumor microenvironment. Understanding the impact of 5-FU on these and other cells in the tumor microenvironment will allow us to understand their role in tumor response to 5-FU and could provide the basis for developing therapies that might enhance its anti-tumor efficacy.

Previous studies have shown that by genetically modifying the BMDCs infiltrating the tumor stroma to make them resistant to TS inhibitors, rendered intestinal

tumors to be also resistant to systemic treatment with a combination of the TS inhibitors raltitrexed and 5-FU (Pena et al, unpublished data). The specific BMDCs in the tumor stroma that may dictate tumor response to TS inhibition have not been studied. Identification of these cells is necessary to determine if they can be specifically genetically manipulated to enhance tumor response to TS inhibitors. Moreover, understanding the mechanisms by which 5-FU directly affects these intestinal stromal cells will facilitate our ability to harness them in order to enhance anti-tumor efficacy while lowering drug induced toxicities to the surrounding normal cells.

MDSCs have previously been shown to be sensitive to 5-FU, as well as gemcitabine treatment both *in vitro*, using immortalized MDSC cell lines derived from Balb/c splenocytes, and *in vivo* using an EL4 thymoma mouse model.(Vincent, Mignot et al. 2010). Anti-inflammatory T-regs in human colorectal cancer patients can respond to a combination therapy consisting of 5-FU, oxaliplatin, and leucovorin (FOLFOX) (Gonzalez-Aparicio, Alzuguren et al. 2011). This combination of drugs was shown to reduce tumor burden and to deplete the number of anti-inflammatory T-regs in the spleens of tumor bearing animals (Ghiringhelli, Larmonier et al. 2004). Not much is known about the response of mast cells to 5-FU administration. To date, there have been no studies carried out examining the effect of TS inhibitors on MDSCs, mast cells, and T-regs simultaneously, in the tumor stroma of colorectal cancer. In this chapter, we quantitatively assessed the effect of a single dose of 5-FU on MDSCs, mast cells, and T-regs in the intestinal tumor stroma in Apc^{Min+} mice and in the ectopic model of CT26 mouse colon carcinoma cells subcutaneously implanted onto Balb/cByJ mice. The results showed that MDSCs, and to a lesser extent, T-regs, were selectively sensitive to 5-FU but

mast cells were not responsive. Similar results were obtained in both *Apc*$^{Min/+}$ mice, which had early stage adenomas, and in the ectopic model representing advanced stage carcinoma, suggesting that their response to the therapy was independent of the stage of carcinogenesis. We also examined their response in hematopoietic organs such as spleen and bone marrow in both normal and tumor bearing mice. To assess their role in tumor response to therapy, we determined the effect of 5-FU on MDSCs, mast cells and T-regs in chimeric mice wherein the BMDCs in the stromal compartment were made resistant to TS inhibitors, while tumor cells were sensitive to the therapy. The results showed that in these mice, the MDSCs and T-regs were no longer sensitive to 5-FU, but were in fact resistant to the drug. The data indicate that BMDCs in the tumor microenvironment can be direct targets of 5-FU and that these cells can be genetically manipulated to alter tumor response to therapy.

3.2 Material and Methods

Cells: GP+E86 producer cells were obtained from ATCC (Manassas, VA). The cells were stably transfected with the retroviral vector pMSCV-OptecTS (MOTS) containing the gene for E. coli TS that was optimized for expression in mammalian cells (Shaw, Berger et al. 2001) to generate the producer cell line GP+E86 (MOTS). The cells were cultured in Dulbecco's Modified Eagle Medium (DMEM) supplemented with 10% heat inactivated Fetal Bovine Serum (FBS) (Atlanta Biologicals, Lawrenceville, GA), 2 mmol/L L-glutamine, and 1× penicillin/streptomycin (Mediatech, Manassas, VA) at 37^{o}C and 5% CO_2 in a humidified atmosphere.

Mice: Balb/cByJ and *Apc*$^{Min/+}$ mice were purchased from Jackson Laboratories (Bar Harbor, ME, USA) but were bred and maintained at the Mouse Experimentation Core Facility of the Center for Colon Cancer Research at the University of South Carolina (USC), Columbia, SC. All aspects of the animal experiments have been conducted in accordance with the guidelines and approval of the USC Institutional Animal Care and Use Committee.

Drug administration: A stock solution of 5 mg/ml of 5-FU (Sigma-Aldrich, St. Louis, MO) was dissolved in PBS and filter sterilized using 0.2 micron syringe filters. Two groups of *Apc*$^{Min/+}$ mice (twenty mice per group) were injected intraperitoneally (*i.p*,) with either 5-FU (50 mg/kg) or PBS as a control. In the Balb/cByJ ectopic model, tumor size was monitored after subcutaneous injection. 5-FU or PBS was administered when the tumor diameter reached 9-11 mm. The drug dose of 50 mg/kg is similar to that used in previous studies and shown to have the maximum depleting effect on MDSCs *in vivo*, in the EL4 thymoma model (Vincent, Mignot et al. 2010).

Tissue harvest and analysis: Five *Apc*$^{Min/+}$ mice from each group were humanely sacrificed at 3, 5, 7 and 10 days after drug administration. For the ectopic model, two tumor bearing mice each from the PBS or 5-FU-treated groups were analyzed also at 3, 5, 7, and 10 days post 5-FU administration. Bone marrow, spleen and tumors were isolated from these animals and processed for analyses by flow cytometry, as described before. Figure 3.1 is a schematic diagram of the schedule of drug administration in the 15-week old *Apc*$^{Min/+}$ mice and subsequent harvest and analyses of the tissues at different time points post 5-FU administration.

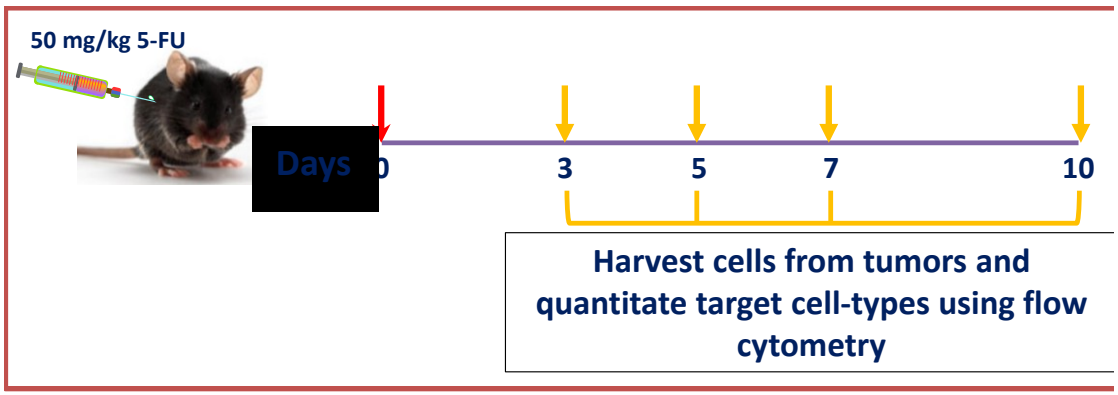

Figure 3.1. Schedule of drug administration and time points for cell analyses. 5-FU was administered *i.p.* in the respective tumor bearing mice. The day of drug injection is designated as Day 0. On days 3, 5, 7, 10 days post 5-FU administration, spleen, bone marrow, and tumors were harvested from the animals, single cell suspensions were prepared, and the target cells quantitated by flow cytometry.

Bone marrow transplantation:

Isolation of bone marrow: Four-week old C57BL/6J donor mice were injected with one dose of 150 mg/kg 5-FU administered *i.p.* to ablate the committed cells from the bone marrow and induce the progenitor cells to initiate the cell cycle. The donor mice were sacrificed after 48 hours and their bone marrow was flushed from the femur and tibia with sterile PBS containing 2% FBS using a 21-gauge needle. The bone marrow was washed twice with 1 ml of sterile PBS to remove traces of FBS and pre-stimulated by culturing for two days in DMEM supplemented with 15% FBS, 20 ng/ml recombinant interleukin 3 (rIL-3, (Thermo Scientific, Rockford, IL), 50 ng/ml recombinant interleukin 6 (rIL-6, Thermo Scientific, Rockford, IL) and 50 ng/ml recombinant rat stem cell factor (rSCF) (Peprotech, Rockhill, NJ) at 37^{o} C and 5% CO_2 in a humidified atmosphere.

Transduction by Co-culture: Sub-confluent GP+E86 (MOTS) producer cells were prepared prior to the start of co-culture by treating each plate with 10 ug/ml *mitomycin C*

(Calbiochem, San Diego, CA) for 90 minutes to stop their division and growth. The cells were washed 4 times in PBS and re-plated in 100-mm tissue culture dishes. The pre-stimulated bone marrow cells prepared above, were harvested by tapping gently on the side of each plate, and by drawing up 5-10 ml cell suspension. The plate is then washed with PBS twice to harvest as many cells as possible. Care was taken to prevent cell lysis. 10 ml of the media containing bone marrow cells was added to each plate of producer cells and polybrene (hexadimethrine bromide, purchased from Sigma-Aldrich, St. Louis, MO) was added to the co-culture media to a final concentration of 6 ug/ml. The bone marrow and producer cells were co-cultured for 48 hours and then harvested for transplantation or plating in methylcellulose semi-solid media.

Harvest and transplant: Age-matched recipient *Apc*$^{Min/+}$ mice were lethally irradiated with 900 Gy administered at 200 Gy/minute using a Varian Clinac Linear Accelerator. The transduced bone marrow cells were harvested by carefully removing the media from the co-culture plates. The media was centrifuged in an Eppendorf 5430R centrifuge for 5 minutes at 2000 rpm at room temperature. The cell pellet was washed twice with PBS to remove traces of FBS. 1 to 3 million bone marrow progenitor cells were injected into the recipient *Apc*$^{Min/+}$ mouse by tail vein injection.

Tissue processing: Tumors, spleen, and bone marrow tissues were processed for analyses by flow cytometry as described in the previous chapter.

3.3 Results

3.3.1 (a) Effect of 5-FU on target cell types in $Apc^{Min/+}$ mice

We analyzed the effect of single dosage of 5-FU on the various cell types and compared them to the tumor stromal cells in control age-matched tumor bearing mice injected with PBS. We administered a single dose of 5-FU or PBS to $Apc^{Min/+}$ mice and determined the effect on the percentages of MDSCs, mast cells, and T-regs in the tumor beds, spleen, and bone marrow at 3, 5, 7, and 10 days post injection. The results in Figure 3.2 shows the fold change in the percentages of the target cell-types post 5-FU administration, as compared to those in mice treated with PBS. All animals were sacrificed and the tissues processed on the same day. As shown in Figure 3.2 the MDSCs in the tumor beds are the most sensitive cells to systemic treatment with 5-FU. They are depleted by almost 50% in the tumor beds of $Apc^{Min/+}$ mice, with maximum depletion on days 3 to 5 after 5-FU administration. The same sensitivity was observed in the spleen (Figure 3.2) and bone marrow, with the bone marrow exhibiting the highest level of depletion on day 5. Gradually though, MDSC levels recovered from the drug treatment and were restored to normal pre-treatment levels in the tumor beds, spleen, and bone marrow by day 10 after 5-FU administration. In contrast, the number of mast cells in the tumor beds increased by almost two-fold at 5 days after drug administration (Figure 3.2). This was accompanied by a corresponding two-fold decrease in the spleen at five days (Figure 3.3). This inverse relationship suggested that mast cells might be mobilized from the spleen to the bone marrow in response to 5-FU treatment. On the hand, the number of mast cells in bone marrow, which is physiologically not a typical localization for mast cells, remains relatively unchanged throughout the course of this study (Figure 3.3). T-regs in the tumor

beds appear to be sensitive to 5-FU and are depleted within three days after treatment, however, they quickly recover to pre-treatment levels within five days (Figure 3.2). There is no significant effect on T-regs in the spleen (Figure 3.3), and in bone marrow (Figure 3.3). It is important to note though that assessing the impact on T-regs is complicated by the fact that there are very low levels of T-regs in all three tissues examined. For example, the percentage of T-regs change from 2.1% in the tumors of PBS treated *Apc*$^{Min/+}$ mice to 1.4% three days post 5-FU treatment. Also as observed in the tumor bed, T-regs recover quickly by the 5th day, showing a very transient response to 5-FU. They do not show a pronounced response to 5-FU in the hematopoietic organs, and seem to display a delayed response to the drug decreasing from the original level by 0.22 folds transiently at around day 7 (Figure 3.3).

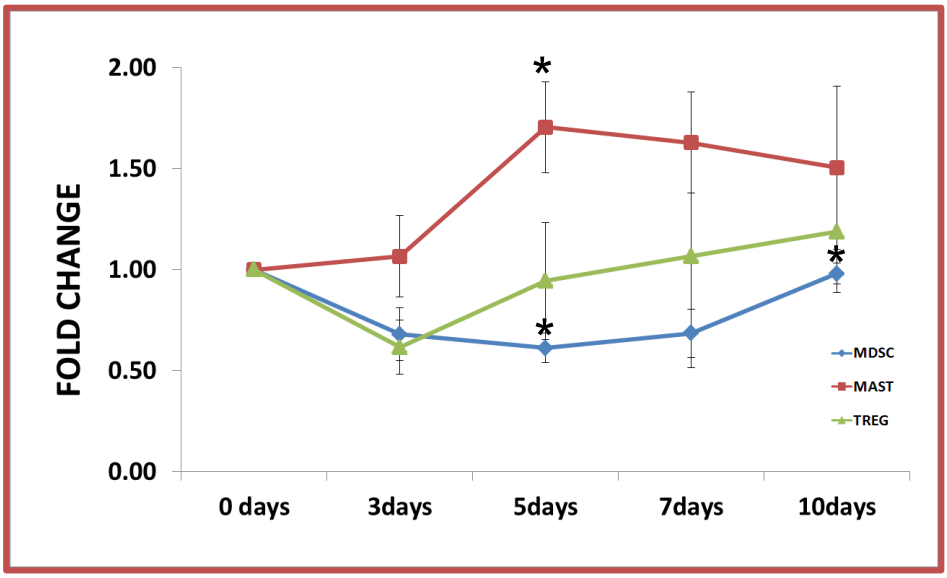

Figure 3.2. Effect of 5-FU on MDSCs, Mast cells, T-regs in tumor beds of *Apc*$^{Min/+}$ mice. 15-week old *Apc*$^{Min/+}$ mice were administered with PBS or 50 mg/kg 5-FU. At 3, 5, 7, and 10 days post drug injection, tumors from 5 mice in each group were excised. Single cell suspensions were prepared and then 1 million cells were stained with antibodies to detect MDSCs (α-CD11b and α-Gr-1), mast cells (α-CD34 and α-CD117), and T-regs (α-CD4 and α-FOXP3). Stained cells were quantitated by flow cytometric analyses.

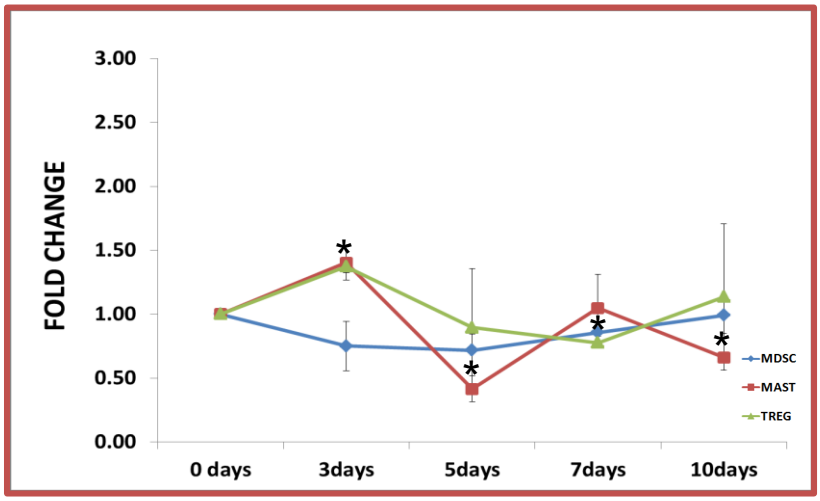

Figure 3.3. Effect of 5-FU on MDSCs, Mast cells, T-regs in the spleens of *Apc*$^{Min/+}$ mice. 15-week old *Apc*$^{Min/+}$ mice were administered with PBS or 50 mg/kg 5-FU. At 3, 5, 7, and 10 days post drug injection, spleens from 5 mice in each group were isolated. Single cell suspensions were prepared and then 1 million cells were stained with antibodies to detect MDSCs (α-CD11b and α-Gr-1), mast cells (α-CD34 and α-CD117), and T-regs (α-CD4 and α-FOXP3). Stained cells were quantitated by flow cytometric analyses.

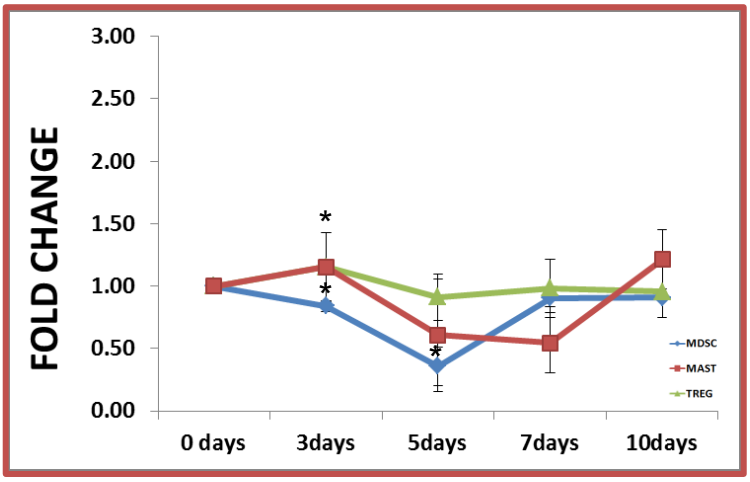

Figure 3.4. Effect of 5-FU on MDSCs, Mast cells, T-regs in the bone marrow of *Apc*$^{Min/+}$ mice. 15-week old *Apc*$^{Min/+}$ mice were administered with PBS or 50 mg/kg 5-FU. At 3, 5, 7, and 10 days post drug injection, bone marrow was flushed from the femur and tibia of 5 mice in each group. Single cell suspensions were prepared and then 1 million cells were stained with antibodies to detect MDSCs (α-CD11b and α-Gr-1), mast cells (α-CD34 and α-CD117), and T-regs (α-CD4 and α-FOXP3).

3.3.1(b) Effect of 5-FU on MDSCs, Mast cells and T-regs in an ectopic mouse model

Our earlier findings suggested that MDSCs, mast cells and T-regs infiltrate the tumor stroma of both adenoma and carcinoma stages of colorectal cancer. In the previous section we determined the effect of 5-FU on these cells in early stage adenomas. In this section, we determined the effect of 5-FU on these cells in a subcutaneous model of colon carcinoma cells, a more advanced stage of the disease. We injected CT26 colon carcinoma cells into the flank of Balb/cByJ mice, allowed the tumors to develop to a diameter of 9-11 mm, and then subjected the mice to 50 mg/kg 5-FU or PBS, harvested tissues, and processed and analyzed as described previously..

The results shown in Figures 3.5, 3.6, and 3.7 indicate that in a model of advanced stage carcinoma, the MDSCs are also selectively sensitive to 5-FU, while mast cells are resistant, and T-regs are moderately affected by the drug. These results further indicate that the kinetics of the effect of 5-FU on MDSCs, mast and T-reg cells are independent of the stage of cancer progression. MDSCs in the Balb/cByJ-CT26 carcinoma model appear to recover quicker from the effects of 5-FU as compared to those in the adenomas in $Apc^{Min/+}$ mice. Instead of the gradual recovery from 5-FU by day 10 post injection seen in $Apc^{Min/+}$ mice, MDSCs in tumor beds of the Balb/cByJ-CT26 ectopic model recover to pre-treatment levels by day 7, with 50% reduction in their numbers only at day 5. This response could be attributed to the higher recruiting ability of the CT26 carcinoma cells allowing MDSCs to be more quickly mobilized to the CT26 tumor stroma to replace the diminished levels after 5-FU administration. Taken together, though, these results show that MDSCs in the stroma of tumors at different stages of colorectal cancer progression, and in hematopoietic organs such as spleen and bone marrow, are similarly depleted in

response to 5-FU therapy, with maximum effects seen on day 5. Similar to *Apc*$^{Min/+}$ mice, mast cells in the Balb/cByJ-CT26-carcinoma model are resistant to 5-FU in the tumor beds and exhibit a two-fold increase in their numbers after 5-FU administration. The depletion of mast cells in the spleen in response to 5-FU is not as pronounced as in the *Apc*$^{Min/+}$ mouse, with the number of splenic mast cells reduced only very slightly by approximately 0.1 fold.

Quantitatively, mast cells were not adversely affected in the spleens or bone marrow of the ectopic colorectal tumor-bearing Balb/cByJ animals. In the bone marrow, we observed an immediate but transient two-fold increase in mast cells on day 5, but the number of mast cells returned to pre-treatment level on day 7. The impact of 5-FU on T-regs was more gradual in the carcinoma model as compared to the adenoma model. Their levels were diminished to less than 50% five days after 5-FU administration, after which they slowly recovered to pre-treatment level by day 10. Understanding the involvement of inflammatory cells at all stages of tumor development will allow us to develop customized therapy schedules that might enhance the antitumor efficacy of TS inhibitors.

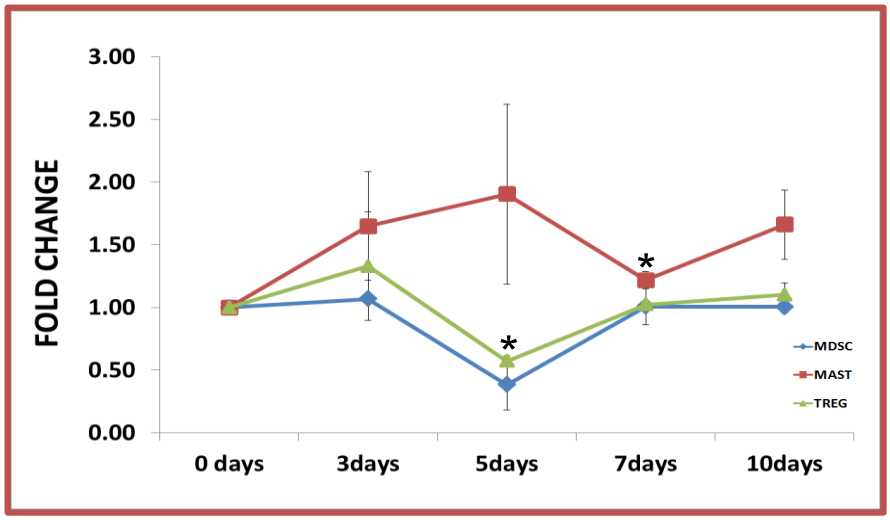

Figure 3.5. Effect of 5-FU on MDSCs, Mast cells, and T-regs in tumor beds of Balb/cByJ mice implanted with CT26 cells. Mice with tumors that were 9-11 mm in diameter were administered with PBS or 50 mg/kg 5-FU. At 3, 5, 7, and 10 days post drug injection; tumors from mice in each group were excised and debulked into single cell suspensions and then stained with antibodies to detect MDSCs (α-CD11b and α-Gr-1), mast cells (α-CD34 and α-CD117), and T-regs (α-CD4 and α-FOXP3). The stained cells were quantitated by flow cytometry.

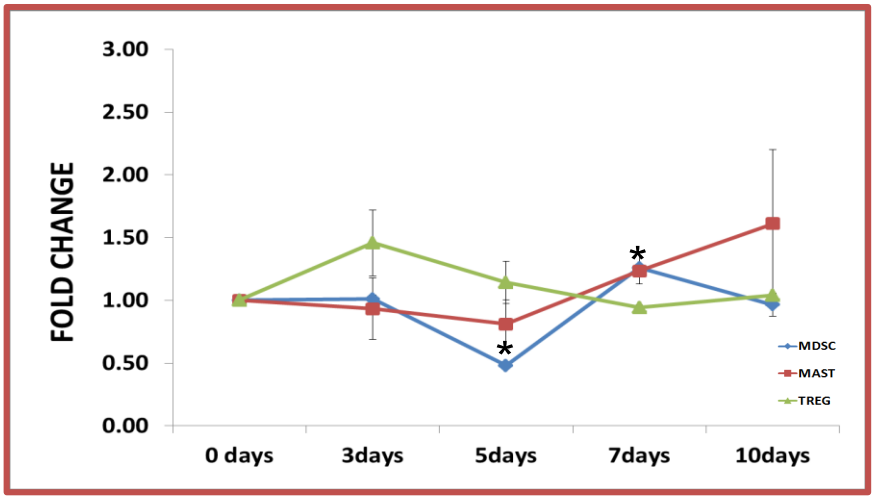

Figure 3.6. Effect of 5-FU on MDSCs, mast cells, and T-regs in spleens of tumor bearing Balb/cByJ mice. Mice bearing tumors with a 9-11 mm diameter were administered with PBS or 50 mg/kg 5-FU. At 3, 5, 7, and 10 days post drug injection; spleens from mice in each group were isolated. Single cell suspensions of splenocytes were stained with antibodies to detect MDSCs (α-CD11b and α-Gr-1), mast cells (α-CD34 and α-CD117), and T-regs (α-CD4 and α-FOXP3). The stained cells were quantitated by flow cytometry.

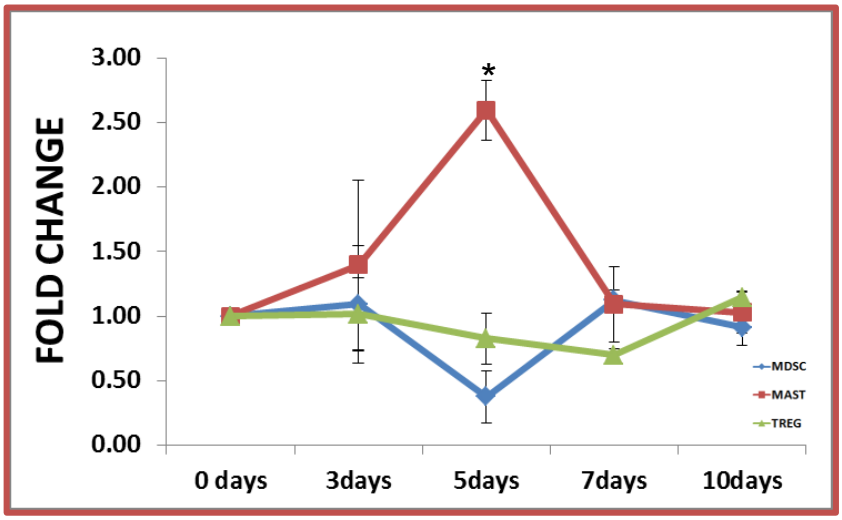

Figure 3.7. Effect of 5-FU on MDSCs, mast cells, and T-regs in the bone marrow of tumor bearing Balb/cByJ mice. Mice bearing tumors with a diameter of 9-11 mm were administered with PBS or 50 mg/kg 5-FU. At 3, 5, 7, and 10 days post drug injection, bone marrow from mice in each group were isolated. Single cell suspension of bone marrow was stained with antibodies to detect MDSCs (α-CD11b and α-Gr-1), mast cells (α-CD34 and α-CD117), T-regs (α-CD4 and α-FOXP3). The stained cells were quantitated by flow cytometry.

3.3.2 Determine the kinetics of response to 5-FU in mice transplanted with ecTS overexpressing chemo-resistant marrow

After quantifying the effect of 5-FU on MDSCs, mast and T-reg cells from tumor bearing *Apc*$^{Min/+}$ and Balb/cByJ mice, we studied the kinetics of the target cells' response to 5-FU administration in *Apc*$^{Min/+}$ mice transplanted with TS over-expressing bone marrow. In earlier studies, we found that in chimeric *Apc*$^{Min/+}$ mice wherein BMDCs in the tumor microenvironment were made resistant to TS inhibitors by transplanting marrow that was overexpressing ecTS while the tumor cells were chemosensitive to the therapy, tumors were also rendered resistant to TS inhibitors. In the current experiment, the goal was to determine the role of the target BMDCs in mediating tumor resistance to 5-FU in the chimeric mice. 4- weeks old *Apc*$^{Min/+}$ mice were lethally irradiated and transplanted with bone marrow overexpressing *E.coli* TS to create chimeric mice whose bone marrow

derived tumor stroma responds differently to chemotherapy as compared to the cancer cells. A schematic diagram of the procedure for creating the chimeric mice is shown in the in Figure 1.6. After complete engraftment of the transplanted marrow, the mice were treated with 50 mg/kg 5-FU followed by analyses of the target cell populations as described in previous sections. As controls, *Apc*$^{Min/+}$ mice transplanted with non-transduced, chemo-sensitive marrow and non-transplanted *Apc*$^{Min/+}$ mice were also analyzed.

The results showed that MDSCs in the tumor beds of mice transplanted with drug resistant bone marrow expressing the *E .coli.* TS increased by approximately 1.8 fold after 5-FU administration in contrast to the MDSCs in mice transplanted with chemo-sensitive non-transduced marrow and in non-transplanted mice wherein the MDSCs in the tumor beds were depleted (Figure 3.8). Ten days post 5-FU administration, the MDSC population in the tumor beds of chimeric mice remained at least 1.5 fold higher than those in the control mice, indicating that they retained their resistance to TS inhibitors throughout the course of the treatment. Interestingly, MDSCs in the spleen and bone marrow in the transplanted mice, retained their sensitivity to 5-FU and were depleted by approximately 50% in both organs, as shown in Figures 3.9 and 3.10. It is however noteworthy that the bone marrow in the mice transplanted with chemoresistant bone marrow recovered quicker as compared to the chemo-sensitive controls, supporting the notion that transplanting mice with chemoresistant bone marrow might provide them with some level of myeloprotection against 5-FU induced toxicity.

The results in Figure 3.8 show that mast cells in the tumor beds of the chimeric mice remained resistant to 5-FU, showing an increase of 1.5 to 2-fold in drug treated

mice as compared to the that was similar to that in mice transplanted with chemoresistant marrow or non-transplanted mice. However, in contrast to the results seen in the un-transplanted mice or transplanted mice with chemosensitive stroma, mast cells in the spleens of mice transplanted with chemoresistant marrow were 1.8-fold higher on day 5 post 5-FU administration (Figure 3.9) rather than being depleted. Mast cells in the bone marrow show a certain threshold level of resistance to 5-FU throughout the course of study. Till day 7 of the treatment all three groups of 5-FU treated mice show an upsurge of mast cell numbers ranging from 1.5 fold in chemo-sensitive mice to 2.5 fold in the mice transplanted with drug resistant bone marrow expressing the *E .coli.* TS. By day 10 after 5-FU administration though, the quantity of mast cells gets lowered to nearly the same numbers as the PBS control groups. This trend is seen in all the three groups of mice, namely, untransplanted, chemo-sensitive, and resistant marrow carrying $Apc^{Min/+}$ mice.

The results in Figure 3.8 further indicate that, T-regulatory cells in the chimeric mice were resistant to 5-FU in tumor beds, with a 1.7 fold higher levels on day 3, as compared to the tumor beds in un-transplanted mice or mice transplanted with chemo-sensitive bone marrow. Similar to the MDSCs, T-regs in the tumor beds of chimeric mice were also resistant to 5-FU throughout the course of the study. They showed little or no effect in response to 5-FU in the spleen, suggesting that the chemo-resistant bone marrow might skew the BMDC response to 5-FU in the hematopoietic organs. Since bone marrow is not the normal residence of differentiated cells such as mast cells and T-regs, it was not an ideal organ for determining the effect of TS inhibitors in these cells. In addition, mast cells and T-regs in the bone marrow behave differently from those in the

tumor beds, since these cells play different roles in the normal stroma of non-cancerous organs.

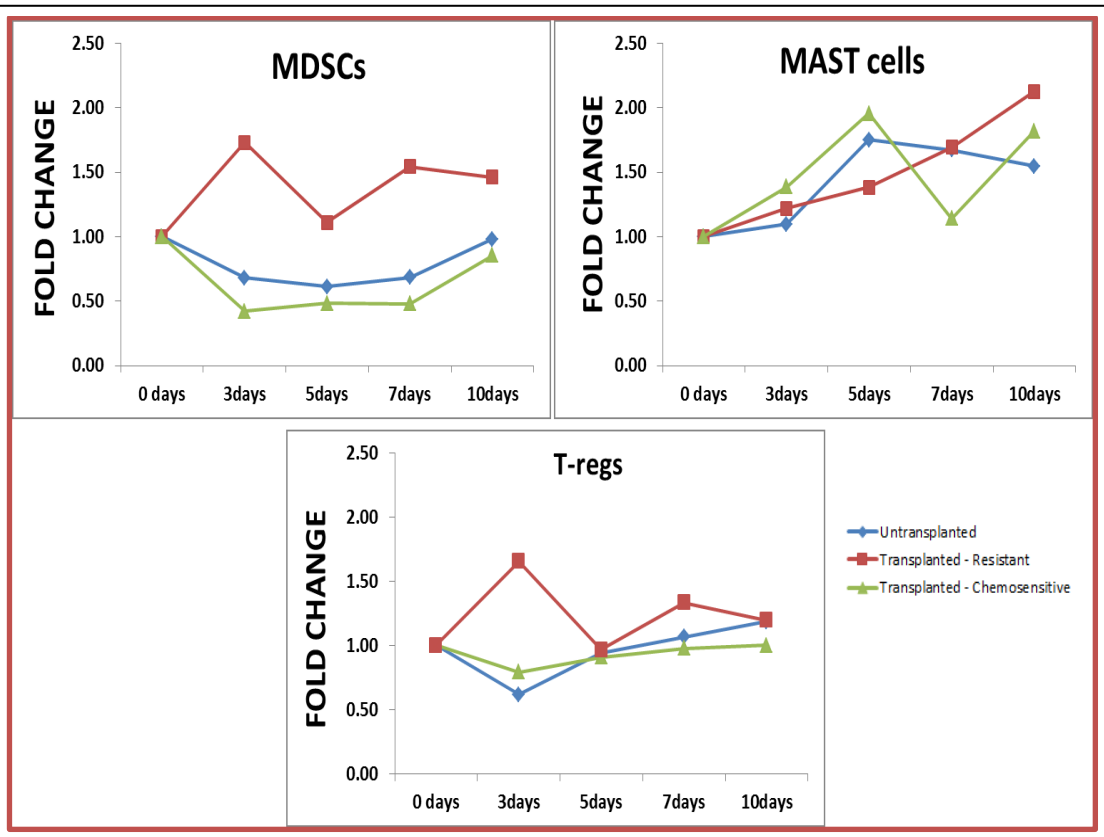

Figure 3.8. Comparison of the effect of 5-FU on MDSCs, Mast cells, and T-regs in the tumor beds of *Apc*$^{Min/+}$ mice that were non-transplanted or transplanted with non-transduced chemosensitive or ecTS-transduced chemoresistant bone marrow. 15-weeks old *Apc*$^{Min/+}$ mice from the different groups were administered with 50 mg/kg 5-FU. At 3, 5, 7, and 10 days post drug injection; tumors from 5 mice in each group were excised. Single cell suspensions were prepared from the tumors and stained with antibodies to detect MDSCs (α-CD11b and α-Gr-1), mast cells (α-CD34 and α-CD117), T-regs (α-CD4 and α-FOXP3) and the stained cells were quantitated by flow cytometry.

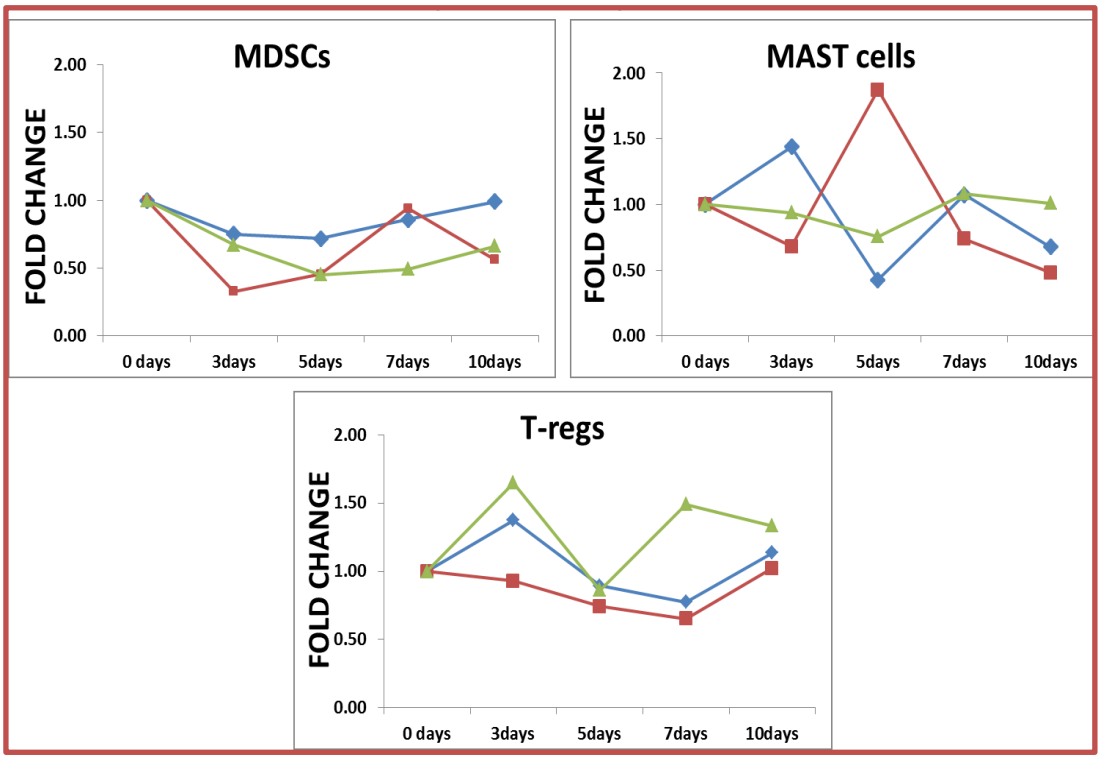

Figure 3.9. Comparison of the effect of 5-FU on MDSCs, Mast cells, and T-regs in the spleens of *Apc*$^{Min/+}$ mice that were non-transplanted or transplanted with non-transduced chemosensitive or ecTS-transduced chemoresistant bone marrow. 15-weeks old *Apc*$^{Min/+}$ mice from the different groups were administered with 50 mg/kg 5-FU. At 3, 5, 7, and 10 days post drug injection, spleens from 5 mice in each group were isolated. Single cell suspensions were prepared from the spleens and stained with antibodies to detect MDSCs (α-CD11b and α-Gr-1), mast cells (α-CD34 and α-CD117), T-regs (α-CD4 and α-FOXP3) and the stained cells were quantitated by flow cytometry.

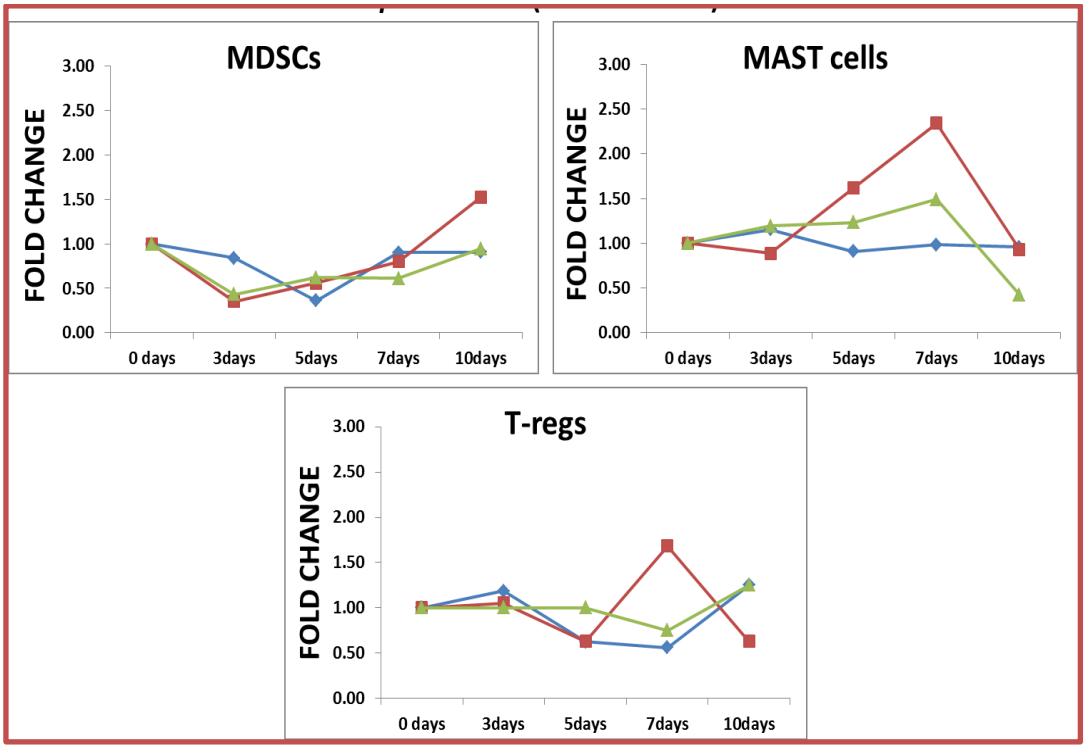

Figure 3.10. Comparison of the effect of 5-FU on MDSCs, Mast cells, and T-regs in the bone marrow of *Apc*$^{Min/+}$ mice that were non-transplanted or transplanted with non-transduced chemosensitive or ecTS-transduced chemoresistant bone marrow. 15-weeks old *Apc*$^{Min/+}$ mice from the different groups were administered with 50 mg/kg 5-FU. At 3, 5, 7, and 10 days post drug injection, bone marrow from the femur and tibia of 5 mice in each group was isolated. Single cell suspension was prepared from the bone marrow and stained with antibodies to detect MDSCs (α-CD11b and α-Gr-1), mast cells (α-CD34 and α-CD117), T-regs (α-CD4 and α-FOXP3) and the stained cells were quantitated by flow cytometry.

3.4 Discussion

The recognition of the direct impact of 5-fluorouracil on the tumor stromal compartment of colorectal cancer *in vivo* is crucial to identifying BMDCs that could influence or determine tumor response to therapy using TS inhibitors. A number of studies have been done to elucidate the effect of 5-FU on the tumor stromal cells in a variety of cancers. For example, 5-FU was found to activate the cleavage of caspase-3 and BH3 interacting-domain death agonist expression in $CD8^+$ T cells *in vitro* (Cheng, Liu et al. 2004) and has

been shown to deplete neutrophils in the peripheral blood of primates (Gillio, Gasparetto et al. 1990). Its effect on MDSCs, mast cells, and T-regs, bone marrow derived cells in the tumor stroma that have been shown to play a role in the development of colorectal cancer, has not been studied simultaneously . Our study simultaneously examined the impact of 5-FU on these cells and the kinetics of their response in the tumor bed and in the hematopoietic organs like bone marrow and spleen. It was important to study the effect of 5-FU on the cells in the environment of the hematopoietic organs and in the tumor beds in order to assess if the effect of drug was systemic or targeted only in the tumor stroma due to changes in the genetic signature and behavior of the BMDCs in the tumor beds in response to signals initiating from the tumor cells. Moreover, examining the impact of a single dose of 5-FU over time allowed us to evaluate the response of the target cell-types after the system recovers from the impact of drug and potentially assess the role they play in tumor recurrence post therapy.

The results from our studies show for the first time, that MDSCs but not mast cells are sensitive to 5-FU in the intestinal tumors. This response was the same irrespective of the location of MDSCs, tumor, spleen or bone marrow, in tumor bearing mice. T-regs on the other hand are present in very low numbers in the tumor beds, that the effect of 5-FU on them was not very pronounced. It had previously been shown that MDSCs undergo caspase-3 and -7 mediated apoptosis within 5 days after treatment with 5-FU *in vitro* (Vincent, Mignot et al. 2010). However, it was not known whether this effect was sustained even after the removal of the therapy *in vivo* or if this response was only transient. The data we obtained from un-transplanted $Apc^{Min/+}$ mice and the Balb/cByJ mice that were subcutaneously implanted with CT26 cells showed that the

depletion of MDSCs in the tumor beds was a transient effect which peaked at 5 days post-treatment. Upon removal of 5-FU, MDSCs gradually re-populate the tumor stroma and return to pre-treatment levels. Similar effects were observed in the hematopoietic organs. On the other hand, mast cells were unaffected by 5-FU treatment and appear to be recruited to the tumor beds from the spleen.

When transplanted with BMDCs that have been genetically modulated to overexpress *E.coli.* TS gene, that had previously been shown to confer resistance to TS inhibitors, the MDSCs in tumor stroma were rendered resistant to 5-FU at all time-points examines post drug administration. This data shows that, tumor infiltrating MDSCs can be manipulated *ex vivo* such that they exhibit resistance to TS inhibition. More importantly, this showed that 1) MDSCs might play a role in mediating tumor response to 5-FU, and 2) manipulating the sensitivity of the cells in the tumor microenvironment can alter tumor response to the therapy. This raises the possibility that increasing the chemosensitivity of these cells might also increase the sensitivity of tumors to the therapy and in this case enhance the anti-tumor efficacy of 5-FU therapy. We further found that MDSCs in the hematopoietic organs were not as resistant to 5-FU as compared to the MDSCs in tumor beds. It is known that colorectal tumors have a much higher level of TS as compared to the normal regions. A plausible explanation could be that the difference in the sensitivity of the MDSCs is due to the fact that MDSCs in tumor stroma may have co-evolved with the cancer cells and their presence in a chronically inflamed environment in tumor associated stroma confers enhanced resistance as compared to MDSCs in non-tumor stroma.

5-FU has been shown to inhibit mastopoiesis *in vitro* at a concentration of 1 ug/ml

administered continuously for 14 days and *in vivo* when administered at 150 mg/kg at 2 days after drug injection (Ophir, Berenshtein et al. 1993). This inhibition of mastopoiesis was transient and followed by a gradual recovery of the cells after 5-FU treatment. This data suggested that mast cells can be targeted by 5-FU. Our data indicates that this effect does not happen at the lower dose that was used in our experiments. However, although the higher concentration of the drug was effective, its potential anti-tumor effects are abrogated by its toxic effect by depleting the committed progenitor cells *in vivo*. Such a dose will be sub-lethal causing extensive hematopoietic damage as a side effect. It is also possible that, upon 5-FU treatment, mast cells might be recruited from the hematopoietic organs or might be differentiating from their progenitor stage and migrating to the tumor bed to help protect the tumors or to recover from drug induced toxicity (Okayama and Kawakami 2006). Additional experiments need to be performed to verify this possibility. It is also possible that *in vivo,* a much higher concentration of 5-FU is needed to target mast cells as compared to MDSCs. In our studies, we only used one dose of 5-FU, 50 mg/kg to minimize its toxic side-effects. It might be worthwhile to perform these studies at higher concentrations of 5-FU to test this possibility. The ultimate goal of these studies, however, are to develop strategies to enhance the toxicity of 5-FU to tumor cells without having to increase the dosage in order to minimize drug induced toxicities. We are therefore pursuing strategies using combinations of 5-FU with drugs that inhibit mast cell activity to determine of this is a viable combination that might enhance the anti-tumor efficacy of 5-FU (Tisdale and Pena, unpublished data.). In summary, the data suggests that the target cell types examined, – MDSCs, mast and T-regs cells may all contribute in different ways to the refractile response to 5-FU in animals transplanted

with genetically engineered HSCs expressing a drug resistant ecTS gene (Pena *et.al.,* unpublished data). These data will be useful in designing strategies that either target BMDCs or genetically modify MDSCs to enhance tumor response to therapeutic agents.

CHAPTER 4

MECHANISMS UNDERLYING THE IMPACT OF 5-FLUOROURACIL ON MDSCS, MAST CELLS, AND T-REGULATORY CELLS

4.1 Introduction

Inhibition of apoptosis and the aberrant proliferation of colonic epithelium, which is typical in the tumor microenvironment, aid the serration or unmanageable growth of the crypt epithelium and facilitate the transition from hyperplastic to dysplastic environment. The tumor stromal cells residing within the micro-environment co-evolve with the cancer cells and over time, they behave in response to molecular signals from the cancer cells to promote tumor progression. Because of this, we propose that an effective anti-neoplastic drug should be able to induce apoptosis not only in aggressively proliferating cancer cells but in the associated tumor stromal cells as well. In order to determine if a BMDC in the tumor stroma has the potential to enhance the efficacy of TS inhibitors, it is essential to know its response, i.e., undergo apoptosis, to 5-FU is administration.

The results in the previous section showed that 5 days after 5-FU administration, there is a rapid depletion of MDSCs while mast cells were resistant to the effects of 5-FU. In this section, we examined the mechanisms underlying the differential response of the three cell types to 5-FU. First, we determined if the cells undergo apoptosis, in response to treatment with 5-FU. Since TS inhibitors are targeted against actively

proliferating cells, we then measured the proliferative indices of the cells to determine if this was the underlying reason for the vulnerability of MDSCs to 5-FU.

Irreparable DNA strand breaks usually results in apoptosis mediated by a cascade of cleaved caspases. In animal models of colorectal cancer, apoptosis of tumor cells in response to anti-neoplastic drugs is largely mediated by caspase-3 and caspase-7 dependent pathways. Previous studies have shown that 5-FU can induce the cleavage of caspase 3 and caspase 7 (Stevenson, Allen et al. 2011; Kim, Kim et al. 2013). Poly (ADP-ribose) polymerase 1 (PARP-1) is a target of caspase cleavage which leads its inactivation, a hallmark of late apoptosis. In the case of colorectal cancers, cleavage of caspase 3 and 7 is the main mediator of PARP1 cleavage at aspartic acid 214 and glycine 215 which generates two PARP-1 fragments of 24 kDA and 89 kDA each. This renders PARP-1 inactive and engages the cell on a path towards programmed cell death.

The apoptotic effect of 5-FU is usually amplified in aggressively proliferating cells. One marker for active proliferation is the nuclear protein Ki-67. During interphase, the Ki-67 antigen is detected in the nucleus, but during mitosis, most of the protein is transported to the chromosomal surface. The Ki-67 protein is functional during all active phases of the cell cycle, but is absent from the resting cells (in G_0 phase). Thus, Ki-67 is a nuclear protein that is strictly associated with active cellular proliferation and is not expressed during G_0 phase, making it a useful marker to identify actively proliferating cells. Antibodies to Ki-67 have been successfully used in a variety of cancers to identify aggressively proliferating cells. This marker has also been used as a labeling index to identify the clinical course or staging of the disease. All aggressively proliferating cells inevitably express Ki-67 protein in their nuclear and chromosomal surfaces.

MDSCs are immature, undifferentiated cells that are broadly classified into monocytes and granulocytes. We examined the apoptotic status of both cell-types that compose the MDSC population. We then performed similar analyses on mast cells which were resistant to 5-FU. The results indicated that MDSCs but not mast cells undergo apoptosis in response to 5-FU. Analyses of their proliferative indices indicated that MDSCs are more highly proliferative as compared to the mast cells, thereby underscoring their enhanced vulnerability to 5-FU. Elucidating the impact and vulnerability of the various BMDCs that make up the tumor microenvironment will allow us to understand their role in tumor response to therapy and their role in promoting tumor cell death or recurrence post therapy. We could then exploit these interactions to tilt the balance toward tumor killing and regression by simultaneously targeting tumor cells and stromal cells in the tumor microenvironment.

4.2 Materials and Methods

Mice: Balb/cByJ mice, C57BL/6J-ApcMin/J mice (*Apc*$^{Min/+}$) and C57BL/6J mice were purchased from Jackson Laboratories (Bar Harbor, ME, USA) but were bred and maintained at the Mouse Core Facility of the Center for Colon Cancer Research at the University of South Carolina (USC), Columbia, SC. All aspects of the animal experiments have been conducted in accordance with the guidelines and approval of the USC Institutional Animal Care and Use Committee.

Drug Administration and harvest: Three *Apc*$^{Min/+}$ mice aged 15-weeks were administered with PBS and three *Apc*$^{Min/+}$ mice with 50 mg/kg 5-FU. Animals were humanely sacrificed 5 days after PBS or 5-FU administration. Their intestines were isolated,

divided into four sections, flushed with PBS to remove fecal material, and cut open longitudinally. The tissues were fixed overnight in 4% paraformaldehyde. The fixed intestines were "swiss-rolled", embedded in paraffin cassettes, and left to dry overnight. 3-5 micron thick sections were cut from the swiss-rolled intestines and mounted on poly-L-lysine coated microscopy slides.

Immunofluorescence: The sections were deparaffinized, rehydrated, and then incubated in a microwave oven at 95^{o}C with 0.01 M citrate buffer, pH 6.0 (Diagnostic Biosystem, Pleasanton, CA) for 10 minutes for antigen retrieval. Sections were blocked with 5% goat serum (Invitrogen, Frederick, MD) and 5% Normal Donkey serum (Jackson Laboratory, Bar Harbor, ME) diluted in 1% BSA in PBS for one hour. To identify apoptotic cells, the samples were incubated overnight with a mixture of primary antibodies against cleaved PARP-1 (Rabbit polyclonal, 1:200 dilution, Santa Cruz Biotechnology, Santa Cruz, CA USA) and a cell-type specific cell surface marker such as CD11b for monocytes, Gr-1 for granulocytes, or MCT1 for mast cells (all the antibodies are rat monoclonal used at 1:200 dilution, all from Abcam, Cambridge, MA) in 1% BSA in PBS. To assess the proliferative indices of the various cell types, the samples were incubated overnight with a mixture of primary antibodies against Ki-67 (Rabbit polyclonal, 1:800 dilution, Abcam, Cambridge, MA) and a cell-type specific surface marker, such as CD11b for monocytes, Gr-1 for granulocytes, or MCT1 for mast cells (all antibodies are rat monoclonal antibodies used at 1:200 dilutions) in 1% BSA in PBS. The next day, the samples were washed with 1% BSA in PBS and then incubated with a mixture of goat anti rat secondary antibody conjugated to Cy-3 (1:200 dilution, Invitrogen, Frederick, MD) and donkey anti-rabbit secondary antibody conjugated to Cy-5 (1:100 dilution, Jackson

Laboratory, Bar Harbor, ME) for 1 hour at 37^{o}C. The sections were again washed with 1% BSA/PBS for 30 minutes at room temperature and then stained with DAPI for nucleus. Stained sections were cover-slipped using ProLong Gold anti-fade reagent (Invitrogen, Frederick, MD).

Imaging and Quantitation: The slides containing sections stained with the various combinations of primary antibodies, i.e., against CD11b and cPARP-1, Gr-1 and cPARP-1, MCT1 and cPARP-1, CD11b and Ki-67, Gr-1 and Ki-67, and MCT1 and Ki-67 were imaged using Zeiss LSM Meta 510 confocal microscope. For each antibody combination, 3 sections obtained from 3 different mice were stained and a minimum of approximately 100 field view images were captured at 40 X magnification from the different slides. For each field view image, we manually counted the number of cells that stained positively for the specific cell type examined and then counted the number of cells that also stained positively for cleaved PARP to determine the number of apoptotic cells, or for Ki-67 to determine the number of proliferating cells. Apoptotic or proliferative indices were calculated as the percentage of cells that stained for both the cell surface marker and cleaved PARP or Ki-67 against the total number of cells that stained positively for the specific cell surface marker.

Statistical Analysis: Statistical analysis was performed on the two separate groups of mice either treated with PBS or 5-FU, to compare the proportion or percentage of cells expressing both cell-specific surface marker, as well as either apoptosis marker cleaved PARP-1 or proliferation marker Ki-67. The mice used in the study were randomly selected from a population of mice, the tumors observed were a sample from a population of tumors within one mouse and the field view observed is a sample from a population of

field views within one tumor. The tumors were nested within the mice and were not identical to each other. Also, the numbers of tumors in each mouse were varied. The field views were nested within the tumors of the mice and the number of regions of field views per tumor was not identical. The PBS vs 5-FU treatment groups were constant throughout the study, while random effects were considered to be those associated with mice, tumors and field views, with the additional restriction that there was nesting aspect to these random effects.

Statistical analysis for this section was done using glmer function in the lme4 package of the widely used statistical software R. PBS and 5-FU treated mice were considered as the two separate groups analyzed by a generalized linear model with a binomial distribution and logit link function. The result was represented by the box and whisker histogram with the median values flanked by upper and lower 25% quartile with whiskers showing the maximum and minimum data points.

4.3 Results

4.3.1 Apoptotic response of the target cell-types to 5-fluorouracil

We used double immunofluorescence staining of intestinal tumor sections, to determine if the 5-FU mediated depletion of MDSCs is due to apoptosis. Typically, MDSCs are identified by a combination of antibodies against CD11-b and Gr-1, however, we were unable to successfully stain with both antibodies in combination with a marker for apoptosis. Thus, in order to gauge the effect of 5-FU on these cells, we separately stained with a combination of antibodies against CD11b and cPARP-1 or with a combination of antibodies against Gr-1 and cPARP-1. The apoptotic index was expressed as the

percentage of cells that stained for both markers against the total number of cells that stained positively for the cell specific surface marker. The representative slide in Figure 4.1 shows a drastic increase in the apoptotic index of monocytes at 5 days after 5-FU administration, as compared to the PBS-treated mice. From a total of 198 field views, we calculated that in PBS-treated mice, 20.25% of the CD11b-positive cells also stained positively for cPARP-1, indicating a baseline level of apoptosis in these cells (Table 4.1). In contrast, upon treatment with 5-FU, 62.2% of the CD11b-positive cells also stained positive for cPARP-1, a 42% increase over the basal level. Statistical analysis of the data collected from the absolute numbers shown in Figure 4.2 indicated a significant increase in the number of apoptotic cells upon treatment with 5-FU.

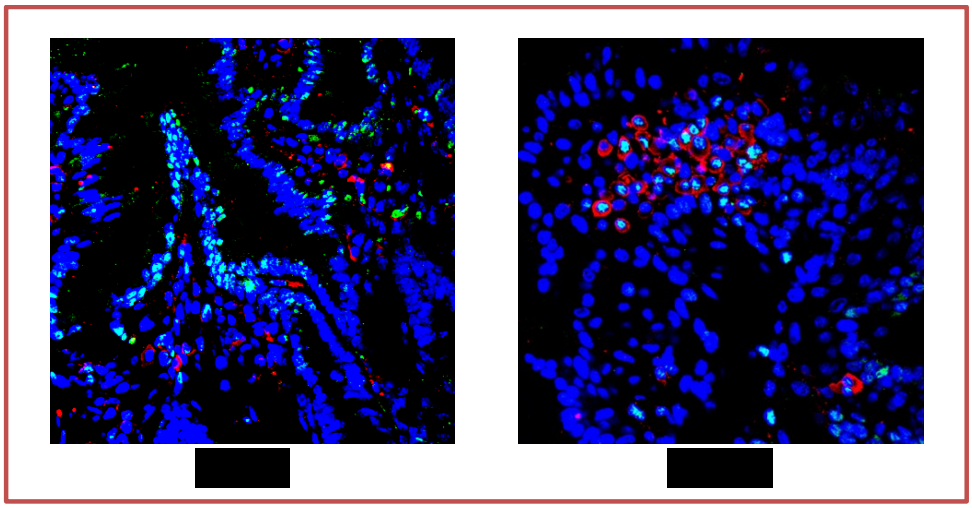

Figure 4.1. Apoptosis induced in monocytes at 5 days after 5-FU administration. Intestinal tissues from *Apc*$^{Min/+}$ mice were fixed in 4% paraformaldehyde overnight and embedded into paraffin cassettes. 3-5 micron sections were cut and double stained with rat monoclonal primary antibody against CD11b (a marker for monocytes) and rabbit polyclonal primary antibody against c-PARP-1 (a marker for apoptosis). The samples were then incubated with Cy-3-conjugated goat anti-rat secondary antibody and Cy5-conjugated donkey anti-rabbit secondary antibody, respectively. 198 total images were taken from the PBS and 5-FU samples together. Representative field views of confocal images of intestinal sections from PBS or 5-FU treated mice are shown. Red = CD11b positive cells (monocytes), Green = cleaved PARP-1 (apoptotic cells). Double positive cells indicate apoptotic monocytes.

Table 4.1. Apoptosis induced in monocytes 5 days after 5-FU administration.

	CD11b+ Cells #	CD11b+ c-PARP+ Cells #	% of apoptotic CD11b Cells
PBS	1817	368	20.25
5-FU	1522	947	62.22

Total numbers of monocytes (CD11b-positive red cells) and the total number of apoptotic monocytes (CD11b-positive, red and c-PARP-positive, green cells) were counted from n=100 field views each for PBS and 5-FU treated mice (n=3 mice per treatment group). The percentage of apoptotic CD11b+ cells in each group was calculated by dividing total apoptotic monocyte cells by total number of monocytes in all the field views. The table shows the total numbers of cells and the percentages of apoptotic monocytes in PBS vs 5-FU treated *Apc*$^{Min/+}$ mice.

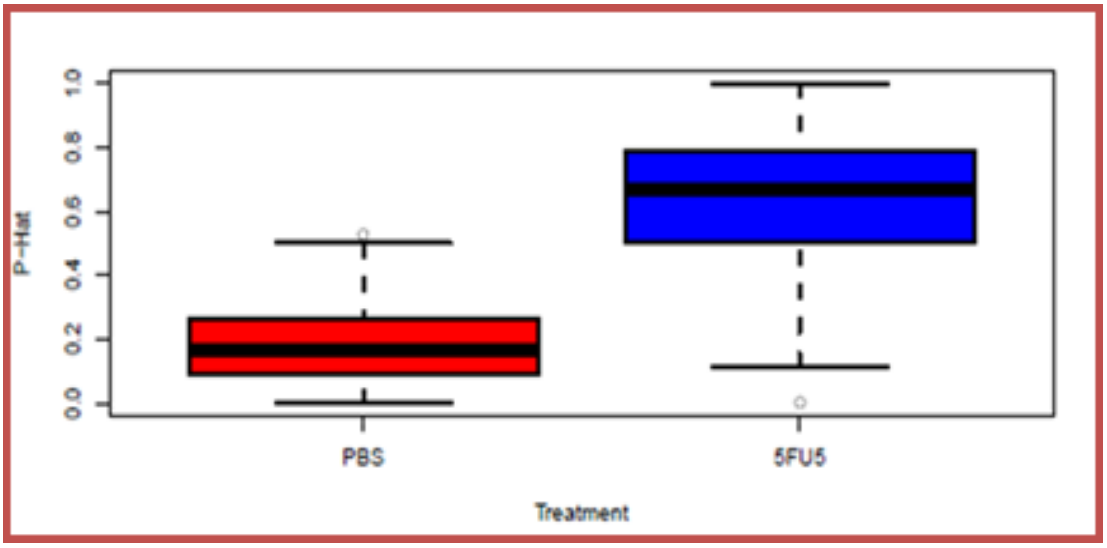

Figure 4.2. Box plots of the number of apoptotic monocytes in PBS versus 5-FU treated mice at 5 days post treatment. This figure is a graphical presentation of the statistical analyses of the number of cells undergoing apoptosis in response to 5-FU. P-Hat is the estimated proportion for the particular combination of Treatment, Mouse, Tumor, and field view, and is obtained by dividing the number of apoptotic monocyte cells by the total number of monocyte cells examined.

We performed a similar analysis of granulocytic cells. The results in Figure 4.3 shows representative field views of double immunofluorescent staining for granulocytes and the apoptosis marker, cleaved PARP-1. As expected, the granulocytes behaved similarly to monocytes, demonstrating a dramatic increase in the apoptotic index in response to 5-FU administration as compared to PBS-treated cells. The granulocytes showed a baseline apoptotic level of 16% in PBS treated *Apc*$^{Min/+}$ mouse intestinal tumor stroma which increased to 67% in 5-FU-treated mice, representing an approximately 4-fold increase as shown in Table 4.2. This statistically significant difference in apoptotic indices is further shown in Figure 4.4 by a box plot of number of apoptotic cells counted from the 200 field views of the images taken from the treatment groups.

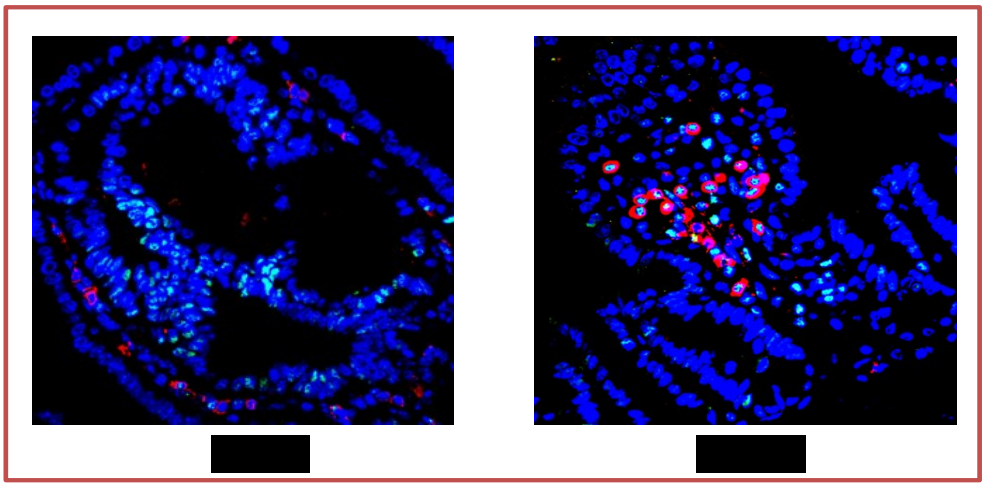

Figure 4.3. Apoptosis induced in granulocytes at 5 days after 5-FU administration. Intestinal tissues from *Apc*$^{Min/+}$ mice were fixed in 4% paraformaldehyde overnight and embedded into paraffin cassettes. 3-5 micron sections were cut and double stained with rat monoclonal primary antibody against Gr-1 (a marker for granulocytes) and rabbit polyclonal primary antibody against c-PARP-1 (a marker for apoptosis). The samples were then incubated with Cy-3-conjugated goat anti-rat secondary antibody and Cy5-conjugated donkey anti-rabbit secondary antibody, respectively. 200 total images were taken from the PBS and 5-FU samples together. Representative field views of confocal images of intestinal sections from PBS or 5-FU treated mice are shown. Red = Gr-1 positive cells (granulocytes), Green = cleaved PARP-1 (apoptotic cells). Double positive cells indicate apoptotic granulocytes.

Table 4.2. Apoptosis induced in granulocytes 5 days after 5-FU administration.

	GR1+ Cells #	GR1+ c-PARP+ Cells #	% of apoptotic GR1 Cells
PBS	1439	238	16.54
5-FU	1350	905	67.04

Total numbers of granulocytes (Gr-1-positive red cells) and the total number of apoptotic granulocytes (Gr-1-positive, red and c-PARP-positive, green cells) were counted from n=100 field views each for PBS and 5-FU treated mice (n=3 mice per treatment group). The percentage of apoptotic Gr-1+ cells in each group was calculated by dividing total apoptotic granulocyte cells by total number of granulocytes in all the field views. The table shows the total numbers of cells and the percentages of apoptotic granulocytes in PBS vs 5-FU treated *Apc*$^{Min/+}$ mice.

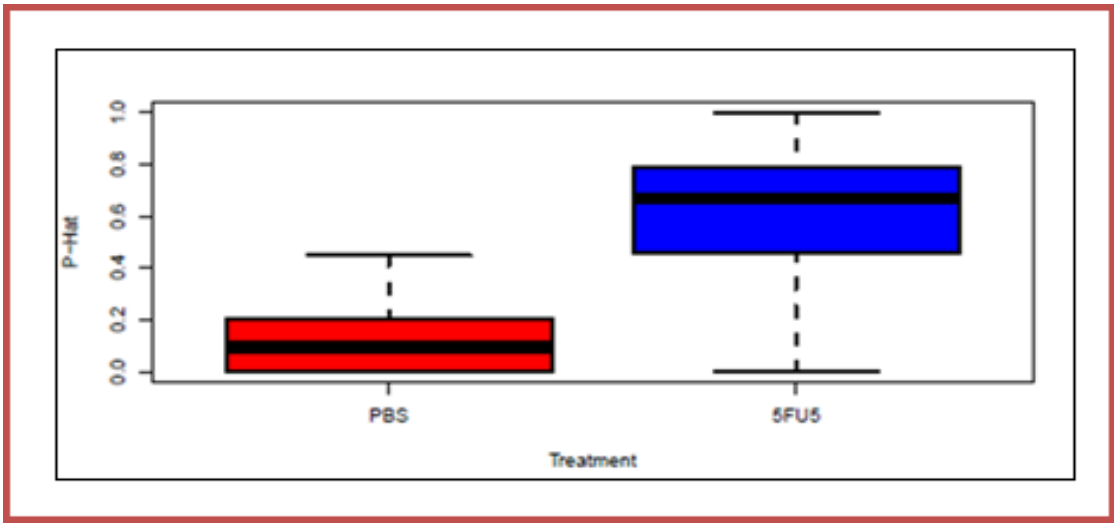

Figure 4.4. Box plots of the number of apoptotic granulocytes in PBS versus 5-FU treated mice at 5 days post treatment. This figure is a graphical presentation of the statistical analyses of the number of granulocyte cells undergoing apoptosis in response to 5-FU. P-Hat is the estimated proportion for the particular combination of Treatment, Mouse, Tumor, and field view, and is obtained by dividing the number of apoptotic granulocyte cells by the total number of granulocyte cells examined.

In contrast to the results obtained with MDSCs, similar analyses of mast cells in the intestinal tumor sections, showed an insignificant increase in apoptotic response to 5-FU administration from a baseline value of 17% in PBS-treated mice to 19% in 5-FU treated mice. Representative immunofluorescence confocal images in Figure 4.5 showed very low numbers of MCT1 positive mast cells with positive staining for cleaved PARP. The total number cells that were positive for MCT1 and/or cleaved PARP-1 staining field views are shown in Table 4.3. The numbers indicate only a 2% increase in the apoptotic index between the PBS and 5-FU treated mice. Finally, Figure 4.6 shows the box plots of a total of 93 field views from both the groups together, indicating no significant difference in the apoptotic indices between PBS and 5-FU treated mice.

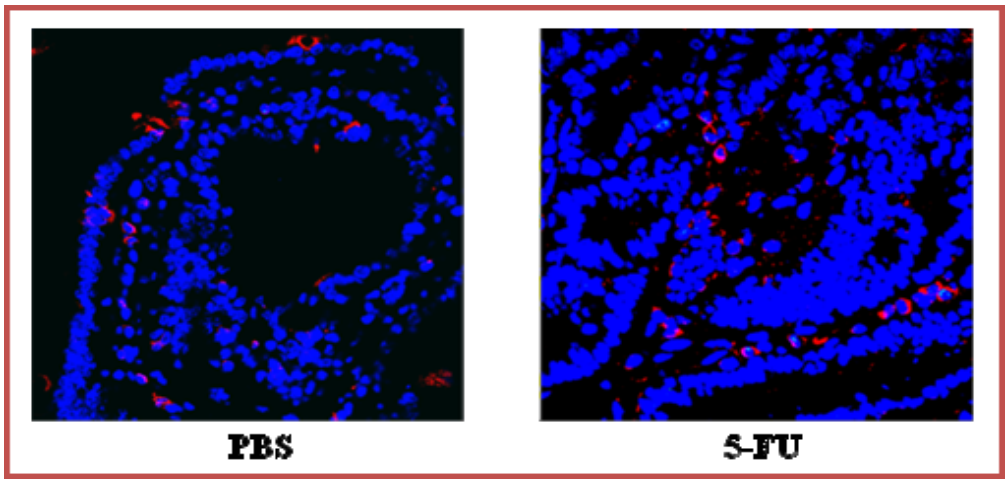

Figure 4.5. Apoptosis induced in mast cells at 5 days after 5-FU administration. Intestinal tissues from *Apc*$^{Min/+}$ mice were fixed in 4% paraformaldehyde overnight and embedded into paraffin cassettes. 3-5 micron sections were cut and double stained with rat monoclonal primary antibody against MCT1 (a marker for mast cells) and rabbit polyclonal primary antibody against c-PARP-1 (a marker for apoptosis). The samples were then incubated with Cy-3-conjugated goat anti-rat secondary antibody and Cy5-conjugated donkey anti-rabbit secondary antibody, respectively. 93 total images were taken from the PBS and 5-FU samples together. Representative field views of confocal images of intestinal sections from PBS or 5-FU treated mice are shown. Red = MCT1 positive cells (mast cells), Green = cleaved PARP-1 (apoptotic cells). Double positive cells indicate apoptotic mast cells.

Table 4.3. Apoptosis induced in mast cells 5 days after 5-FU administration.

	MCT1+ Cells #	MCT1+ c-PARP+ Cells #	% of apoptotic MCT1 Cells
PBS	1232	211	17.13
5-FU	730	140	19.18

Total numbers of mast cells (MCT1-positive red cells) and the total number of apoptotic mast cells (MCT1-positive, red and c-PARP-positive, green cells) were counted from n=100 field views each for PBS and 5-FU treated mice (n=3 mice per treatment group). The percentage of apoptotic MCT1+ cells in each group was calculated by dividing total apoptotic mast cells by total number of mast cells in all the field views. The table shows the total numbers of cells and the percentages of apoptotic mast cells in PBS vs 5-FU treated *Apc*$^{Min/+}$ mice.

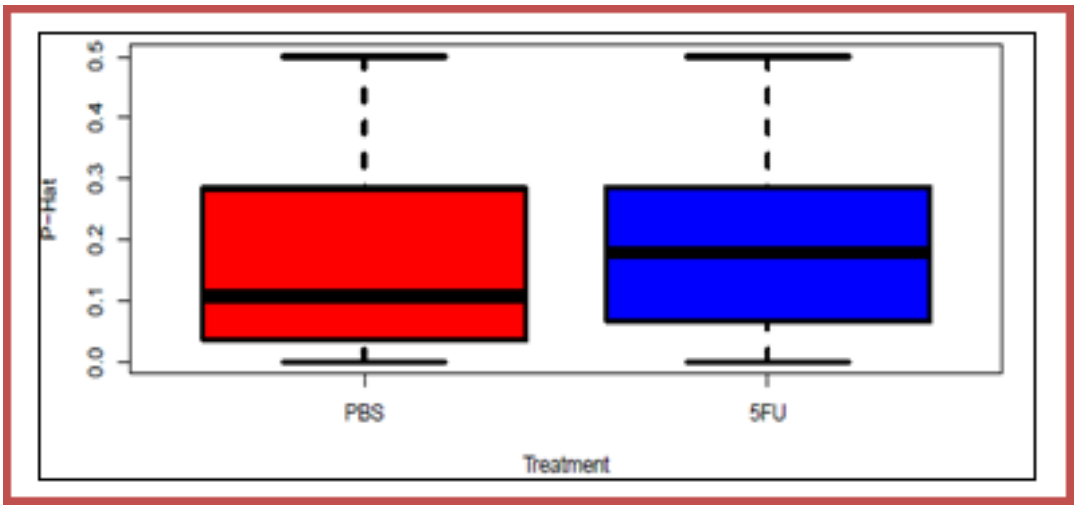

Figure 4.6. Box plots of the number of apoptotic mast cells in PBS versus 5-FU treated mice at 5 days post treatment. This figure is a graphical presentation of the statistical analyses of the number of mast cells undergoing apoptosis in response to 5-FU. P-Hat is the estimated proportion for the particular combination of Treatment, Mouse, Tumor, and field view, and is obtained by dividing the number of apoptotic mast cells by the total number of mast cells examined.

These results from these analyses corroborate with the data obtained by flow cytometric analyses obtained in earlier sections, demonstrating that mast cells were not depleted in response to 5-FU administration. All the samples analyzed by fluorescence immunohistochemical staining showed a baseline level of 15-20% apoptotic cells in the intestinal tumor stroma of control PBS treated mice. This number probably represents normal turnover or homeostasis in the intestinal tumor stroma. The samples used in the analyses for apoptotic indices were obtained from 3 different mice in each group for each of the different cell-types. The results of the trends presented here are consistent within each mice in each treatment group.

4.3.2 Proliferative indices of the target cell-types in PBS and 5-FU treated mice

TS inhibitors specifically target actively proliferating cells, thus, we examined the proliferative index of the MDSCs and mast cells to determine if this is the underlying reason for their differential response to 5-FU. As in the previous experiment, we used an immunofluorescence based analyses to determine the percentages of proliferating cell types in PBS or 5-FU treated mice. Fixed sections on slides were stained with antibodies against cell-specific surface markers and with an antibody against Ki-67 as a marker for proliferation. The number of cells that stained positive for the cell surface markers and those that stained for both cell surface marker and Ki-67 were determined, and the percentage of double stained cells against the total number of cell surface marker positive cells was used as a measure of the proliferative indices. The results showed that in PBS treated mice, the monocytes and granulocytes had much higher percentages of proliferating cells as compared to mast cells. Figures 4.7 and 4.9 show representative

images of intestinal tumor sections stained for monocytes and granulocytes, respectively. The data in Tables 4.4 and 4.5 indicate that the baseline proliferation indices in PBS-treated mice were 26.23% and 32.01% for monocytes and granulocytes, respectively. In response to 5-FU, the proliferation rates decreased by approximately two-fold to 11.89%, and 17.13% for monocytes, granulocytes, respectively. Box plots of the statistically significant changes in the percentage of proliferating cells in response to 5-FU are shown in Figures 4.8 and 4.9.

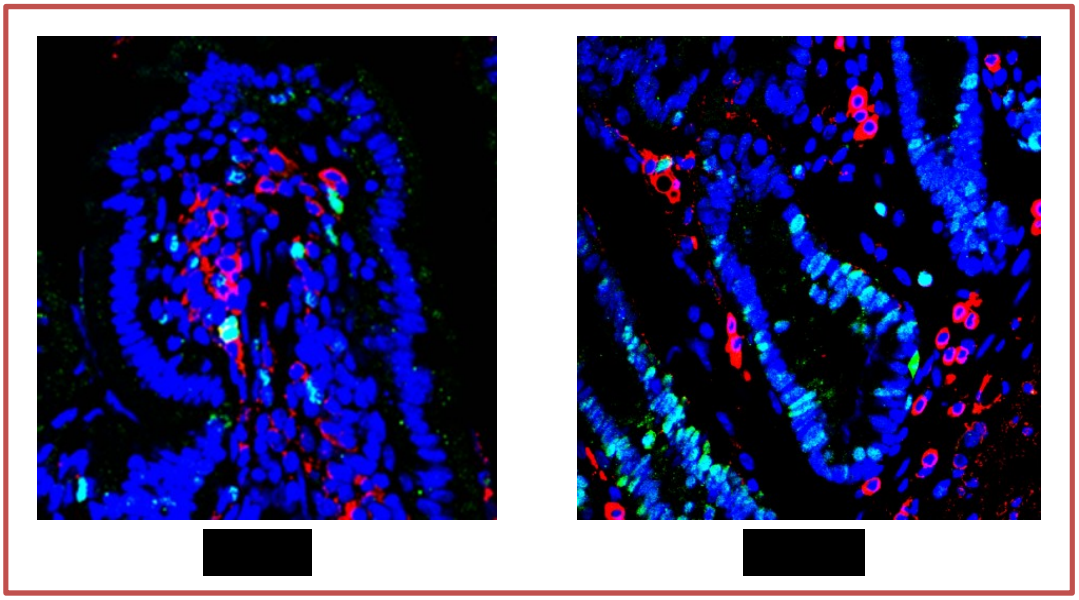

Figure 4.7. Proliferation levels of monocytes at 5 days after 5-FU administration. Intestinal tissues from *Apc*$^{Min/+}$ mice were fixed in 4% paraformaldehyde overnight and embedded into paraffin cassettes. 3-5 micron sections were cut and double stained with rat monoclonal primary antibody against CD11b (a marker for monocytes) and rabbit polyclonal primary antibody against Ki-67 (a marker for proliferation). The samples were then incubated with Cy-3-conjugated goat anti-rat secondary antibody and Cy5-conjugated donkey anti-rabbit secondary antibody, respectively. 216 total images were taken from the PBS and 5-FU samples together. Representative field views of confocal images of intestinal sections from PBS or 5-FU treated mice are shown. Red = CD11b positive cells (monocytes), Green = Ki-67 (proliferating cells). Double positive cells indicate proliferating monocytes.

Table 4.4. Reduction in the level of proliferation of monocytes 5 days after 5-FU administration.

	CD11b+ Cells #	CD11b+ Ki-67+ Cells #	% of proliferating CD11b Cells
PBS	1998	524	26.23
5-FU	1463	174	11.89

Total numbers of monocytes (CD11b-positive red cells) and the total number of proliferating monocytes (CD11b-positive, red and Ki-67-positive, green cells) were counted from n=100 field views each for PBS and 5-FU treated mice (n=3 mice per treatment group). The percentage of proliferating CD11b+ cells in each group was calculated by dividing total proliferating monocyte cells by total number of monocytes in all the field views. The table shows the total numbers of cells and the percentages of proliferating monocytes in PBS vs 5-FU treated *Apc*$^{Min/+}$ mice.

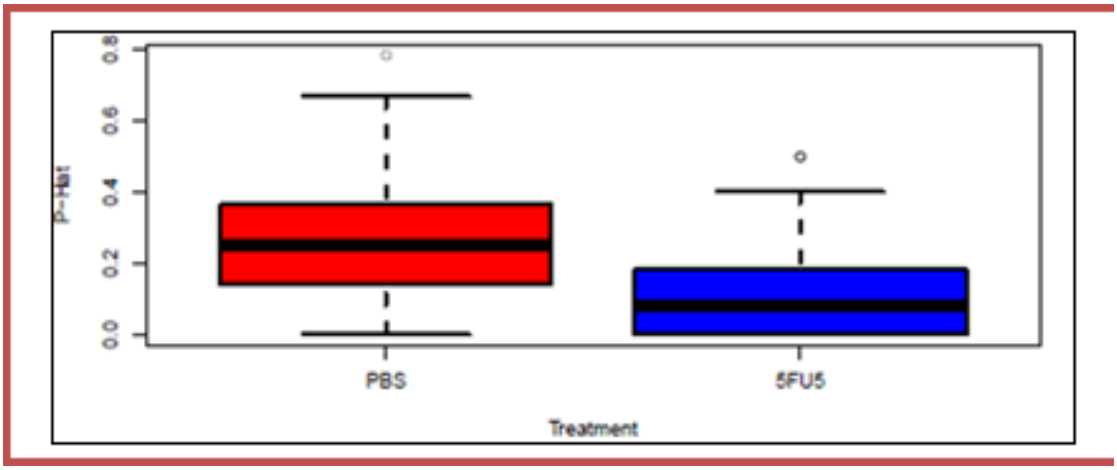

Figure 4.8. Box plots of the number of proliferating monocytes in PBS versus 5-FU treated mice at 5 days post treatment. This figure is a graphical presentation of the statistical analyses of the number of monocyte cells undergoing proliferation in response to 5-FU. P-Hat is the estimated proportion for the particular combination of Treatment, Mouse, Tumor, and field view, and is obtained by dividing the number of proliferating monocyte cells by the total number of monocyte cells examined.

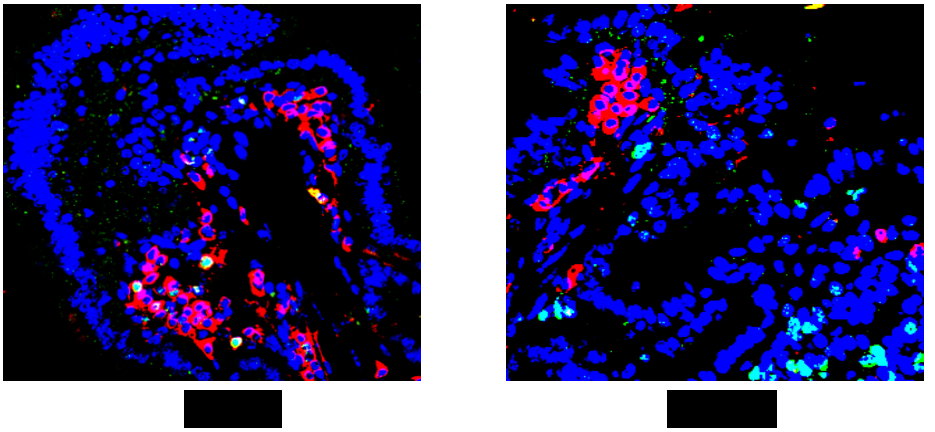

Figure 4.9. Proliferation levels of granulocytes at 5 days after 5-FU administration. Intestinal tissues from *Apc*$^{Min/+}$ mice were fixed in 4% paraformaldehyde overnight and embedded into paraffin cassettes. 3-5 micron sections were cut and double stained with rat monoclonal primary antibody against Gr-1 (a marker for granulocytes) and rabbit polyclonal primary antibody against Ki-67 (a marker for proliferation). The samples were then incubated with Cy-3-conjugated goat anti-rat secondary antibody and Cy5-conjugated donkey anti-rabbit secondary antibody, respectively. 194 total images were taken from the PBS and 5-FU samples together. Representative field views of confocal images of intestinal sections from PBS or 5-FU treated mice are shown. Red = Gr-1 positive cells (granulocytes), Green = Ki-67 (proliferating cells). Double positive cells indicate proliferating granulocytes.

Table 4.5. Reduction in the level of proliferation of granulocytes 5 days after 5-FU administration.

	GR1+ Cells #	GR1+ Ki67+ Cells #	% of proliferating GR1 cells
PBS	2009	643	32.01
5-FU	1127	193	17.13

Total numbers of granulocytes (Gr-1-positive red cells) and the total number of proliferating granulocytes (Gr-1-positive, red and Ki-67-positive, green cells) were counted from n=100 field views each for PBS and 5-FU treated mice (n=3 mice per treatment group). The percentage of proliferating Gr-1+ cells in each group was calculated by dividing total proliferating granulocyte cells by total number of granulocytes in all the field views. The table shows the total numbers of cells and the percentages of proliferating granulocytes in PBS vs 5-FU treated *Apc*$^{Min/+}$ mice.

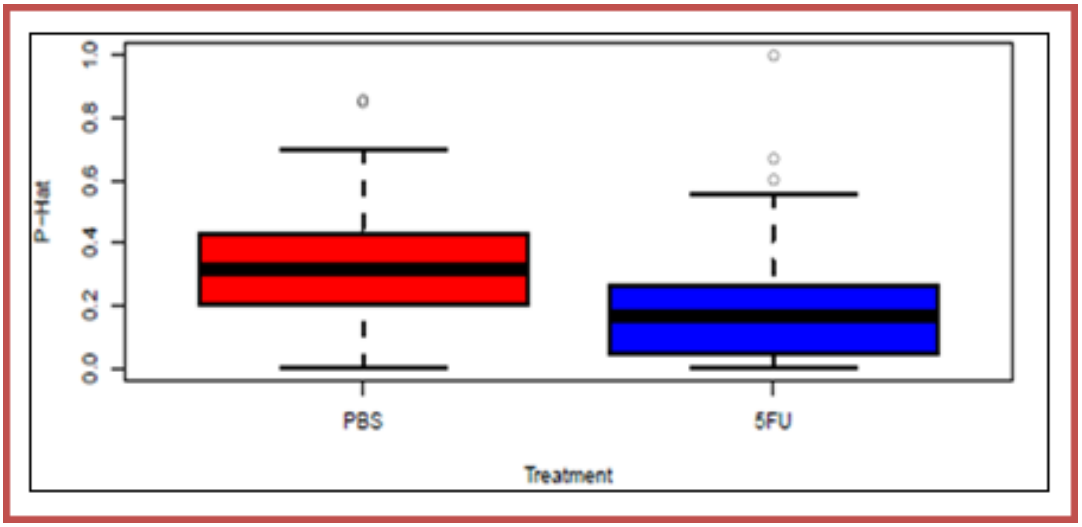

Figure 4.10. Box plots of the number of proliferating granulocytes in PBS versus 5-FU treated mice at 5 days post treatment. This figure is a graphical presentation of the statistical analyses of the number of granulocyte cells undergoing proliferation in response to 5-FU. P-Hat is the estimated proportion for the particular combination of Treatment, Mouse, Tumor, and field view, and is obtained by dividing the number of proliferating granulocyte cells by the total number of granulocyte cells examined.

Similar analyses for mast cells showed a much lower basal level of proliferation of 7.06%, approximately 3-5 folds lower as compared to monocytes and granulocytes. Representative slides of immunofluorescent double staining with antibodies against MCT1 and the Ki-67 proliferation marker in Figure 4.11 shows very little or no co-localization of the two antibodies. This is further supported by the data in Table 4.6 obtained from 50 field each views of the PBS and 5-FU treated samples showing only 7% of mast cells proliferating in PBS treated mice that is reduced to 3% in 5-FU treated mice. Although, we observed a 50% reduction from 7% to 3% in the 5-FU treated mice, the absolute numbers of proliferating mast cells are very low as compared to proliferating monocytes or granulocytes. These numbers are consistent with the data obtained from analyses done by flow cytometric methods. Taken together, the data indicate that MDSCs

have a much higher proliferation rate that is approximately 3-5 fold higher than that in mast cells that potentially render them more sensitive to the effects of 5-FU.

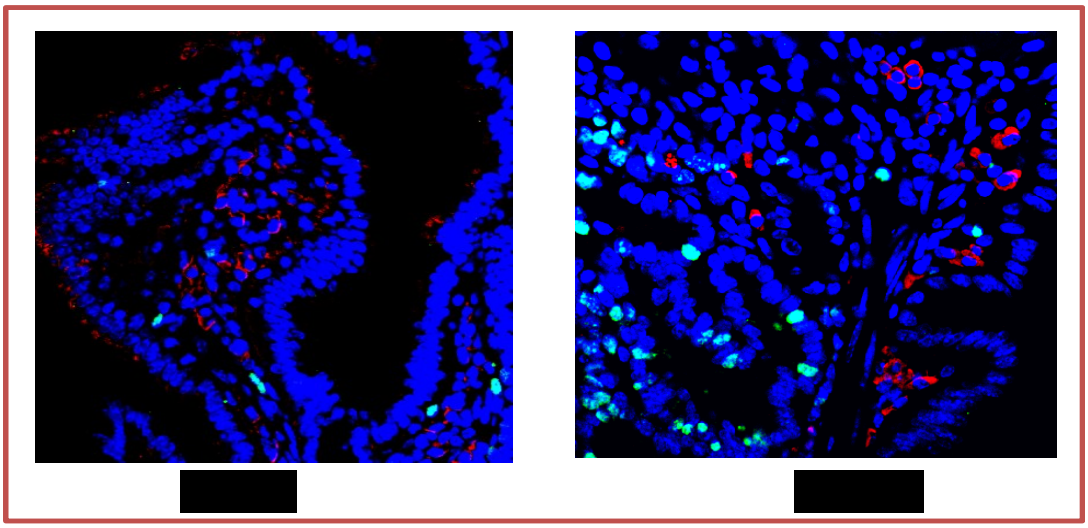

Figure 4.11. Proliferation levels of mast cells at 5 days after 5-FU administration. Intestinal tissues from *Apc*$^{Min/+}$ mice were fixed in 4% paraformaldehyde overnight and embedded into paraffin cassettes. 3-5 micron sections were cut and double stained with rat monoclonal primary antibody against MCT1 (a marker for mast cells) and rabbit polyclonal primary antibody against Ki-67 (a marker for proliferation). The samples were then incubated with Cy-3-conjugated goat anti-rat secondary antibody and Cy5-conjugated donkey anti-rabbit secondary antibody, respectively. 100 total images were taken from the PBS and 5-FU samples together. Representative field views of confocal images of intestinal sections from PBS or 5-FU treated mice are shown. Red = MCT1 positive cells (mast cells), Green = Ki-67 (proliferating cells). Double positive cells indicate proliferating mast cells.

Table 4.6. Reduction in the level of proliferation of mast cells 5 days after 5-FU administration.

	MCT1+ Cells #	MCT1+ Ki-67l+ Cells #	% of proliferating MCT1 Cells
PBS	1048	74	7.06
5-FU	784	24	3.06

Total numbers of mast cells (MCT1-positive red cells) and the total number of proliferating mast cells (Gr-1-positive, red and Ki-67-positive, green cells) were counted from n=100 field views each for PBS and 5-FU treated mice (n=3 mice per treatment group). The percentage of proliferating MCT1+ cells in each group was calculated by dividing total proliferating mast cells by total number of mast cells in all the field views. The table shows the total numbers of cells and the percentages of proliferating mast cells in PBS vs 5-FU treated *Apc*$^{Min/+}$ mice.

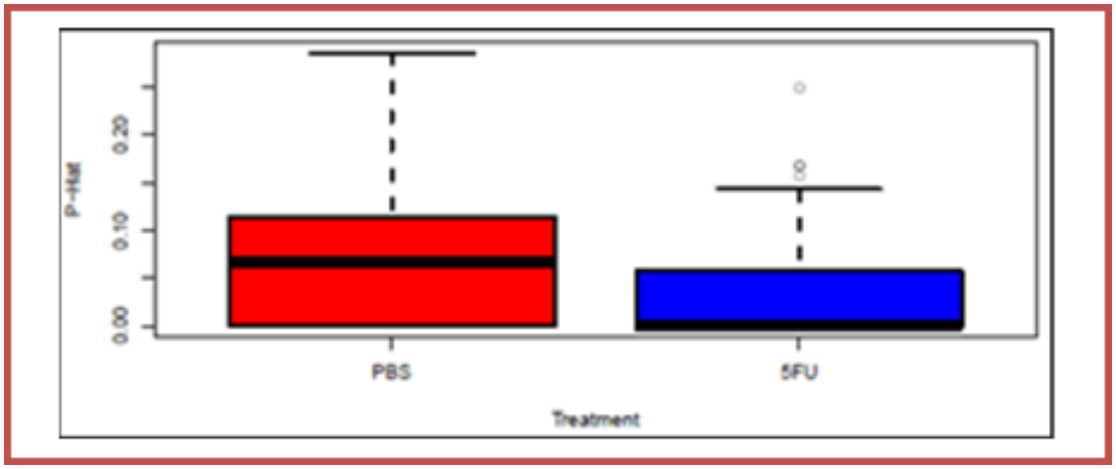

Figure 4.12. Box plots of the number of proliferating mast cells in PBS versus 5-FU treated mice at 5 days post treatment. This figure is a graphical presentation of the statistical analyses of the number of mast cells undergoing proliferation in response to 5-FU. P-Hat is the estimated proportion for the particular combination of Treatment, Mouse, Tumor, and field view, and is obtained by dividing the number of proliferating mast cells by the total number of mast cells examined.

4.4 Discussion

MDSCs are a major contributor for tumor immune escape due to their strong immune-suppressive abilities. MDSCs are present at such high levels in tumor bearing murine models because aggravation of inflammation effectively enhances MDSC generation as well as immune-suppressive ability. Under inflamed conditions induced by tumors, MDSCs show a much higher resistance to apoptosis as compared to the normal healthy conditions. Nevertheless, in tumor bearing rodent models, MDSCs have been reported to be depleted from the animal model system by the use of specific drugs like 5-FU and gemcitabine (Vincent, Mignot et al. 2010). This depletion has been attributed to the activation of a cleaved caspase 3 and 7 mediated apoptotic pathway, post drug treatment (Vincent, Mignot et al. 2010) in immortalized MDSC cell lines but it has not been elucidated *in vivo* and has especially not been studied in colorectal cancer model. It has also been reported that MDSCs are susceptible to regulation by the Fas mediated pathway. Mast cells on the other hand, have though been implicated in the initiation of polyps, progression of colorectal tumors and mobilization of MDSCs, their response to 5-FU has not been studied before. Thus, with the goal of identifying the underlying mechanism behind 5-FU mediated MDSC depletion and to uncover the rationale behind mast cells insensitivity to the therapy, we examined the proliferative and apoptotic status of these cells pre- and post- 5-FU administration. We have studied both the sub-classes of MDSCS separately, namely, monocytes and granulocytes along with mast cells in the intestinal tissues from the same group of tumor bearing animals. Our experiments simultaneously examined the Fas-Caspase mediated apoptosis, manifesting itself as the cleavage of PARP-1 along with active-cell-cycle Ki-67 expression in the same murine

model system of *Apc*$^{Min/+}$ mice.

From our results, it can be postulated that monocytes and granulocytes show a similar range of apoptotic indices 5 days post 5-FU administration. This could be the underlying reason for the measurable depletion of MDSCs from the quantitative analyses done in the previous section. These high apoptotic indices were not observed with the mast cells, which substantiates our earlier results. Monocytes and granulocytes also seem to have a relatively higher level of proliferation in untreated animals as compared to the mast cells. Although, 5-FU quantitatively reduced the absolute number of proliferating mast cells, the depletion was not as prominent as MDSCs. Also, there is a possibility that 5-FU might be targeting some of the mast cells in the tumor beds and this depletion is being compensated by maturation or recruitment of other mast cell progenitors, hence not showing any measurable effect of the drug during flow cytometry assays. Nevertheless, our study indicated that 5-FU does not target the existing mast cells in the tumor beds as immensely as monocytes and granulocytes. The data from Ki-67 experiments point towards the possibility that the mast cells are not as sensitive as MDSCs because of their much lower rate of proliferation. This is an interesting result because it identifies MDSCs as the potential target cells, which could be utilized to develop strategies to enhance tumor sensitivity by combining 5-FU with other anti-inflammatory or anti-neoplastic drugs (i.e., IL-β inhibitors (Bruchard, Mignot et al. 2013)). We could extend this research by sensitizing mast cells to 5-FU therapy by targeting pathways that are crucial in maintaining their active polyp-inducing state. It is also possible that since mast cells are a differentiated cell-type, their turn-over rate in the tumor stroma can be targeted such that

there is a reduction in tumor associated mast cells that, in turn, could limit or prevent the mobilization of MDSCs and T-regs to the stroma.

Proliferation and apoptosis appear to go hand in hand in deciphering the impact of 5-FU on BMDCs in the tumor microenvironment. Both aspects can correlate to the effect of 5-FU on the target cell-types. As a TS inhibitor, 5-FU non-selectively targets proliferating cells including both cancer and non-cancer proliferating cells. This is substantiated by the data showing enhanced PARP cleavage in monocytes and granulocytes and not in mast cells.

CHAPTER 5

CONCLUSION AND FUTURE DIRECTIONS

5.1 Conclusion

The results from this study emphasize on the role of host derived immune cells originating from the bone marrow and infiltrating the tumor microenvironment on tumor response to therapy, specifically to 5-FU, a TS inhibitor. These tumor stromal cells could be sensitive to TS inhibitor therapy and prone to 5-FU attack, such as MDSCs, or could be insensitive to TS inhibition, such as the Mast cells. Each of the cell-types uniquely contributes to tumor survival, progression, and metastasis. This project examined three target cells which have the potential to dictate tumor response to therapy and influence the manner in which the tumor recovers from anti-neoplastic therapy. This project postulates that certain cells are more intriguing than others, with respect to their response to therapy, owing to their proliferation rate that could potentially make them vulnerable to 5-FU dosing. 5-FU is known to cause apoptosis in cancer cells as well as in rapidly proliferating normal cells in the patient. It is critical to reduce drug induced toxicity while enhancing the efficacy and specificity of the drug so that it can target only cancer and tumor associated stromal cells. The results from this study indicate stromal cells derived from the bone marrow can be exploited to develop methods to sensitize the tumor to TS inhibitor therapy. The proof-of-the-principle studies that we have conducted, wherein bone marrow cells in the tumor microenvironment that were made resistant to TS

inhibitors also rendered tumor cells resistant to these inhibitors, suggest that these cells can be exploited to enhance tumor response to 5-FU. Cells such as monocytes and granulocytes, can be further modulated to enhance tumor sensitivity to the therapy. They can also be genetically modified to modulate tumor response so that the rebound of cancer cells from the therapy and therefore, time to tumor recurrence is extended.

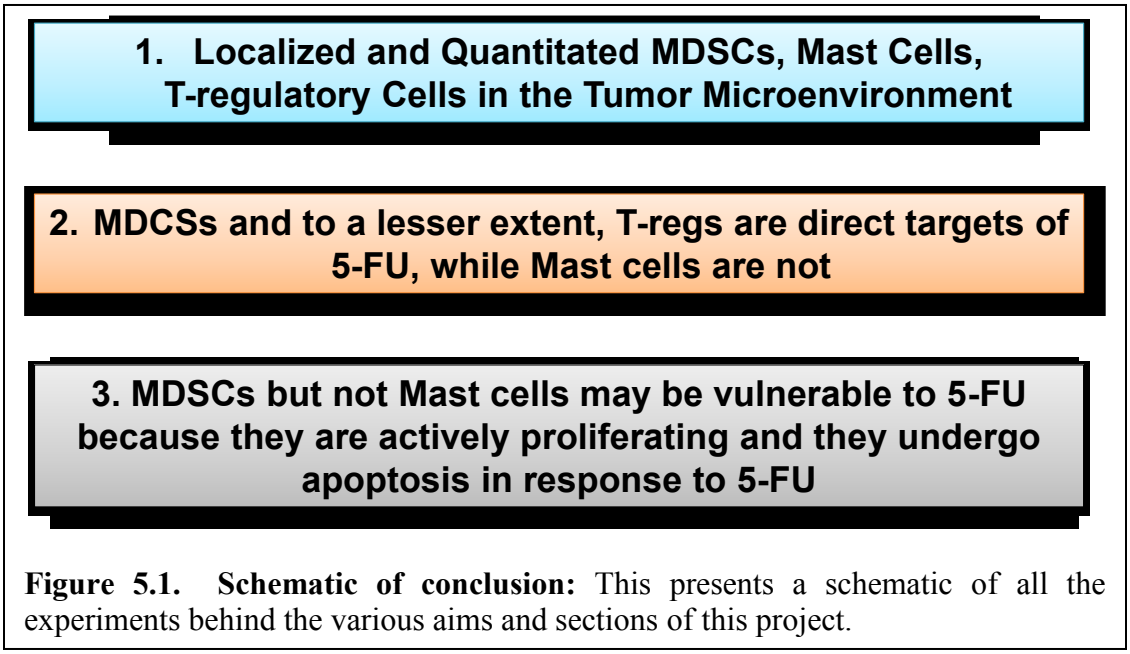

Figure 5.1. Schematic of conclusion: This presents a schematic of all the experiments behind the various aims and sections of this project.

5.2 Future Directions

The results from these studies point to a number of experiments that can be pursued in the future. First, TS inhibitors can be combined with other drugs that target cells that may are resistant to the therapy, such as mast cells. Mast cells are thought to promote tumor recurrence to therapy, and by inhibiting them tumor relapse after 5-FU treatment might be prolonged or inhibited. Mast cell inhibitors such as Cromolyn, Nedocromil, or TNFα may be used in combination with 5-FU to study their effect on tumor burden and tumor

recurrence. Studies from other labs have shown that loss of MDSCs in response to 5-FU can activate the recruitment of CD8+ killer T cells that further enhance the killing of tumor cells by 5-FU (Bruchard, Mignot et al. 2013). However, the dying MDSCs can also activate the NLRP3 inflammasome which results in the release of IL1-B that promotes the recruitment of CD4+ helper T cells that aids in tumor recurrence post therapy. This raises the possibility of using inhibitors against IL-1β in combination with 5-FU attenuate the strong inflammatory response and block the recruitment of pro-tumorigenic CD4+ T cells..

Finally, it is also critical to study the impact of 5-FU on other cells in the tumor microenvironment such as neutrophils, tumor associated macrophages, mesenchymal stem cells, myofibroblasts, and cancer-associated fibroblasts among many other cell-types, to determine their role in dictating tumor response to chemotherapy. Such studies have not been undertaken before. Furthermore, one of the major goals of this project is to be able to specifically target tumor and tumor stromal with the therapy, while sparing the normal cells from drug induced toxicity and side-effects. The use of promoters that are specifically expressed in the tumor stroma to drive the expression of chemosensitizing genes in stromal cells will be useful in achieving this goal.

REFERENCES

Abbitt, K. B., M. J. Cotter, et al. (2009). "Antibody ligation of murine Ly-6G induces neutropenia, blood flow cessation, and death via complement-dependent and independent mechanisms." J Leukoc Biol **85**(1): 55-63.

Almand, B., J. I. Clark, et al. (2001). "Increased production of immature myeloid cells in cancer patients: a mechanism of immunosuppression in cancer." J Immunol **166**(1): 678-689.

Attar, E. C., T. Ervin, et al. (2000). "Side effects of chemotherapy. Case 3. Acute interstitial pneumonitis related to gemcitabine." J Clin Oncol **18**(3): 697-698.

Balkwill, F. and A. Mantovani (2001). "Inflammation and cancer: back to Virchow?" Lancet **357**(9255): 539-545.

Baniyash, M. (2006). "Chronic inflammation, immunosuppression and cancer: new insights and outlook." Semin Cancer Biol **16**(1): 80-88.

Bauer, O. and E. Razin (2000). "Mast Cell-Nerve Interactions." News Physiol Sci **15**: 213-218.

Bettelli, E., Y. Carrier, et al. (2006). "Reciprocal developmental pathways for the generation of pathogenic effector TH17 and regulatory T cells." Nature **441**(7090): 235-238.

Beyer, M. and J. L. Schultze (2006). "Regulatory T cells in cancer." Blood **108**(3): 804-811.

Bischoff, S. C. and S. Kramer (2007). "Human mast cells, bacteria, and intestinal immunity." Immunol Rev **217**: 329-337.

Blatner, N. R., A. Bonertz, et al. (2010). "In colorectal cancer mast cells contribute to systemic regulatory T-cell dysfunction." Proc Natl Acad Sci U S A **107**(14): 6430-6435.

Bokemeyer, C., I. Bondarenko, et al. (2009). "Fluorouracil, leucovorin, and oxaliplatin with and without cetuximab in the first-line treatment of metastatic colorectal cancer." J Clin Oncol **27**(5): 663-671.

Bronte, V., P. Serafini, et al. (2003). "IL-4-induced arginase 1 suppresses alloreactive T cells in tumor-bearing mice." J Immunol **170**(1): 270-278.

Bronte, V., P. Serafini, et al. (2003). "L-arginine metabolism in myeloid cells controls T-lymphocyte functions." Trends Immunol **24**(6): 302-306.

Bruchard, M., G. Mignot, et al. (2013). "Chemotherapy-triggered cathepsin B release in myeloid-derived suppressor cells activates the Nlrp3 inflammasome and promotes tumor growth." Nat Med **19**(1): 57-64.

Burstein, H. J. (2000). "Side effects of chemotherapy. Case 1. Radiation recall dermatitis from gemcitabine." J Clin Oncol **18**(3): 693-694.

Cambien, B., B. F. Karimdjee, et al. (2009). "Organ-specific inhibition of metastatic colon carcinoma by CXCR3 antagonism." Br J Cancer **100**(11): 1755-1764.

Chantrain, C. F., O. Feron, et al. (2008). "Bone marrow microenvironment and tumor progression." Cancer Microenviron **1**(1): 23-35.

Cheng, H., Y. Liu, et al. (2004). "5-Fluorouracil enhances apoptosis sensitivity of T lymphocytes mediated by CD3 epsilon." Cell Biochem Funct **22**(3): 187-195.

Chu, E., M. A. Callender, et al. (2003). "Thymidylate synthase inhibitors as anticancer agents: from bench to bedside." Cancer Chemother Pharmacol **52 Suppl 1**: S80-89.

Clark, R. A., S. J. Huang, et al. (2008). "Human squamous cell carcinomas evade the immune response by down-regulation of vascular E-selectin and recruitment of regulatory T cells." J Exp Med **205**(10): 2221-2234.

Clarke, S. L., G. J. Betts, et al. (2006). "CD4+CD25+FOXP3+ regulatory T cells suppress anti-tumor immune responses in patients with colorectal cancer." PLoS One **1**: e129.

Colombo, M. P. and S. Piconese (2007). "Regulatory-T-cell inhibition versus depletion: the right choice in cancer immunotherapy." Nat Rev Cancer **7**(11): 880-887.

Colombo, M. P. and S. Piconese (2009). "Polyps wrap mast cells and Treg within tumorigenic tentacles." Cancer Res **69**(14): 5619-5622.

Condamine, T. and D. I. Gabrilovich (2011). "Molecular mechanisms regulating myeloid-derived suppressor cell differentiation and function." Trends Immunol **32**(1): 19-25.

Correale, P., M. S. Rotundo, et al. (2010). "Regulatory (FoxP3+) T-cell tumor infiltration is a favorable prognostic factor in advanced colon cancer patients undergoing chemo or chemoimmunotherapy." J Immunother **33**(4): 435-441.

Cortez-Retamozo, V., M. Etzrodt, et al. (2012). "Origins of tumor-associated macrophages and neutrophils." Proc Natl Acad Sci U S A **109**(7): 2491-2496.

Corzo, C. A., T. Condamine, et al. (2010). "HIF-1alpha regulates function and differentiation of myeloid-derived suppressor cells in the tumor microenvironment." J Exp Med **207**(11): 2439-2453.

Costi, M. P., S. Ferrari, et al. (2005). "Thymidylate synthase structure, function and implication in drug discovery." Curr Med Chem **12**(19): 2241-2258.

Danenberg, P. V., H. Malli, et al. (1999). "Thymidylate synthase inhibitors." Semin Oncol **26**(6): 621-631.

Davis, C., R. Price, et al. (2011). "Hematopoietic derived cell infiltration of the intestinal tumor microenvironment in Apc Min/+ mice." Microsc Microanal **17**(4): 528-539.

Dawicki, W. and J. S. Marshall (2007). "New and emerging roles for mast cells in host defence." Curr Opin Immunol **19**(1): 31-38.

de Gramont, A., A. Figer, et al. (2000). "Leucovorin and fluorouracil with or without oxaliplatin as first-line treatment in advanced colorectal cancer." J Clin Oncol **18**(16): 2938-2947.

De Palma, M., M. A. Venneri, et al. (2003). "Targeting exogenous genes to tumor angiogenesis by transplantation of genetically modified hematopoietic stem cells." Nat Med **9**(6): 789-795.

DeNardo, D. G., D. J. Brennan, et al. (2011). "Leukocyte complexity predicts breast cancer survival and functionally regulates response to chemotherapy." Cancer Discov **1**(1): 54-67.

Denkert, C., S. Loibl, et al. (2010). "Tumor-associated lymphocytes as an independent predictor of response to neoadjuvant chemotherapy in breast cancer." J Clin Oncol **28**(1): 105-113.

Diaz-Montero, C. M., M. L. Salem, et al. (2009). "Increased circulating myeloid-derived suppressor cells correlate with clinical cancer stage, metastatic tumor burden, and doxorubicin-cyclophosphamide chemotherapy." Cancer Immunol Immunother **58**(1): 49-59.

Doering, C. B., D. Archer, et al. (2010). "Delivery of nucleic acid therapeutics by genetically engineered hematopoietic stem cells." Adv Drug Deliv Rev **62**(12): 1204-1212.

Dolcetti, L., I. Marigo, et al. (2008). "Myeloid-derived suppressor cell role in tumor-related inflammation." Cancer Lett **267**(2): 216-225.

Dolcetti, L., E. Peranzoni, et al. (2010). "Hierarchy of immunosuppressive strength among myeloid-derived suppressor cell subsets is determined by GM-CSF." Eur J Immunol **40**(1): 22-35.

Dove, W. F., K. A. Gould, et al. (1995). "Emergent issues in the genetics of intestinal neoplasia." Cancer Surv **25**: 335-355.

Duluc, D., Y. Delneste, et al. (2007). "Tumor-associated leukemia inhibitory factor and IL-6 skew monocyte differentiation into tumor-associated macrophage-like cells." Blood **110**(13): 4319-4330.

Dvorak, H. F. (1986). "Tumors: wounds that do not heal. Similarities between tumor stroma generation and wound healing." N Engl J Med **315**(26): 1650-1659.

Dwight, R. W., G. A. Higgins, et al. (1972). "Preoperative radiation and surgery for cancer of the sigmoid colon and rectum." Am J Surg **123**(1): 93-103.

Erdman, S. E. and T. Poutahidis (2010). "Roles for inflammation and regulatory T cells in colon cancer." Toxicol Pathol **38**(1): 76-87.

Farrugia, D. C., H. E. Ford, et al. (2003). "Thymidylate synthase expression in advanced colorectal cancer predicts for response to raltitrexed." Clin Cancer Res **9**(2): 792-801.

Fichtner-Feigl, S., M. Terabe, et al. (2008). "Restoration of tumor immunosurveillance via targeting of interleukin-13 receptor-alpha 2." Cancer Res **68**(9): 3467-3475.

Findlay, M. P., D. Cunningham, et al. (1997). "Lack of correlation between thymidylate synthase levels in primary colorectal tumours and subsequent response to chemotherapy." Br J Cancer **75**(6): 903-909.

Fong, Y., N. Kemeny, et al. (1996). "Treatment of colorectal cancer: hepatic metastasis." Semin Surg Oncol **12**(4): 219-252.

Frankenstein, Z., U. Alon, et al. (2006). "The immune-body cytokine network defines a social architecture of cell interactions." Biol Direct **1**: 32.

Fujii, M., M. Kochi, et al. (2010). "Recent advances in chemotherapy for advanced gastric cancer in Japan." Surg Today **40**(4): 295-300.

Gabrilovich, D. (2004). "Mechanisms and functional significance of tumour-induced dendritic-cell defects." Nat Rev Immunol **4**(12): 941-952.

Gabrilovich, D. I., V. Bronte, et al. (2007). "The terminology issue for myeloid-derived suppressor cells." Cancer Res **67**(1): 425; author reply 426.

Gabrilovich, D. I. and S. Nagaraj (2009). "Myeloid-derived suppressor cells as regulators of the immune system." Nat Rev Immunol **9**(3): 162-174.

Galon, J., A. Costes, et al. (2006). "Type, density, and location of immune cells within human colorectal tumors predict clinical outcome." Science **313**(5795): 1960-1964.

Garcia-Barros, M., F. Paris, et al. (2003). "Tumor response to radiotherapy regulated by endothelial cell apoptosis." Science **300**(5622): 1155-1159.

Gerard, C. and B. J. Rollins (2001). "Chemokines and disease." Nat Immunol **2**(2): 108-115.

Ghiringhelli, F., N. Larmonier, et al. (2004). "CD4+CD25+ regulatory T cells suppress tumor immunity but are sensitive to cyclophosphamide which allows immunotherapy of established tumors to be curative." Eur J Immunol **34**(2): 336-344.

Giannopoulos, K., M. Schmitt, et al. (2008). "The high frequency of T regulatory cells in patients with B-cell chronic lymphocytic leukemia is diminished through treatment with thalidomide." Leukemia **22**(1): 222-224.

Gillio, A. P., C. Gasparetto, et al. (1990). "Effects of interleukin-3 on hematopoietic recovery after 5-fluorouracil or cyclophosphamide treatment of cynomolgus primates." J Clin Invest **85**(5): 1560-1565.

Gmeiner, W. H. (2005). "Novel chemical strategies for thymidylate synthase inhibition." Curr Med Chem **12**(2): 191-202.

Gonzalez-Aparicio, M., P. Alzuguren, et al. (2011). "Oxaliplatin in combination with liver-specific expression of interleukin 12 reduces the immunosuppressive microenvironment of tumours and eradicates metastatic colorectal cancer in mice." Gut **60**(3): 341-349.

Gounaris, E., N. R. Blatner, et al. (2009). "T-regulatory cells shift from a protective anti-inflammatory to a cancer-promoting proinflammatory phenotype in polyposis." Cancer Res **69**(13): 5490-5497.

Gounaris, E., S. E. Erdman, et al. (2007). "Mast cells are an essential hematopoietic component for polyp development." Proc Natl Acad Sci U S A **104**(50): 19977-19982.

Greifenberg, V., E. Ribechini, et al. (2009). "Myeloid-derived suppressor cell activation by combined LPS and IFN-gamma treatment impairs DC development." Eur J Immunol **39**(10): 2865-2876.

Grem, J. L. (2000). "5-Fluorouracil: forty-plus and still ticking. A review of its preclinical and clinical development." Invest New Drugs **18**(4): 299-313.

Haile, L. A., R. von Wasielewski, et al. (2008). "Myeloid-derived suppressor cells in inflammatory bowel disease: a new immunoregulatory pathway." Gastroenterology **135**(3): 871-881, 881 e871-875.

Hall, B. M., J. E. Fortney, et al. (2004). "Stromal cells expressing elevated VCAM-1 enhance survival of B lineage tumor cells." Cancer Lett **207**(2): 229-239.

Hanahan, D. and R. A. Weinberg (2000). "The hallmarks of cancer." Cell **100**(1): 57-70.

Hanahan, D. and R. A. Weinberg (2011). "Hallmarks of cancer: the next generation." Cell **144**(5): 646-674.

Hanna, E., J. Quick, et al. (2009). "The tumour microenvironment: a novel target for cancer therapy." Oral Dis **15**(1): 8-17.

Heib, V., M. Becker, et al. (2008). "Advances in the understanding of mast cell function." Br J Haematol **142**(5): 683-694.

Heidelberger, C., N. K. Chaudhuri, et al. (1957). "Fluorinated pyrimidines, a new class of tumour-inhibitory compounds." Nature **179**(4561): 663-666.

Heijmans, J., N. V. Buller, et al. (2012). "Role of mast cells in colorectal cancer development, the jury is still out." Biochim Biophys Acta **1822**(1): 9-13.

Hofmeister, V., D. Schrama, et al. (2008). "Anti-cancer therapies targeting the tumor stroma." Cancer Immunol Immunother **57**(1): 1-17.

Huang, B., Z. Lei, et al. (2008). "SCF-mediated mast cell infiltration and activation exacerbate the inflammation and immunosuppression in tumor microenvironment." Blood **112**(4): 1269-1279.

Ichikawa, M., R. Williams, et al. (2011). "S100A8/A9 activate key genes and pathways in colon tumor progression." Mol Cancer Res **9**(2): 133-148.

Jenq, R. R. and M. R. van den Brink (2010). "Allogeneic haematopoietic stem cell transplantation: individualized stem cell and immune therapy of cancer." Nat Rev Cancer **10**(3): 213-221.

Jin, D. K., K. Shido, et al. (2006). "Cytokine-mediated deployment of SDF-1 induces revascularization through recruitment of CXCR4+ hemangiocytes." Nat Med **12**(5): 557-567.

Jutila, M. A., F. G. Kroese, et al. (1988). "Ly-6C is a monocyte/macrophage and endothelial cell differentiation antigen regulated by interferon-gamma." Eur J Immunol **18**(11): 1819-1826.

Kaler, P., V. Galea, et al. (2010). "Tumor associated macrophages protect colon cancer cells from TRAIL-induced apoptosis through IL-1beta-dependent stabilization of Snail in tumor cells." PLoS One **5**(7): e11700.

Kerkar, S. P. and N. P. Restifo (2012). "Cellular constituents of immune escape within the tumor microenvironment." Cancer Res **72**(13): 3125-3130.

Kettunen, H. L., A. S. Kettunen, et al. (2003). "Intestinal immune responses in wild-type and Apcmin/+ mouse, a model for colon cancer." Cancer Res **63**(16): 5136-5142.

Kidd, S., E. Spaeth, et al. (2012). "Origins of the tumor microenvironment: quantitative assessment of adipose-derived and bone marrow-derived stroma." PLoS One **7**(2): e30563.

Kim, S. L., S. H. Kim, et al. (2013). "Synergistic antitumor effect of 5-fluorouracil in combination with parthenolide in human colorectal cancer." Cancer Lett **335**(2): 479-486.

Kimura, T., J. R. McKolanis, et al. (2013). "MUC1 vaccine for individuals with advanced adenoma of the colon: a cancer immunoprevention feasibility study." Cancer Prev Res (Phila) **6**(1): 18-26.

Kitamura, Y. and J. Fujita (1989). "Regulation of mast cell differentiation." Bioessays **10**(6): 193-196.

Kusmartsev, S. and D. I. Gabrilovich (2003). "Inhibition of myeloid cell differentiation in cancer: the role of reactive oxygen species." J Leukoc Biol **74**(2): 186-196.

Kusmartsev, S., S. Nagaraj, et al. (2005). "Tumor-associated CD8+ T cell tolerance induced by bone marrow-derived immature myeloid cells." J Immunol **175**(7): 4583-4592.

Kusmartsev, S., Y. Nefedova, et al. (2004). "Antigen-specific inhibition of CD8+ T cell response by immature myeloid cells in cancer is mediated by reactive oxygen species." J Immunol **172**(2): 989-999.

Levings, M. K., R. Bacchetta, et al. (2002). "The role of IL-10 and TGF-beta in the differentiation and effector function of T regulatory cells." Int Arch Allergy Immunol **129**(4): 263-276.

Li, W., K. Wu, et al. (2013). "HMGB1 recruits myeloid derived suppressor cells to promote peritoneal dissemination of colon cancer after resection." Biochem Biophys Res Commun **436**(2): 156-161.

Li, Y. Y., L. L. Hsieh, et al. (2009). "Interleukin-6 (IL-6) released by macrophages induces IL-6 secretion in the human colon cancer HT-29 cell line." Hum Immunol **70**(3): 151-158.

Lin, Y. C., J. Mahalingam, et al. (2013). "Activated but not resting regulatory T cells accumulated in tumor microenvironment and correlated with tumor progression in patients with colorectal cancer." Int J Cancer **132**(6): 1341-1350.

Ling, K. L., S. E. Pratap, et al. (2007). "Increased frequency of regulatory T cells in peripheral blood and tumour infiltrating lymphocytes in colorectal cancer patients." Cancer Immun **7**: 7.

Liu, J., Y. Zhang, et al. (2011). "Mast cell: insight into remodeling a tumor microenvironment." Cancer Metastasis Rev **30**(2): 177-184.

Loddenkemper, C., M. Schernus, et al. (2006). "In situ analysis of FOXP3+ regulatory T cells in human colorectal cancer." J Transl Med **4**: 52.

Love, R. R., H. Leventhal, et al. (1989). "Side effects and emotional distress during cancer chemotherapy." Cancer **63**(3): 604-612.

Lutsiak, M. E., R. T. Semnani, et al. (2005). "Inhibition of CD4(+)25+ T regulatory cell function implicated in enhanced immune response by low-dose cyclophosphamide." Blood **105**(7): 2862-2868.

Ma, C. and X. Dong (2011). "Colorectal cancer-derived Foxp3(+) IL-17(+) T cells suppress tumour-specific CD8+ T cells." Scand J Immunol **74**(1): 47-51.

Maltby, S., K. Khazaie, et al. (2009). "Mast cells in tumor growth: angiogenesis, tissue remodelling and immune-modulation." Biochim Biophys Acta **1796**(1): 19-26.

Marigo, I., L. Dolcetti, et al. (2008). "Tumor-induced tolerance and immune suppression by myeloid derived suppressor cells." Immunol Rev **222**: 162-179.

Markiewski, M. M., R. A. DeAngelis, et al. (2008). "Modulation of the antitumor immune response by complement." Nat Immunol **9**(11): 1225-1235.

Mauritz, R., E. Giovannetti, et al. (2009). "Polymorphisms in the enhancer region of the thymidylate synthase gene are associated with thymidylate synthase levels in normal tissues but not in malignant tissues of patients with colorectal cancer." Clin Colorectal Cancer **8**(3): 146-154.

McKnight, J. A. (2003). "Principles of chemotherapy." Clin Tech Small Anim Pract **18**(2): 67-72.

McLean, M. H., G. I. Murray, et al. (2011). "The inflammatory microenvironment in colorectal neoplasia." PLoS One **6**(1): e15366.

Medina-Echeverz, J., J. Fioravanti, et al. (2011). "Successful colon cancer eradication after chemoimmunotherapy is associated with profound phenotypic change of intratumoral myeloid cells." J Immunol **186**(2): 807-815.

Mougiakakos, D., A. Choudhury, et al. (2010). "Regulatory T cells in cancer." Adv Cancer Res **107**: 57-117.

Movahedi, K., M. Guilliams, et al. (2008). "Identification of discrete tumor-induced myeloid-derived suppressor cell subpopulations with distinct T cell-suppressive activity." Blood **111**(8): 4233-4244.

Mueller, M. M. and N. E. Fusenig (2004). "Friends or foes - bipolar effects of the tumour stroma in cancer." Nat Rev Cancer **4**(11): 839-849.

Murdoch, C., M. Muthana, et al. (2008). "The role of myeloid cells in the promotion of tumour angiogenesis." Nat Rev Cancer **8**(8): 618-631.

Murphy, J. T., J. M. Tucker, et al. (2004). "Raltitrexed increases tumorigenesis as a single agent yet exhibits anti-tumor synergy with 5-fluorouracil in ApcMin/+ mice." Cancer Biol Ther **3**(11): 1169-1176.

Muzes, G., B. Molnar, et al. (2012). "Regulatory T cells in inflammatory bowel diseases and colorectal cancer." World J Gastroenterol **18**(40): 5688-5694.

Nagendra, S. and A. J. Schlueter (2004). "Absence of cross-reactivity between murine Ly-6C and Ly-6G." Cytometry A **58**(2): 195-200.

Ohtsu, A. (2003). "The latest advances in chemotherapy for gastrointestinal cancers." Int J Clin Oncol **8**(4): 234-238.

Okayama, Y. and T. Kawakami (2006). "Development, migration, and survival of mast cells." Immunol Res **34**(2): 97-115.

Okita, R., T. Saeki, et al. (2005). "CD4+CD25+ regulatory T cells in the peripheral blood of patients with breast cancer and non-small cell lung cancer." Oncol Rep **14**(5): 1269-1273.

Omura, K. (2008). "Advances in chemotherapy against advanced or metastatic colorectal cancer." Digestion **77 Suppl 1**: 13-22.

Ophir, A., E. Berenshtein, et al. (1993). "5-fluorouracil and mast cell precursors in mice." Exp Hematol **21**(12): 1558-1562.

Ostrand-Rosenberg, S. and P. Sinha (2009). "Myeloid-derived suppressor cells: linking inflammation and cancer." J Immunol **182**(8): 4499-4506.

Parise, O., Jr., F. Janot, et al. (1994). "Thymidylate synthase activity, folates, and glutathione system in head and neck carcinoma and adjacent tissues." Head Neck **16**(2): 158-164.

Partridge, A. H., H. J. Burstein, et al. (2001). "Side effects of chemotherapy and combined chemohormonal therapy in women with early-stage breast cancer." J Natl Cancer Inst Monogr(30): 135-142.

Peddareddigari, V. G., D. Wang, et al. (2010). "The tumor microenvironment in colorectal carcinogenesis." Cancer Microenviron **3**(1): 149-166.

Peranzoni, E., S. Zilio, et al. (2010). "Myeloid-derived suppressor cell heterogeneity and subset definition." Curr Opin Immunol **22**(2): 238-244.

Pflugh, D. L., S. E. Maher, et al. (2002). "Ly-6 superfamily members Ly-6A/E, Ly-6C, and Ly-6I recognize two potential ligands expressed by B lymphocytes." J Immunol **169**(9): 5130-5136.

Placencio, V. R., X. Li, et al. (2010). "Bone marrow derived mesenchymal stem cells incorporate into the prostate during regrowth." PLoS One **5**(9): e12920.

Porta, C., B. Subhra Kumar, et al. (2007). "Tumor promotion by tumor-associated macrophages." Adv Exp Med Biol **604**: 67-86.

Prussin, C. and D. D. Metcalfe (2003). "4. IgE, mast cells, basophils, and eosinophils." J Allergy Clin Immunol **111**(2 Suppl): S486-494.

Reed, J. A., N. S. McNutt, et al. (1996). "Expression of the mast cell growth factor interleukin-3 in melanocytic lesions correlates with an increased number of mast cells in the perilesional stroma: implications for melanoma progression." J Cutan Pathol **23**(6): 495-505.

Ribechini, E., P. J. Leenen, et al. (2009). "Gr-1 antibody induces STAT signaling, macrophage marker expression and abrogation of myeloid-derived suppressor cell activity in BM cells." Eur J Immunol **39**(12): 3538-3551.

Rose, M. G., M. P. Farrell, et al. (2002). "Thymidylate synthase: a critical target for cancer chemotherapy." Clin Colorectal Cancer **1**(4): 220-229.

Sanchez-Munoz, F., A. Dominguez-Lopez, et al. (2008). "Role of cytokines in inflammatory bowel disease." World J Gastroenterol **14**(27): 4280-4288.

Schabowsky, R. H., S. Madireddi, et al. (2007). "Targeting CD4+CD25+FoxP3+ regulatory T-cells for the augmentation of cancer immunotherapy." Curr Opin Investig Drugs **8**(12): 1002-1008.

Schwarz, Y. X., M. Yang, et al. (1999). "Follicular dendritic cells protect malignant B cells from apoptosis induced by anti-Fas and antineoplastic agents." J Immunol **163**(12): 6442-6447.

Sebens, S. and H. Schafer (2012). "The tumor stroma as mediator of drug resistance--a potential target to improve cancer therapy?" Curr Pharm Biotechnol **13**(11): 2259-2272.

Serafini, P., R. Carbley, et al. (2004). "High-dose granulocyte-macrophage colony-stimulating factor-producing vaccines impair the immune response through the recruitment of myeloid suppressor cells." Cancer Res **64**(17): 6337-6343.

Serebrennikova, O. B., C. Tsatsanis, et al. (2012). "Tpl2 ablation promotes intestinal inflammation and tumorigenesis in Apcmin mice by inhibiting IL-10 secretion and regulatory T-cell generation." Proc Natl Acad Sci U S A **109**(18): E1082-1091.

Shaw, D., F. G. Berger, et al. (2001). "Retroviral expression of Escherichia coli thymidylate synthase cDNA confers high-level antifolate resistance to hematopoietic cells." Hum Gene Ther **12**(1): 51-59.

Shiao, S. L. and L. M. Coussens (2010). "The tumor-immune microenvironment and response to radiation therapy." J Mammary Gland Biol Neoplasia **15**(4): 411-421.

Shinar, G., R. Milo, et al. (2007). "Input output robustness in simple bacterial signaling systems." Proc Natl Acad Sci U S A **104**(50): 19931-19935.

Shoemaker, A. R., K. A. Gould, et al. (1997). "Studies of neoplasia in the Min mouse." Biochim Biophys Acta **1332**(2): F25-48.

Showalter, S. L., T. N. Showalter, et al. (2008). "Evaluating the drug-target relationship between thymidylate synthase expression and tumor response to 5-fluorouracil. Is it time to move forward?" Cancer Biol Ther **7**(7): 986-994.

Sica, A. and V. Bronte (2007). "Altered macrophage differentiation and immune dysfunction in tumor development." J Clin Invest **117**(5): 1155-1166.

Siddiqui, S. A., X. Frigola, et al. (2007). "Tumor-infiltrating Foxp3-CD4+CD25+ T cells predict poor survival in renal cell carcinoma." Clin Cancer Res **13**(7): 2075-2081.

Sinha, P., V. K. Clements, et al. (2007). "Prostaglandin E2 promotes tumor progression by inducing myeloid-derived suppressor cells." Cancer Res **67**(9): 4507-4513.

Sinha, P., C. Okoro, et al. (2008). "Proinflammatory S100 proteins regulate the accumulation of myeloid-derived suppressor cells." J Immunol **181**(7): 4666-4675.

Sinnamon, M. J., K. J. Carter, et al. (2008). "A protective role of mast cells in intestinal tumorigenesis." Carcinogenesis **29**(4): 880-886.

Sonda, N., M. Chioda, et al. (2011). "Transcription factors in myeloid-derived suppressor cell recruitment and function." Curr Opin Immunol **23**(2): 279-285.

Soria, G. and A. Ben-Baruch (2008). "The inflammatory chemokines CCL2 and CCL5 in breast cancer." Cancer Lett **267**(2): 271-285.

Stevenson, L., W. L. Allen, et al. (2011). "Calbindin 2 (CALB2) regulates 5-fluorouracil sensitivity in colorectal cancer by modulating the intrinsic apoptotic pathway." PLoS One **6**(5): e20276.

Studeny, M., F. C. Marini, et al. (2002). "Bone marrow-derived mesenchymal stem cells as vehicles for interferon-beta delivery into tumors." Cancer Res **62**(13): 3603-3608.

Sugasawa, H., T. Ichikura, et al. (2008). "Gastric cancer cells exploit CD4+ cell-derived CCL5 for their growth and prevention of CD8+ cell-involved tumor elimination." Int J Cancer **122**(11): 2535-2541.

Sunderkotter, C., T. Nikolic, et al. (2004). "Subpopulations of mouse blood monocytes differ in maturation stage and inflammatory response." J Immunol **172**(7): 4410-4417.

Suzuki, H., N. Chikazawa, et al. (2010). "Intratumoral CD8(+) T/FOXP3 (+) cell ratio is a predictive marker for survival in patients with colorectal cancer." Cancer Immunol Immunother **59**(5): 653-661.

Swartz, M. A., N. Iida, et al. (2012). "Tumor microenvironment complexity: emerging roles in cancer therapy." Cancer Res **72**(10): 2473-2480.

Taketo, M. M. (2009). "Role of bone marrow-derived cells in colon cancer: lessons from mouse model studies." J Gastroenterol **44**(2): 93-102.

Taketo, M. M. and W. Edelmann (2009). "Mouse models of colon cancer." Gastroenterology **136**(3): 780-798.

Tanaka, T. and H. Ishikawa (2013). "Mast cells and inflammation-associated colorectal carcinogenesis." Semin Immunopathol **35**(2): 245-254.

Theoharides, T. C., D. Kempuraj, et al. (2007). "Differential release of mast cell mediators and the pathogenesis of inflammation." Immunol Rev **217**: 65-78.

Udagawa, T., M. Puder, et al. (2006). "Analysis of tumor-associated stromal cells using SCID GFP transgenic mice: contribution of local and bone marrow-derived host cells." FASEB J **20**(1): 95-102.

Umansky, V. and A. Sevko (2012). "Tumor Microenvironment and Myeloid-Derived Suppressor Cells." Cancer Microenviron.

Umemura, N., M. Saio, et al. (2008). "Tumor-infiltrating myeloid-derived suppressor cells are pleiotropic-inflamed monocytes/macrophages that bear M1- and M2-type characteristics." J Leukoc Biol **83**(5): 1136-1144.

Utrera-Barillas, D., M. Castro-Manrreza, et al. (2010). "The role of macrophages and mast cells in lymphangiogenesis and angiogenesis in cervical carcinogenesis." Exp Mol Pathol **89**(2): 190-196.

Vincent, J., G. Mignot, et al. (2010). "5-Fluorouracil selectively kills tumor-associated myeloid-derived suppressor cells resulting in enhanced T cell-dependent antitumor immunity." Cancer Res **70**(8): 3052-3061.

Whitlock, E. P., J. S. Lin, et al. (2008). "Screening for colorectal cancer: a targeted, updated systematic review for the U.S. Preventive Services Task Force." Ann Intern Med **149**(9): 638-658.

Willhauck, M. J., N. Mirancea, et al. (2007). "Reversion of tumor phenotype in surface transplants of skin SCC cells by scaffold-induced stroma modulation." Carcinogenesis **28**(3): 595-610.

Wolf, A. M., D. Wolf, et al. (2003). "Increase of regulatory T cells in the peripheral blood of cancer patients." Clin Cancer Res **9**(2): 606-612.

Woo, E. Y., C. S. Chu, et al. (2001). "Regulatory CD4(+)CD25(+) T cells in tumors from patients with early-stage non-small cell lung cancer and late-stage ovarian cancer." Cancer Res **61**(12): 4766-4772.

Wu, L., C. Yan, et al. (2012). "Inhibition of PPARgamma in myeloid-lineage cells induces systemic inflammation, immunosuppression, and tumorigenesis." Blood **119**(1): 115-126.

Xia, Q., Y. Ding, et al. (2011). "Mast Cells in Adjacent Normal Colon Mucosa rather than Those in Invasive Margin are Related to Progression of Colon Cancer." Chin J Cancer Res **23**(4): 276-282.

Yang, Z., B. Zhang, et al. (2010). "Mast cells mobilize myeloid-derived suppressor cells and Treg cells in tumor microenvironment via IL-17 pathway in murine hepatocarcinoma model." PLoS One **5**(1): e8922.

Youn, J. I., S. Nagaraj, et al. (2008). "Subsets of myeloid-derived suppressor cells in tumor-bearing mice." J Immunol **181**(8): 5791-5802.

Zhang, B., Z. Wang, et al. (2013). "Circulating and tumor-infiltrating myeloid-derived suppressor cells in patients with colorectal carcinoma." PLoS One **8**(2): e57114.

Ziegler, S. F. (2006). "FOXP3: of mice and men." Annu Rev Immunol **24**: 209-226.

Zischek, C., H. Niess, et al. (2009). "Targeting tumor stroma using engineered mesenchymal stem cells reduces the growth of pancreatic carcinoma." Ann Surg **250**(5): 747-753.